공학박사 학위논문

Practical Application of Bacterial Quorum Quenching and Development of Quorum Quenching Medium for Biofouling Control in Membrane Bioreactor for Wastewater Treatment

정족수감지 억제 미생물의 실적용과 고정화 담체 개발을 통한

하폐수 처리용 분리막 생물반응기에서의 생물막오염 제어

2016 년 8 월

서울대학교 대학원

화학생물공학부

이 선 기

Abstract

Practical Application of Bacterial Quorum Quenching and Development of Quorum Quenching Medium for Biofouling Control in Membrane Bioreactor for Wastewater Treatment

Seonki Lee

School of Chemical and Biological Engineering

The Graduate School

Seoul National University

Since bacterial quorum quenching (QQ) was reported as an effective biofouling control strategy in membrane bioreactor (MBR) for wastewater treatment, various media entrapping the QQ bacteria have been developed and their efficiencies for biofouling control was confirmed. However, most studies on QQ-MBR have been carried out using laboratory-scale reactors fed with synthetic wastewater. Moreover, a few studies have been conducted to explore how to increase the performance of QQ-media for biofouling control in MBR.

In this study, pilot-scale MBRs were constructed and operated with real wastewater to bring the QQ-MBR closer to potential practical applications. In

addition, factors affecting the performance of QQ-media were investigated and a new cylinder-type medium was developed to enhance the performance of QQ-MBR.

First, pilot-scale QQ-MBRs with QQ bacteria entrapping beads (QQ-beads) were installed and operated at a domestic wastewater treatment plant, feeding a real municipal wastewater. The rate of transmembrane pressure (TMP) rise-up was significantly alleviated in QQ-MBR compared to that of control MBR. QQ-MBR saved the energy consumption by reducing coarse bubble aeration without compromising the effluent water quality. The addition of QQ-beads decreased the EPS concentration, as well as microbial floc size in the mixed liquor. In addition, the biological QQ activity and mechanical stability of QQ-beads were well maintained for at least four months, indicating QQ-MBR has good potential for practical applications.

Second, a cylinder-type medium (QQ-cylinder), a new shape of moving medium, was developed to improve the performance of QQ-MBR. QQ-cylinders and QQ-beads with various sizes were compared in batch-scale in terms of QQ activity and physical washing effect under identical loading volumes. It was found that QQ activity of QQ-media was highly dependent on their total surface area regardless of the shape of the media while physical washing effect of media was greatly affected by the shape and size of media. Based on those results, the effects of shape and size on performance of QQ-media were investigated to determine design factors to improve their performance. Furthermore, the improved anti-biofouling ability of QQ-cylinders relative to QQ-beads was confirmed in a continuous laboratory-scale MBR.

Keywords

Membrane bioreactor (MBR), Biofouling control, Quorum quenching, Media, Bead, Cylinder

Student Number: 2011-21059

Table of Contents

List of Figures

List of Tables

Chapter I

Introduction

I.1. Backgrounds

For over 30 years, the membrane bioreactor (MBR) has attracted considerable attention in the field of wastewater treatment and reuse due to its compactness and high water quality. For example, the global market for MBR system grew to $838.2 million in 2011 and is projected to increase up to $3.44 billion by 2018. This represents a compound annual growth rate (CAGR) of 22.4% over this time period (Hai et al., 2013). However, a critical issue in MBR that awaits a technological advancement to solve is membrane biofouling, which leads to high operating cost and short membrane life. Many studies utilizing diverse approaches have been conducted and reported to mitigate this chronic issue of membrane biofouling in MBRs including membrane surface modification (Rana and Matsuura, 2010), physical strategies (Rosenberger et al., 2011; Zsirai et al., 2012), and adding specific media (Lee et al., 2006; Yang et al., 2013). However, despite of tremendous efforts to reduce membrane biofouling, the underlying problem still remains because they did not essentially consider the mechanism of natural biofilm formation.

Since the regulation of microbial group behaviors by cell to cell communication (i.e., quorum sensing) was reported to be involved in the biofilm formation (Davies et al., 1998), the disruption of quorum sensing (i.e., quorum quenching, QQ) has been regarded as an ultimate approach of membrane biofouling control on diverse surface (Choudhary and Schmidt-Dannert, 2010).

Recently, Yeon et al. (2009a) revealed that quorum sensing (QS) plays a key role in biofilm formation on membrane surface in MBRs. Furthermore, they proved that the biofouling could be mitigated effectively by disrupting signal molecules such as *N*-acyl homoserine lactones (AHLs) using a quorum quenching (QQ) enzyme (Kim

et al., 2011; Yeon et al., 2009a). After that, bacterial QQ was developed to overcome the limitations of enzymatic QQ strategy (e.g., high cost and low stability of enzyme). In detail, QQ bacterium, *Rhodococcus* sp. BH4 bacterium which produces QQ enzymes that decompose a wide range of AHLs was isolated from a real MBR plant. Since then, many researchers isolated the different QQ bacteria and developed various media for immobilizing QQ microorganisms with greater stability, good mass transfer of substrates and protection of QQ bacteria in MBR system. (Oh et al., 2012). Especially, spherical QQ-beads (QQ-beads) have been favored because they have not only a biological (QQ) effect but also a physical washing effect through collisions between moving beads and membrane surface (Kim et al., 2013b). Other researchers also reported that the biofouling was mitigated by adding QQ-beads into MBRs (Khan et al., 2016; Maqbool et al., 2015).

In previous studies, QQ has been reported as an effective biofouling control approach in MBRs. However, most studies examining QQ-MBR have been performed in lab-scale reactors using synthetic wastewater. Although significantly inhibition of biofouling by QQ has been demonstrated, such an approach has not been fully investigated in a larger pilot-scale MBR using real wastewater. Because the microbial environment in lab-scale reactors is notably different from that in real full-scale reactors due to the different scales of the technological equipment and the different raw wastewater characteristics. Furthermore, they used only spherical QQ-beads as moving QQ-media in most previous studies, and thus there is insufficient information about the effect of the shape and size of QQ media on the performance of biofouling control in MBRs.

I.2. Objectives

The objective of this study was to develop more effective biofouling control strategy based on bacterial quorum quenching (QQ) in MBR for wastewater treatment. Pilot-scale MBRs with QQ-beads were installed and operated with real wastewater to confirm the potential of QQ-MBR for practical application, i.e., for crossing over from laboratory to field. In addition, the effects of the shape and size of QQ-medium on biofouling control were investigated, and cylinder-typed media (QQ-cylinder), as a new type of moving media, were developed to enhance the performance of QQ-MBR.

(1) Performance of QQ bacteria Entrapping Beads for Biofouling Control in Pilot-Scale QQ-MBRs Fed with Real Wastewater

QQ bacteria entrapping beads (QQ-beads) were applied to pilot-scale MBRs fed with real wastewater to evaluate their potential practical application. The effect of QQ-beads on biofouling control was evaluated under real wastewater condition. In addition, the anti-biofouling property of QQ-beads was compared with that of commercial-beads. Moreover, the effects of QQ-beads on operating cost and effluent quality of MBRs were evaluated. Finally, the long-term stabilities of QQ-beads were investigated.

(2) Effect of the Shape and Size of Quorum Quenching Media on Biofouling Control in QQ-MBR

QQ bacteria entrapping cylinder (QQ-cylinder) was developed to improve the performance of QQ-MBR. QQ-cylinders with various sizes were compared

with spherical QQ-beads at batch scale in terms of QQ activity and physical washing effect. The enhanced anti-biofouling performance of QQ-cylinders was also evaluated in a continuous laboratory-scale MBR. Based on those results, the effect of the shape and size on the performance of the QQ-medium was investigated to determine the key parameters affecting its performance in QQ-MBRs.

Chapter II

Literature Review

II.1. Membrane Bioreactor (MBR)

II.1.1. Conventional Activated Sludge (CAS) Process

Conventional activated sludge process is a biological process and has been used for removing organic pollution (biochemical oxygen demand, BOD). As illustrated in Figure II-1, the CAS process is carried out in two main compartments: the aeration tank and the clarification tank. In the aeration tank, the wastewater and activated sludge are mixed so that the degradation of pollutant in feed can occur. Then, the activated sludge is separated out of the liquid in the other compartment by sedimentation. Most of the sludge precipitated out is returned to the aeration tank to repeat the process, but an excess sludge is wasted. Without this wasting, the activated sludge concentration would increase too high, reducing the sedimentation efficiency in the clarification tank (Pombo et al., 2011).

Generally, a CAS system is a bulky system due to the large reactors required. First, the aeration tank is large, because a CAS system is often operated at a biomass concentration of about 3 to 5 g/l. Moreover, gravitational sedimentation is a relatively slow process, also requiring large settling tanks (van 't Oever, 2005).

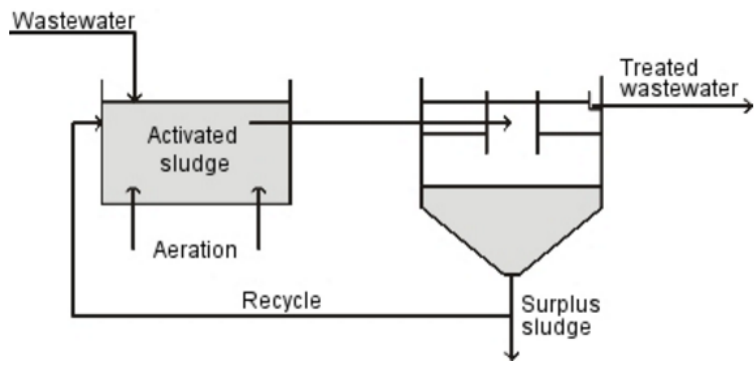

Figure II-1. Diagram of a conventional activated sludge process. (Pombo et al., 2011)

II.1.2. Advantages and Disadvantages of MBR

Membrane bioreactor (MBR) is a technology which combines a conventional activated sludge process with a membrane filtration process like microfiltration (MF) or ultrafiltration (UF). MBR process can produce high quality effluent due to high selectivity of filtration membrane. Other advantages of MBRs over conventional process include small footprint because of removal of settling tank. In addition, it is possible to operate at higher mixed liquor suspended solid (MLSS) concentrations compared to CAS process because of removing all suspended solids from the treated water according to the pore size of membrane (cut-off threshold). Thus, considering the food to microorganism ratio (F/M ratio), the reactor volume of MBR with high MLSS can be reduced by increasing loading rate of wastewater.

The advantages offered by MBR over CAS processes are widely recognized and of these the ones most often cited are (Judd, 2008):

(i) Production of high quality, clarified and largely disinfected permeate product in a single stage; the membrane has an effective pore size <0.1 μm - significantly smaller than the pathogenic bacteria and viruses in the sludge.

(ii) Independent control of solids and hydraulic retention time (SRT and HRT, respectively). In a CAS separation of solids is achieved by sedimentation, which then relies on growth of the mixed liquor solid particles (of flocs) to a sufficient size (>50 μm) to allow their removal by settlement. This then demands an appropriately long HRT for growth. In an MBR, the particles need only be larger than the membrane pore size.

(iii) Operation at higher mixed liquor suspended solids (MLSS) concentration, which reduced the required reactor size and promotes the

development of specific nitrifying bacteria, thereby enhancing ammonia removal.

(iv) Reduced sludge production, which results from operation at long SRTs because the longer the solids are retained in the biotank the lower the waste solids (sludge) production.

Although MBR processes have these advantages, compared with conventional activated sludge process, MBR are to some extent constrained primarily by:

(i) Greater process complexity; membrane separation demands additional operational protocols relating to the maintenance of membrane permeability.

(ii) Higher capital equipment and operating cost; the membrane component of the MBR incurs a significant capital cost over and above that of an CAS and maintaining membrane cleanliness demands further capital equipment (capex) and operating cost (opex).

II.1.3. MBR Configuration

The first MBR installation (Membrane Sewage System-MST) commercialized in the 70's and 80's was based on sidestream configurations, was made by Dorr-Oliver, Inc., with flat sheet ultrafiltration membrane operated at excessive pressure (3.5 bar inlet pressure) and low flux rate (17 l/(m^2 h)), yielding mean permeability (Judd, 2006). However, installation of the first large full-scale MBR for industrial wastewater treatment was at the General Motors plant in Mansfield, Ohio (U.S.) in the early 1990s (Knoblock et al., 1994). Later Yamamoto et al. (1989) innovated the submerged MBR (SMBR) configuration where the membrane module was directly submerged into the reactor with mixed liquor and operated under suction pressure.

As shown in Figure II-2, there are two MBR configurations. The filtration membrane are a separated unit process requiring an intermediate pumping step in side-stream MBR, while the filtration membranes are immersed in and integral to the biological reactor in submerged MBR (Judd, 2015). The key facets of each configuration are summarized (Table II-1).

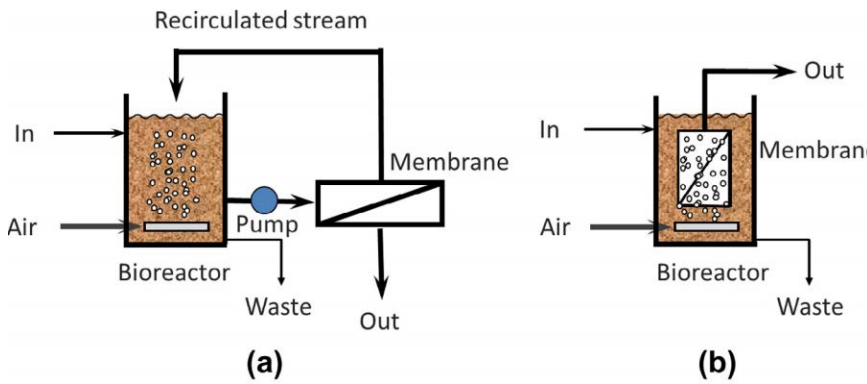

Figure II-2. MBR configurations. (a) Sidestream (external) and (b) submerged (internal).

Table II-1. Key facets of the MBR configurations. (Judd, 2004)

Sidestream	Submerged
Longest history (since early 1970s).	Most recent development (since 1990).
Membrane placed external to bioreactor.	Membrane placed in bioreactor.
Pumped system with permeation rate determined by transmembrane pressure and crossflow.	Permeate removed under hydrostatic head, with or without permeate suction, at rate partly determined by aeration
Higher flux and hydraulic resistance; lower aeration and membrane area requirement.	Lower flux and hydraulic resistance; greater aeration and membrane area requirement.
Stabilized flux with periodic chemical cleaning.	Stabilized flux with periodic chemical cleaning for flat plate membrane configuration; short backwash cycle with periodic chemical cleaning for hollow fiber configuration.
Greater overall energy demand; greater process (hydrodynamic) control.	Lower overall energy demand; reduced process (hydrodynamic) control.

II.1.4. Trend in MBR Market

Conventional technologies in wastewater treatment such as CAS system are gradually replaced by MBR system. As a result, the global MBR market was worth $838.2 million in 2011 and is expected to witness positive growth and revenue sales though 2018 (Frost&Sullivan, 2013). Figure II-3 shows the trends in global MBR market and treatment volume. It is growing at a compound annual growth rate (CAGR) of 22.4%, which is faster than the total market for wastewater treatment plant of 7.3% CAGR (Sze Chai Kwok, 2010). In addition, the large MBR plants appear to be getting ever larger. Figure II-4 and Table II-2 show the large-scale MBR plant (over 100 MLD) in the world.

Meanwhile, MBR employs either submerged membranes or sidestream membranes, but submerged membranes take a vast majority of the MBR market globally regardless of the region. It is because that the capital and operating cost of submerged system are much lower than those of sidestream system. Submerged MBR does not require the housed membrane module and high pumping velocity even though submerged MBR necessarily requires tighter pretreatment to prevent fouling such as fiber clogging (hollow fiber) and channel blocking (flat sheet) compared to sidestream MBR. Thus, more than 99% of MBRs around the globe rely on submerged membranes based on the treated water volume, and this trend is expected to continue in the future (Yoon, 2015).

In submerged MBR, perhaps a roughly equal number of hollow fiber and flat sheet membrane supplier exist. Some of the membrane manufacturers are summarized in Table II-3. Especially, Kubota, Evoqua (formerly Siemens), Asahi Kasei, and GE are the major suppliers playing globally and the number of

membranes are based on PVDF in the MBR market.

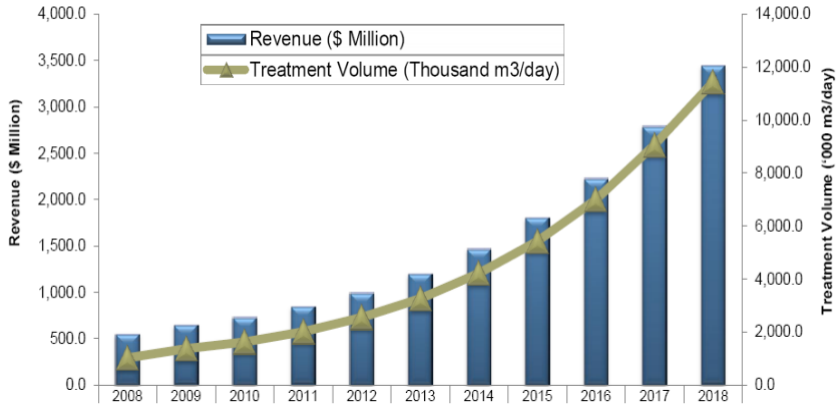

Figure II-3. Global MBR market value MBR and treatment volume. (Frost&Sullivan, 2013)

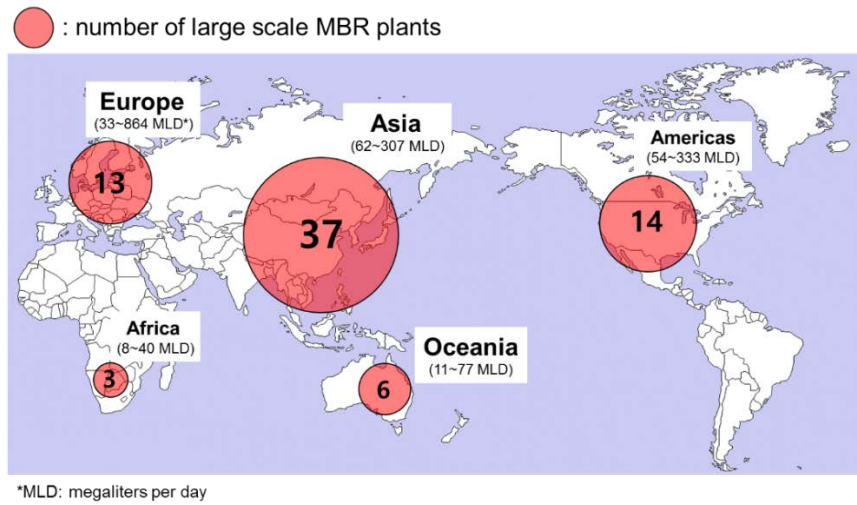

Figure II-4. The number of large scale MBR plants in the world.

(Source: http://www.thembrsite.com)

Table II-2. Large-scale MBR plants in the world.

(Judd, S., the MBR site, http://www.thembrsite.com)

Installations	Location	Technology Provider	(Expected)Date of Commissioning	**PDF (MLD)**
Henriksdal, Sweden	nr Stockholm, Sweden	GEWPT	2016-2019	864
Seine Aval	Acheres, France	GEWPT	2016	357
Canton WWTP	Ohio, USA	Ovivo USA/ Kubota	2015-2017	333
Water Affairs Integrative EPC	Xingyi, Guizhou, China	OW		307
Euclid, OH, USA	Ohio, USA	GEWPT	2018	250
9th and 10th WWTP	Kunming, Yunnan, China	OW	2013	250
Shunyi	Beijing, China	GEWPT	2016	234
Macau	Macau Special Administrative Region, China	GEWPT	2017	210
Wuhan Sanjintang WWTP	Hubei Province, China	OW	2015	200
Jilin WWTP (Phase 1, upgrade)	Jilin Province, China	OW	2015	200
Caotan WWTP PPP project	Xian, Shaanxi, China	OW		200
Brussels Sud	Brussels, Belgium	GEWPT	2017	190
Macau	China	GEWPT	2014	189
Riverside	California, USA	GEWPT	2014	186
Brightwater	Washington, USA	GEWPT	2011	175
Visalia	California, USA	GEWPT	2014	171

PDF: Peak daily flow, Megaliters per day (MLD)
GEWPT: GE Water and Process Technologies
OW: (Beijing) Origin Water

Table II-3. Summary of commercial MBR membrane module products.

(Santos and Judd, 2010)

Immersed (iMBR)	
Flat sheet	Hollow fiber
A3-*MaxFlow*[DE]	Asahi Kasei-*Microzoa*®[JP]
Alfa Laval[SE]	Beijing Origin Water Technology Co.[CN]
Brightwater-*Membright*®[IRL]	*Ecologix-EcoFlon*[TM], *EcoFil*[CN]
Colloide-*Sub snake*[NIR]	ENE Co., Ltd.-*SuperMAK*[KR]
Ecologix-*Ecoplate*[TM], *EcoSepro*[CN]	GE Zenon-Zeeweed®[US]
Huber-*VRM*®; *VUM*®/*GreyUse*[DE]	Hangzhou H-Filtration Membrane Technology Engineering Co., Ltd.MR[CN]
Jiangsu Lantian Peier Memb. Co. Ltd.[CN]	Koch Membrane System-*Puron*®[US]
KOReD-*Neofil*[KR]	Korean Membrane System-*KSMBR*®[KR]
Kubota-ES/EK[JP]	Litree-*LH3*[CN]
Microdyn-Nadir-*Biocel*®[DE]	Memstar-SMM[SG]
Pure Envitech Co., Ltd.-*ENVIS*[KR]	Mitsubishi Rayon-*Sterapore SUR*®; *Sterapore SADF*®[JP]
Shanghai Megavision Memb. Tech.[CN]	Philos[KR]
Toray-*TRM*[JP]	Porous Fibers S.L.-Micronet ®[JP]
Vina Filter-*Vinap*[CN]	SENUO Filtration Technology Co., Ltd.-*SENUOFIL*[CN]
Weise-*MicroClear*®[DE]	Shanghai Dehong Biology Medicine Siece & Tech. Development Co., Ltd.[CN]
	Siemens Water Tech.-*Memjet*[TM DE]
	Sumitomo-*PoreFlon*®[JP]
	Superstring MBR Tech. Corp.-*SuperUF*[CN]
	Tianjin Motimo-*FP AIV*[CN]
	Vina Filter-*F08*[CN]
	Zena Membranes-*P5*[CZ]

Table II-3 *(Continue)*

Sidestream (sMBR)
Multitube/multichannel
A3-*MaxFlow*[DE] Alfa Laval[SE] Brightwater-*Membright*®[IRL] Colloide-*Sub snake*[NIR] Ecologix-*Ecoplate*[TM], *EcoSepro*[CN] Huber-*VRM*®; *VUM*®/*GreyUse*[DE] Jiangsu Lantian Peier Memb. Co. Ltd.[CN] KOReD-*Neofil*[KR] Kubota-ES/EK[JP] Microdyn-Nadir-*Biocel*®[DE] Pure Envitech Co., Ltd.-*ENVIS*[KR] Shanghai Megavision Memb. Tech.[CN] Toray-*TRM*[JP] Vina Filter-*Vinap*[CN] Weise-*MicroClear*®[DE]

II.1.5. MBR Costs

There are capital cost and operating cost factors to take into account when considering implementing MBR technology. The trade-off between capital and operating costs is well recognized. Often, greater investment in capital equipment can increase the process robustness (i.e., high stability) and therefore decrease the operating cost such as maintenance cost. For example, higher fluxes permit reduced capital costs through the correspondingly reduced membrane area requirement. However, higher flux leads to frequent membrane fouling, demanding more frequent cleaning and increasing the process discontinue.

i) Capital cost

As a consequence of low membrane prices, membrane takes only a very small portion of total capital costs (Churchouse and Wildgoose, 1999). As system size grows, specific membranes costs for unit flow rate decreases below \$100/(m^3/d). Since other specific costs for civil and system engineering are also declining, membrane cost takes around 5% of the total capital costs regardless of the plant size (Yoon, online MBR site, http://onlinembr.info).

ii) Operating cost

Figure II-5 shows one of the examples of distribution of the energy consumptions in the full-scale flat sheet and hollow fiber MBRs. In both MBR systems, aeration is the major component of energy consumption as the blowers providing air for the membrane scouring and for the biological process (dissolved oxygen supply) contribute to nearly 50-70% of the total energy demand.

Especially, the coarse bubble aeration is the largest consumer being 36-56% and 0.3-0.48 kWh/m^3 because most MBR plants have been operated at high aeration intensity to control membrane fouling. The other energy consumption are related to mixers, recirculation pumps, permeate extraction and sludge discharge (Krzeminski et al., 2012).

The parameters measuring the energy consumption for aeration are defined as follows (Verrecht et al., 2010):

i) Specific aeration demand based on membrane area (SAD_m) is defined as scouring air flow rate per membrane area.

$$SAD_m = \frac{Q_{air}}{Area_{memb}}$$

ii) Specific aeration demand based on permeate volume (SAD_p) is defined as scouring air flow rate per permeate volume.

$$SAD_p = \frac{Q_{air}}{Q_{permeate}}$$

Moreover, there are some methods for calculating and measuring filtration and aeration energy. For example, each equation for filtration and aeration energy is introduced, respectively.

(i) The filtration energy can be calculated by integrating the TMP over time (t_f) as follows (Weerasekara et al., 2014):

$$\text{Specific filtration energy (kWh/m}^3\text{)} = \frac{1}{\eta t_f}\int_0^{t_f} TMP\ dt$$

where t_f is the filtration time and η is the pump efficiency (which was usually assumed as 0.6).

(ii) Aeration intensity can be expressed using the velocity gradient, G value, which is defined as follows (Mueller et al., 2002):

$$G(s^{-1}) = \sqrt{\frac{Q_a \times [P_1 \times \ln\left(\frac{P_2}{P_1}\right)]}{(3.61 \times V \times \mu)}}$$

where Q_a is the air flow rate (m^3/h), P_1 is the absolute pressure at the reactor surface, P_2 is the absolute pressure at the point of air injection (kPa), V is the liquid volume (m^3), and μ is the absolute viscosity (pa s).

In addition, power dissipated of aeration, P (W) can be calculating by using the velocity gradient as follows (Weiner and Matthews, 2003):

$$G^2 = \frac{P}{\mu V}$$

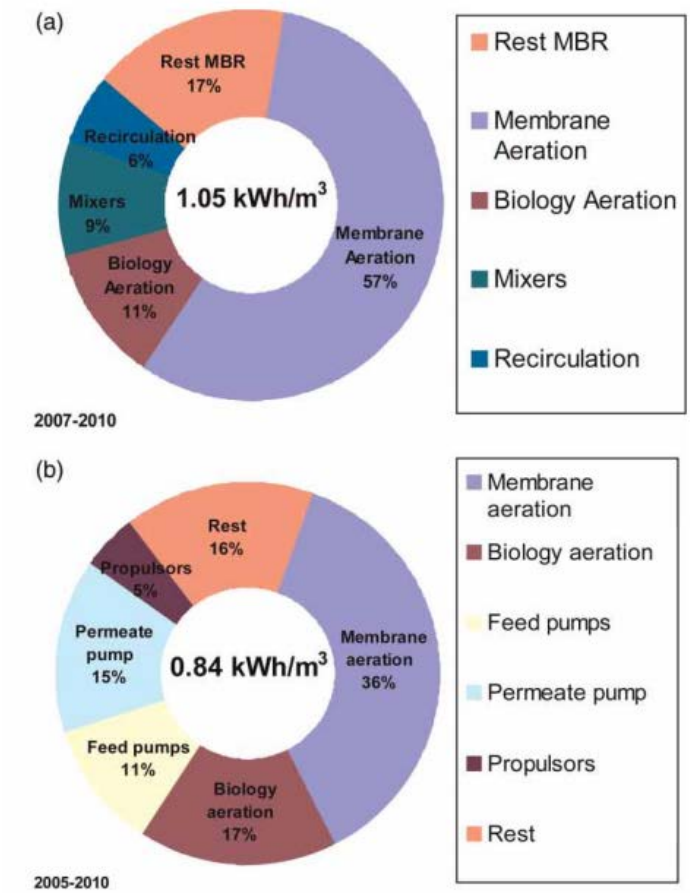

Figure II-5. Energy consumption distribution of MBR equipment. (a) Flat sheet MBR (Heenvliet). (b) Hollow fiber MBR (Varsseveld).

II.1.6. Membrane Fouling in MBR

Membrane fouling means the loss of permeability. In practice, this is observed as an increase in the transmembrane pressure (TMP) as an increase in membrane fouling in MBRs operated at constant flux.

Membrane fouling can be classified as reversible fouling and irreversible fouling (Tsuyuhara et al., 2010). Physically reversible fouling can be restored through appropriate physical washing procedures such as backwashing or hydrodynamic scouring (surface washing), and chemically reversible fouling only can be removed by chemical cleaning. Irreversible fouling occurs by chemisorption and pore plugging mechanisms. In case of irreversible fouling, the loss in transmembrane flux cannot be recovered physically or chemically. This means that the membranes should be treated by extensive chemical cleaning or be replaced.

Previous studies have demonstrated that membrane fouling and the characteristics of foulants are determined by feed water composition and concentration, water chemistry (pH, ionic strength, and divalent cation concentration), membrane properties (surface morphology, hydrophobicity, charge and molecular weight cut-off), temperature and operating condition (e.g., flux) (Li and Elimelech, 2004; Zhou and Smith, 2002).

Normally, foulants can be classified into the following four categories: Particulates (Guo et al., 2012):

i) Particulates: inorganic or organic particles act as foulants which can physically bind the membrane surface and block the pores, or hinder transport to the surface by the development of a cake layer;

ii) Organic: dissolved components and colloids (e.g., polysaccharide and proteins) which would attach to the membrane by adsorption;

iii) Inorganic: dissolved components (e.g., iron, manganese and silica) which tend to precipitate onto the membrane surface due to pH change (scaling) or due to oxidation (e.g., iron or manganese oxides). Coagulant/flocculant residuals may also be present as inorganic foulants; and

iv) Microbiological organisms: the microbiological category covers vegetative matter such as algae, and microorganisms such as bacteria which can adhere to the membrane surfaces and cause biofouling (biofilm formation).

II.1.7. Fouling Control in MBR

As mentioned previously, membrane fouling is the biggest challenge in MBR operation. Thus, many researchers have been tried to overcome the fouling problem in MBR over 30 years (Figure II-6). Especially, aeration, relaxation, backwashing, chemical cleaning and mechanical washing by adding particles are widely used as effective fouling control methods.

II.1.7.1. Aeration

An aeration process is the most popular method to reduce the membrane fouling in MBR system. Membrane fouling can be mitigated by shear stress and surface tension induced by air bubbles (Hazlett, 1995). However, an aeration process significantly increases the energy consumption of MBR operation. Thus intermittent aeration, in which aeration was switched on and off alternatively was used (Nagaoka and Nemoto, 2005; Yeom et al., 1999). In addition, cyclic aeration alternating between the high and low aeration intensity was used to effectively control membrane fouling in MBRs (Monsalvo et al., 2015; Wu and He, 2012). However, the irreversible interactions between soluble compounds or bacteria and membrane material cannot be controlled by only aeration (Johir et al., 2011).

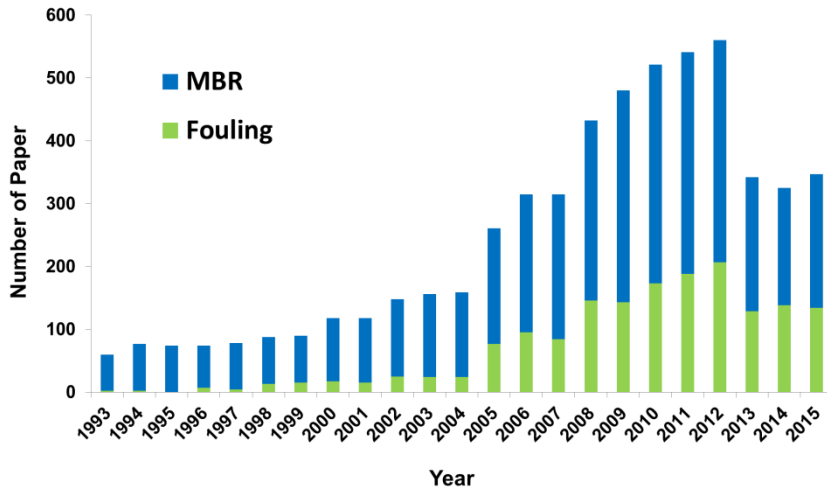

Figure II-6. The number of research papers since 1993. (Source: Web of science)

II.1.7.2. Relaxation

Relaxation is defined as pausing the suction for permeate while continuing to scour the membrane with shear force induced by aeration. Relaxation is a commonly used in submerged MBR operation for either hollow fiber or flat sheet membranes (Judd, 2010; Monclus et al., 2010; Yuniarto et al., 2013). Although relaxation reduces the membrane fouling, too long and highly frequent relaxation reduces the permeate production. Thus some researchers have been tried to find optimize the relaxation condition (i.e., interval and frequency) through experiments (Annop et al., 2014; Wu et al., 2008) or simulation approaches (Ludwig et al., 2011).

II.1.7.3. Backwashing

Backwashing, which is also called backflusing or backpulsing, is also widely used as a membrane fouling control method. A standard definition of backwashing is the reversing of permeation back through the membrane (Judd, 2010). However, backwashing can be diversely conducted by using other than permeation, such as chemicals, air and others that can improve the permeability (Yusuf et al., 2015). Typically, sodium hypochlorite, NaOCl (100-1000 mg/L) is used as a chemical. As expected, optimization of backwashing process is also essential because of trade-off between fouling control and permeation production (Aidan et al., 2007).

Meanwhile, backwashing is often applicable for hollow fiber membranes. However, in flat sheet membranes, backwashing is usually not applied due to low mechanical stability of membrane module while Microdyn-nadir GmbH (flat sheet membrane) can operate the backflushing mode (Amini et al., 2013).

II.1.7.4. Chemical cleaning

There is two kind of membrane cleaning methods using chemicals. One is the backwashing with chemicals such as chlorine (or bleach), so called maintenance cleaning or chemically enhanced backwash or clean in place (CIP), and thus membrane module stays in the reactor during cleaning. It is typically performed once or twice a week, and 100-1000 mg/L bleach solution is back flowed through the permeate line. Another is recovery cleaning. Often chemicals are immersed in a membrane tank after mixed liquor is transferred to another tank such as aeration tank, membrane module can be cleaned without being removed. Commonly, higher concentration (> 1000 mg/L) of bleach solution and additional chemicals (citric acid, etc.) are used.

II.1.7.5. Mechanical Washing by Adding Particles

Many previous researchers have been studied the adding particles, such as granular activated carbon (GAC) and powder activated carbon (PAC), to reduce the membrane fouling because of the removal of organic matter by its adsorption ability (Hu, 2007; Nguyen et al., 2012). However, recently, adding particles has been used for mechanical washing which reduces the membrane fouling by detachment of foulants through the collision between added particles and membrane surface (Johir et al., 2011; Rosenberger et al., 2011; Siembida et al., 2010). Especially, Rosenberger et al. (2011) applied the plastic particles into flat sheet membrane module (BIO-CEL, Microdyn-nadir, Germany). As shown in Figure II-7, an upward flow is induced between membrane sheets by air bubbles (airlift principle) and liquid which flowed upward returns to bottom of the reactor in the downflow region outside the

membrane module. The plastic particles in the membrane tanks results in a circulating fluidized bed flow regime. They showed that the permeability of MBR with circulating particles was relatively maintained compared to conventional MBR (Siembida et al., 2010). However, the membrane surface can be damaged by the collision with polypropylene particles (Figure II-8). Furthermore, Kurita et al. (2014) reported that granules significantly reduced the membrane fouling physically but, they could not inhibit the irreversible fouling generated by long-term operation (Figure II-9).

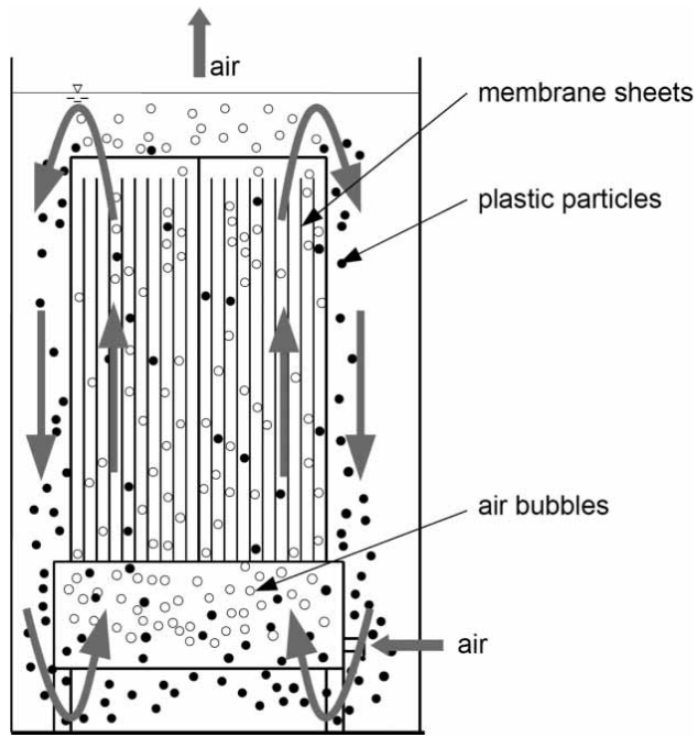

Figure II-7. Scheme of the MCP flow field in a membrane tank with a submerged flat sheet module. (MCP: mechanical cleaning process).

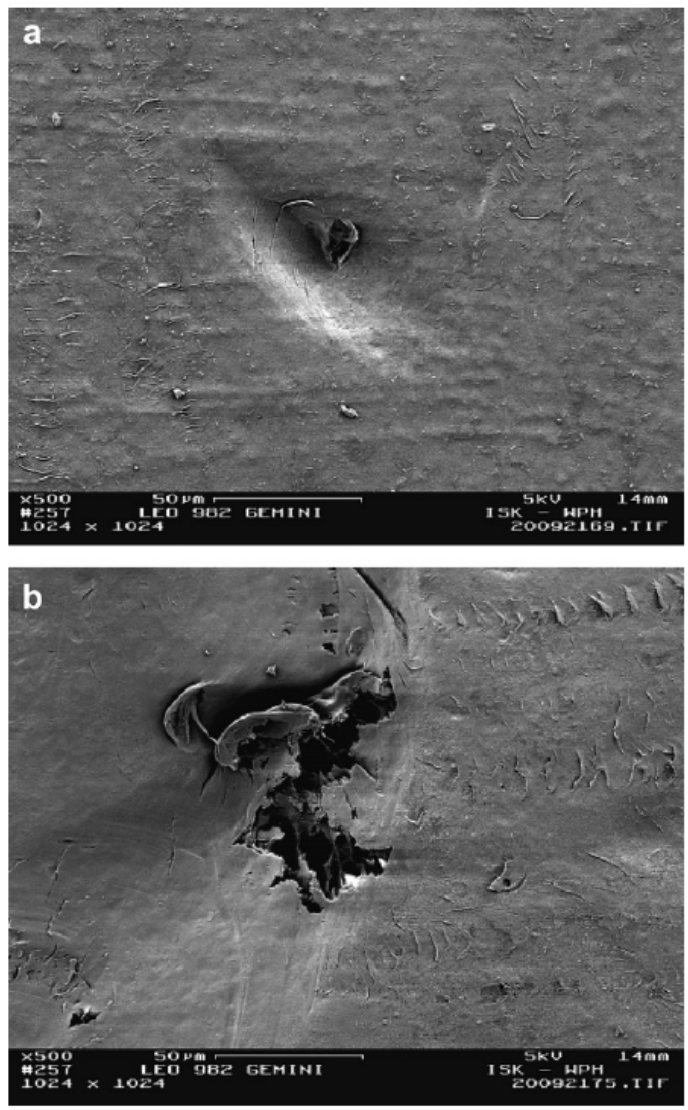

Figure II-8. SEM images of membrane surface. (a) Membrane operated without plastic particles. (b) Membrane operated with plastic particles. (Siembida et al., 2010)

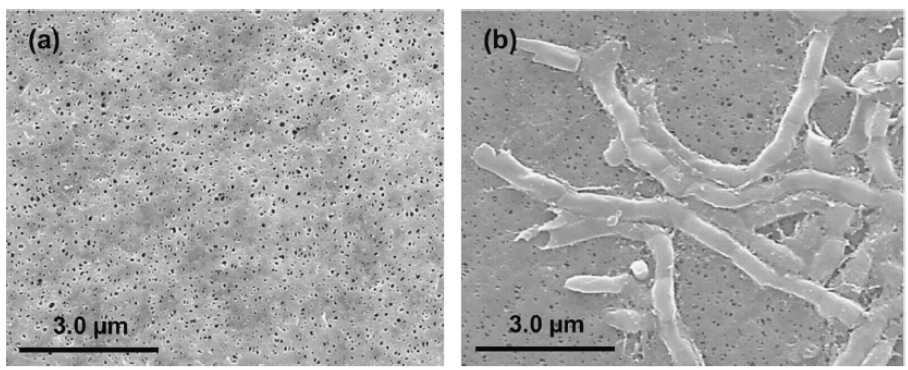

Figure II-9. SEM images of membrane surface at four months of operation (after physical cleaning): (a) without granules and (b) with granules.

II.1.7.6. Biological Approaches

Biological-based strategies offer the advantages of higher efficiency, low toxicity, more sustainability and less bacterial resistance over other control approaches. Among the commonly tested biological approaches for biofilm control are enzymatic disruption (ED), energy uncoupling (EU), cell wall hydrolysis and quorum quenching (QQ).

(i) Enzymatic disruption (ED) refers to degradation of foulant by enzymes which are capable of decomposing protein or polysaccharides. Especially, EPS-degrading enzymes have been successfully applied for biofilm detachment, such as protease (e.g., proteinase K and trypsin), polysaccharases (e.g., Dispersin B, Mutanase and dextranase) and DNases (Chaignon et al., 2007; Guezennec et al., 2012; Petersen et al., 2005).

(ii) Energy uncoupling (EU) by the addition of chemicals [e.g., 2,4-dinitrophenol (DNP), carbonyl cyanide chlorophenylhydrazone (CCCP), and 3,3',4',5-tetrachlorosalicylanilide (TCS)] can transport protons through the cellular membrane thus dissipating the proton gradient and inhibiting adenosine triphosphate (ATP) synthesis. It was reported that DNP suppressed ATP synthesis and AI-2 production and removed biofilm bacteria from nylon membrane surfaces (Xu and Liu, 2011).

(iii) Hydrolytic enzymes of cell walls such as the antimycotic protein lysozyme have been applied to prevent microbial attachment and could act more

specifically than conventional biocides (Xiong and Liu, 2010).

However, until now, a limited amount of biological approaches has been applied to control biofouling in MBRs. However, some review papers introduced the quorum quenching as a successful biological-based antifouling strategy in MBR (Drews, 2010; Malaeb et al., 2013).

II.1.7.7. Microbial Community and Fouling in MBR

In MBRs, many factors, including reactor design and operation, cleaning strategies, membrane properties and biomass conditions can affect directly MBR fouling potential (Meng et al., 2012; Yamato et al., 2006). Miura et al. (2007b) found that relative abundance of *Betaproteobacteria* significantly increased and became the most dominant phylogenetic group in the mature biofilms when aeration rate was increased to 5000 L/h from 3500 L/h. Lim et al. (2004) reported the presence of *Paracoccus* sp. and *Flavobacterium* sp. for continually aeration with and *Pseudomonas, Moraxella, Vibrio, Staphylococcus warneri, Micrococcus* sp. and *Nocardia* sp. for intermittently aeration with hollow fiber MBRs. Huang et al. (2008a) found that the MBR biofilm community composition was similar independent of sludge age at lower fluxes whereas distinct biofilm communities were developed on membrane surfaces at higher fluxes. However, more studies about other parameters and conditions are still needed particularly relating to reactor design, temperature and characteristic of wastewater and how these impact biofouling communities.

When characterizing the microbial communities and their associated products in MBRs, it is important to consider: a) the use of real wastewater or synthetic wastewater. A lower microbial diversity index is generally attributed to

systems with synthetic influent regardless of operation mode and reactor scale (Hiraishi et al., 1998); b) long-term monitoring of the biofouling communities due to deviations in operational conditions and in membrane properties, as foulants attach to the surface, can have a significant impact on the bacterial ecophysiology. It has been reported that short-term tests for membrane adhesion not a suitable predictor for membrane biofouling, which showed significantly reduced adhesion of biofoulants in short-term tests, but no reduction in long-term experiments (Miller et al., 2012); and c) influence of repeated cleaning and the relationship between the biofouling bacterial communities and the cleaning chemicals.

II.2. Quorum Sensing (QS)

II.2.1. Definition

Quorum sensing, cell to cell communication, is the regulation of gene expression related the group behaviors in response to cell density. Quorum sensing bacteria produce and release signal molecules called autoinducers whose external concentration increases as a function of increasing cell density (Waters and Bassler, 2005). In Figure II-10, although each individual cell still synthesizes low level of signal molecules, in aggregate, the group produces higher concentration. At a threshold level, signal molecules binds with a transcription factor, and in turn the transcription factor modulates expression of QS genes (Fuqua et al., 2001). Gram-positive and Gram-negative bacteria use QS communication circuits to regulate a diverse array of physiological activities. These processes include symbiosis, virulence, competence, conjugation, antibiotic production, motility, sporulation, and biofilm formation (Miller and Bassler, 2001).

II.2.2. Mechanism

QS mechanism can be divided into three general classes based on the type of signal molecules (Figure II-11).

(i) Gram-negative bacteria with *N*-acyl-homoserine lactone (AHL).

(ii) Gram-positive bacteria with oligopeptide signal molecules.

(iii) Interspecies communication with AI-2 molecules.

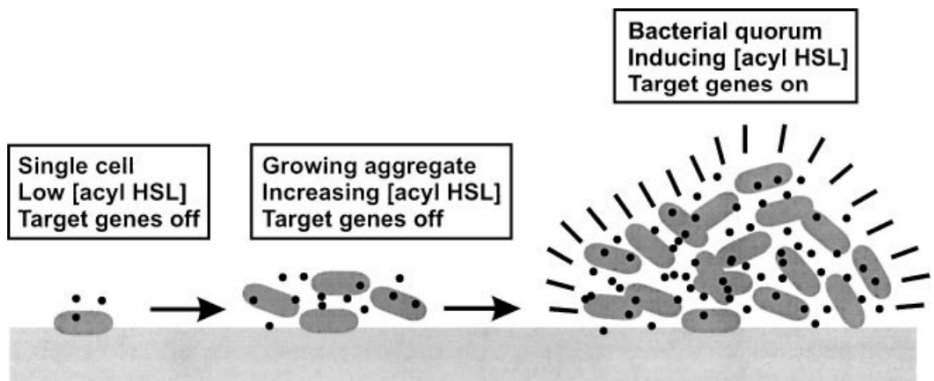

Figure II-10. Population density-dependent gene regulation. A single population of bacteria accumulating on a surface. Filled dots indicates the intercellular signal molecule. (Fuqua et al., 2001)

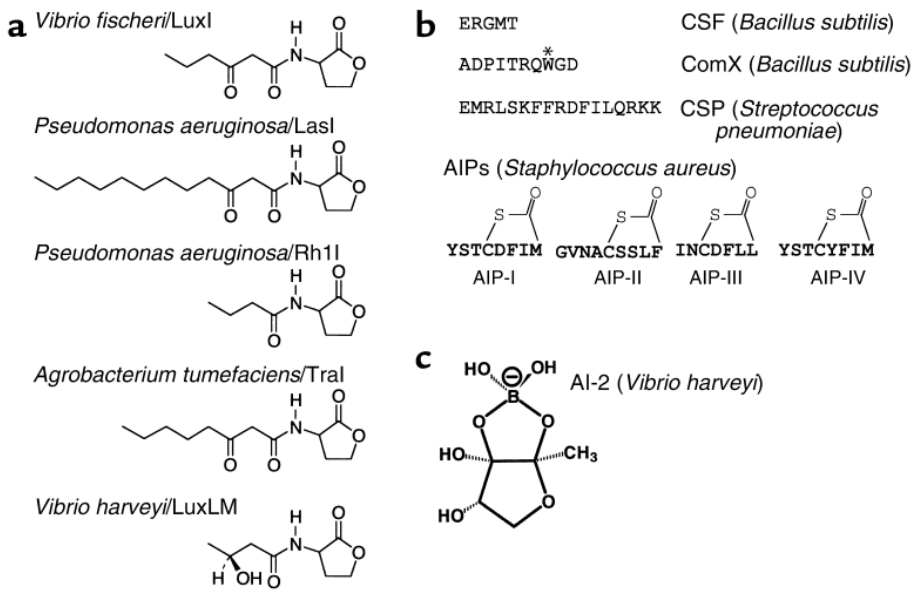

Figure II-11. Structures of different signal molecules. (a) AHL signal molecules. (b) Oligo peptide signal molecules. (c) AI-2 signal molecules. (Federle and Bassler, 2003)

II.2.2.1. Gram-Negative Bacteria QS

Figure II-12 shows the stages of QS process in AHL-mediated QS in Gram-negative bacteria. Generally, the stages of QS step includes the signal synthesis, diffusion, signal binding to receptor binding to promoter and QS gene expression. In detail, in this QS system all have in common the use of an AHL signal molecules whose synthesis is dependent on a *luxI* homologue, as well as *lux R* homologue encoding a transcriptional activator protein detecting AHL molecules and inducing gene expression (Waters and Bassler, 2005). As shown in Figure II- 13, LuxI-like signal molecule synthases (square) are responsible for specific AHL signal molecules (triangles). These AHLs freely diffuse across the cell membrane. Upon reaching a critical concentration of signal molecules, LuxR-like protein (circle) and signal molecules are combined, and together the LuxR-AHL complex activates transcription of the target gene related group behavior (Bassler, 1999).

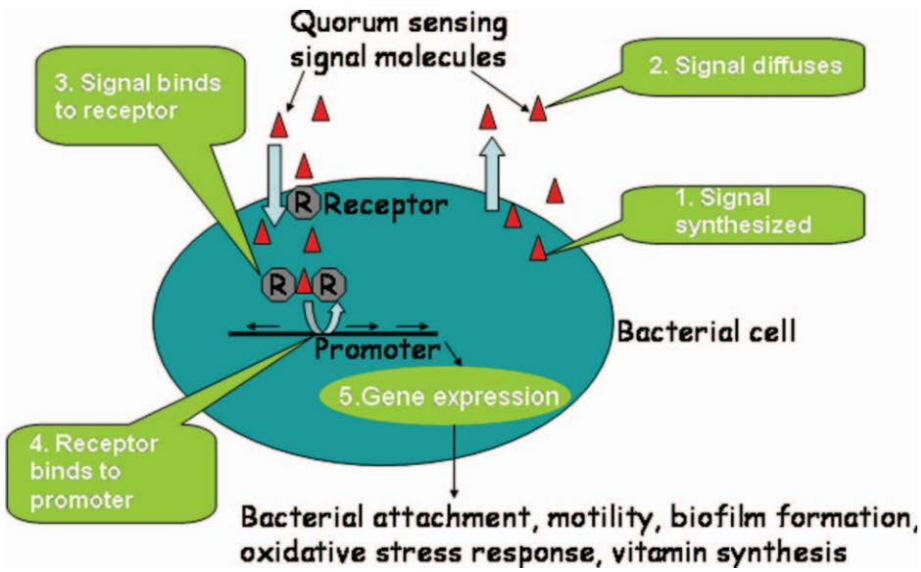

Figure II-12. Different stages of QS process in generalized model of AHL QS in Gram-negative marine bacteria. Thick arrows show the main direction of signal transport due to diffusion (short chain AHLs or active transport (long chain AHLs). (Dobretsov et al., 2009)

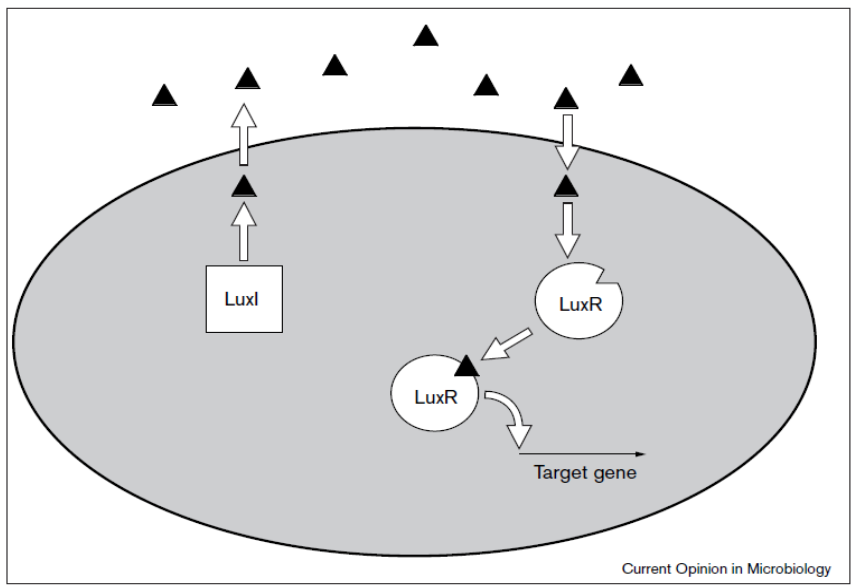

Figure II-13. LusI/LuxR quorum sensing. (Bassler, 1999)

II.2.2.2. Gram-Positive Bacteria QS

Similar to Gram-negative QS, Gram-positive bacteria employ a common signaling substructure while Gram-positive bacteria use the peptide signal molecules via a dedicated AHL (ATP-binding cassette) exporter protein. As shown in Figure II-14, the peptide molecules (extracellular pheromones) are recognized by two-component sensor kinase proteins interacting with cytoplasmic response regulator proteins (Kleerebezem et al., 1997; Novick and Muir, 1999). The sensors auto-phosphorylate on a conserved histidine residue (H), and subsequently transfer the phosphoryl group to cognate response regulators which are phosphorylated on conserved aspartate residues (D). Following phosphorylation (P indicates the phosphorelay cascade), response regulator proteins activate/repress transcription of specific target gene (Bassler, 1999).

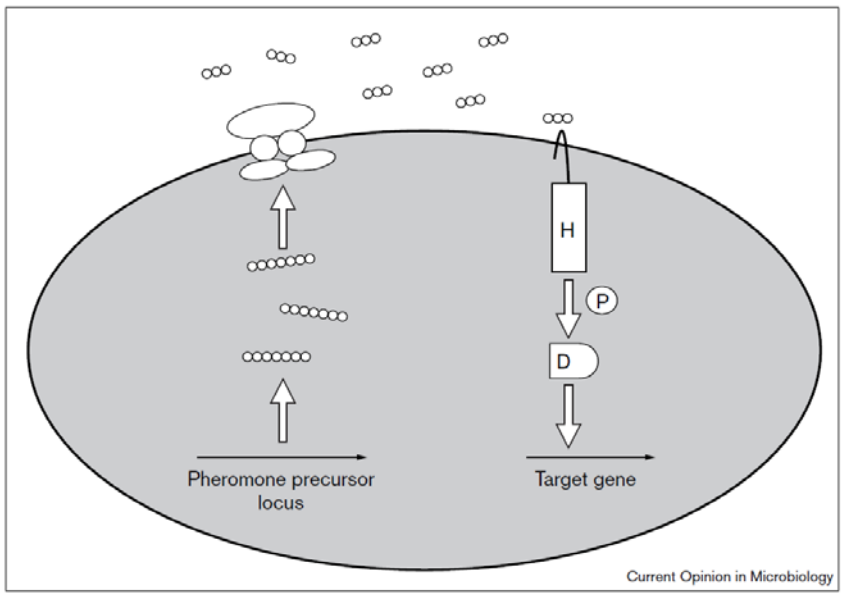

Figure II-14. Peptide quorum sensing. (Bassler, 1999)

.

II.2.2.3. Interspecies QS (AI-2)

In previously mentioned, AHLs and peptides represent the two major classes of bacterial QS signal molecules, used by Gram-negative and Gram positive bacteria, respectively. Recently, a family of molecules termed autoinducer-2 (AI-2) has been found (Chen et al., 2002). It has been proposed that AI-2 is a non-species signal molecules that mediates intra- and interspecies communication among Gram-negative and Gram-positive bacteria (Thiel et al., 2009).

AI-2 QS was firstly found in the *V. harveyi* which is a marine luminous bacterium. This bacterium possesses two QS circuits to control expression of the luciferase structural gene (*luxCDABE*) (Federle and Bassler, 2003). Figure II-15 shows that *V. harveyi* produces and responds to AHLs and AI-2 signal molecules in the first and second circuits, respectively. Triangles and circles represent AHL signal molecules and AI-2 signal molecules, respectively. Synthesis of AHLs and AI-2 molecules is dependent on LuxLM and LuxS, respectively. LuxN and LuxQ is detector for AI-1 and AI-2, respectively. Signals from both sensors are channeled to the shared integrator protein LuxU and LuxO. Each step flows phosphorelay cascade. Finally, LuxO–phosphate controls the expression of the luciferase structural operon *luxCDABE* (Bassler, 1999). Therefore, even though, if one QS circuit was blocked, *V. harveyi* produces luciferase gene using other QS circuit.

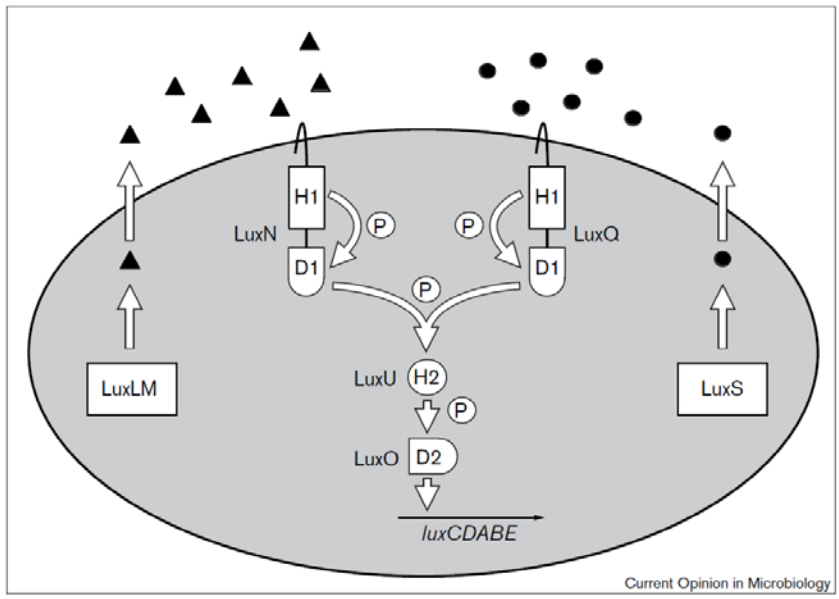

Figure II-15. Quorum sensing in *V. harveyi* with two QS circuits. (Bassler, 1999)

II.2.3. Role of QS in Biofilm Formation

Since biofilm is composed of much higher density of bacteria cell than freely planktonic cell, it stands to reason that quorum sensing and biofilm have a close relationship. Some researchers reported that quorum sensing, a way of bacterial cell density-dependent cell to cell communication, and phenotype regulation is known to associate with biofilm formation (Dobretsov et al., 2009; Sauer et al., 2002). In addition, Figure II-16 shows the hypothetical images of QS signal gradients and biofilm structures. (Parsek and Greenberg, 2005). Others (Cvitkovitch et al.; Sauer et al., 2002; Solano et al., 2014) reported the biofilm development (e.g., attachment, maturation and dispersion) for several species could be influenced by QS as shown in Figure II-17. Furthermore, in Figure II-18, biofilm of wild-type *P. aeruginosa* was thicker than that of lasR, rhlR mutant. Solano et al. (2014) illustrated the relationship between biofilm dispersion and quorum sensing (Figure II-19). Until now, there are growing evidences that QS is one of the important mechanisms for biofilm formation. However, many researchers studied QS and biofilm in respect of medical science. For example, biofilm formed by QS mutant or biofilm treated with QS inhibitors were much susceptible of the antibiotics or biocides. (Brackman et al., 2011; Tomlin et al., 2005).

Recently, Yeon et al. (2009a) revealed that QS plays a key role in biofilm formation on membrane surface in MBRs. They showed that blue color indicating the presence of AHL signal molecules was not detected at the early stage but the blue color development gradually became stronger as the membrane fouling proceeded (Figure II-20).

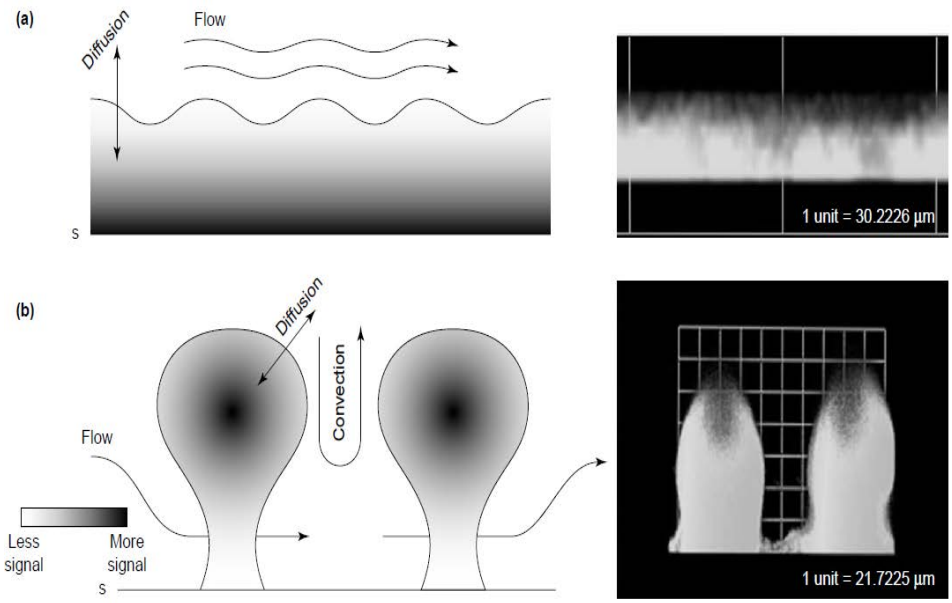

Figure II-16. Hypothetical signal gradients in a biofilm system. This schematic represents a side-view of (a) a flat and (b) a structured biofilm (s indicates the surface or substratum). This diagram represents speculation regarding potential signal gradients (indicated by the gray scale), with higher signal concentrations indicated by darker coloration. The two images at the right of the figure represent side-views of confocal images of a flat and a structured biofilm of *P. aeruginosa* PAO1 (Parsek and Greenberg, 2005).

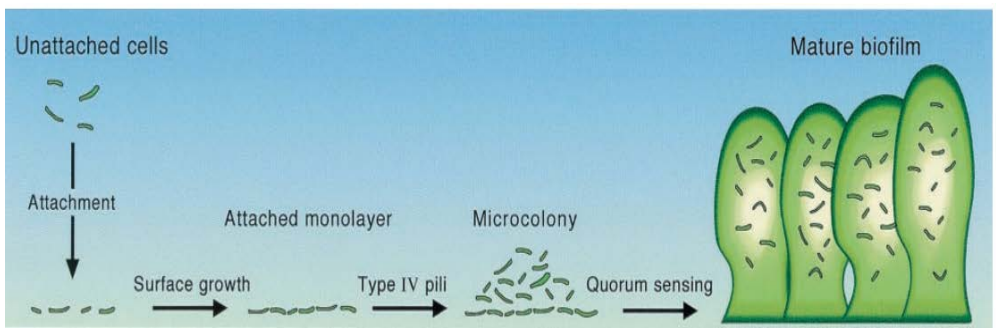

Figure II-17. Diagram of the *P. aeruginosa* biofilm-maturation pathway. Unattached cells that approach a surface may attach. Attachment involves specific functions. Attached cells will proliferate on a surface and use specific functions to actively move into micro-colonies. The high-density micro-colonies differentiate into mature biofilms by a 3-oxo-C12-HSL-dependent mechanism. (Parsek and Greenberg, 2000)

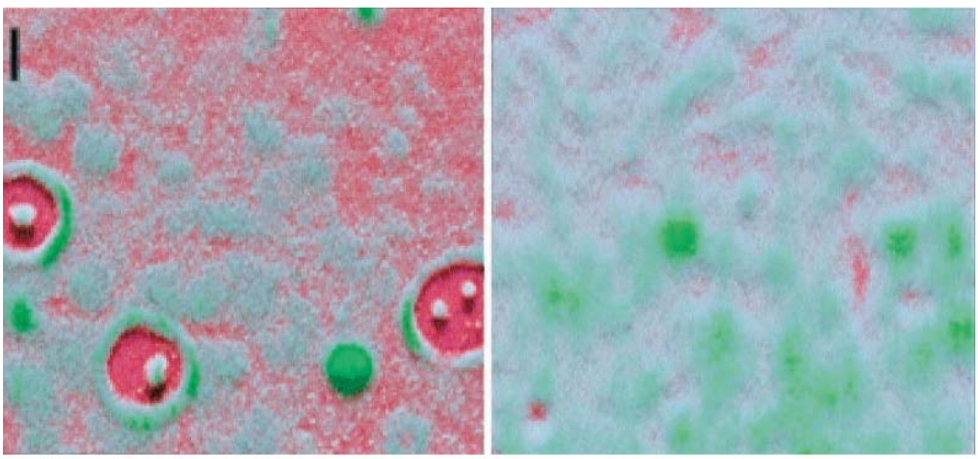

Figure II-18. Scanning confocal microscope images of a mature *P. aeruginosa* wild-type biofilm (Right) and a quorum-sensing mutant biofilm (Left). In this case the quorum-sensing mutant was a lasR, rhlR double mutant. The glass surface is red, and the green is from the green fluorescent protein encoded by the GFP gene in the recombinant *P. aeruginosa*. The wild-type biofilm consists of thick microcolonies. The immature mutant biofilm appears thinner, and more of the glass surface is exposed. With the lasR, rhlR mutant shown here (but not with lasI, rhlI mutants) zones of clearing around microcolony towers are often observed. The colors were applied to the image by computer enhancement with Adobe PHOTOSHOP 5.0. The black marker bar is 100 mm in length. (Parsek and Greenberg, 2000)

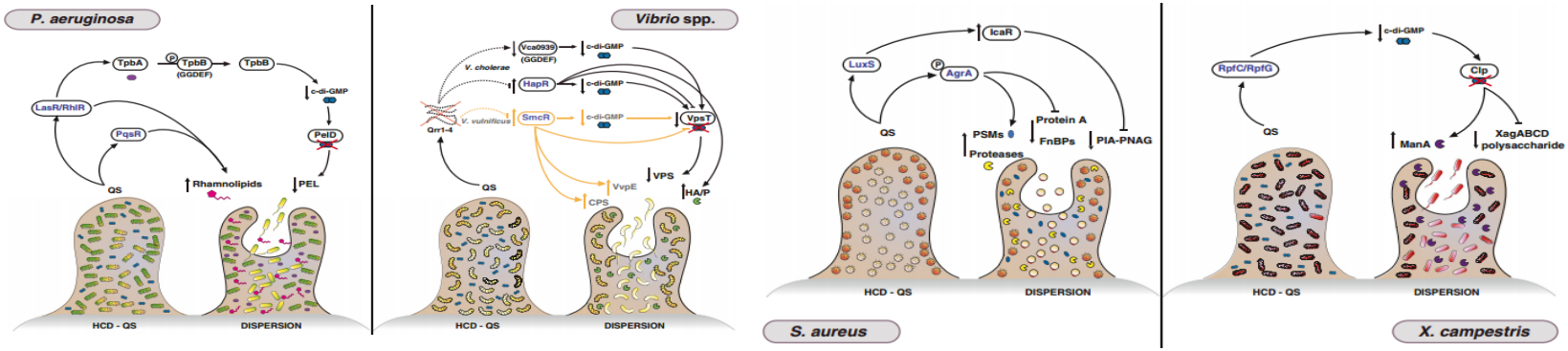

Figure II-19. Biofilm dispersion mechanisms activated at high cell density by QS in bacteria. Schematic representation of biofilm mushroom-like pillars indicating the mechanisms of biofilm dispersion activated by QS signal accumulation in each bacterial species. In P. aeruginosa, QS positively regulates the expression of the periplasmic tyrosine phosphatase TpbA. TpbA dephosphorylates the membrane-anchored GGDEF protein TpbB deactivating its DGC activity and thus reducing c-di-GMP levels in the cell. As a result, the c-di-GMP receptor PelD is no longer bound to c-di-GMP and PEL polysaccharide production is decreased. QS also promotes the synthesis of rhamnolipids whose overproduction results in biofilm detachment. In Vibrio spp., QS signal accumulation provokes a cessation in qrr1-4 small RNAs transcription. In V. cholerae, qrr1-4 cannot longer base pair with the vca0939 mRNA, which encodes a GGDEF domain protein, and thus its translation is inhibited and c-di-GMP levels decrease. On the other hand, the expression of the HCD master transcriptional regulators HapR and SmcR of V. cholerae and V. vulnificus increases. HapR and SmcR downregulate. (Solano et al., 2014)

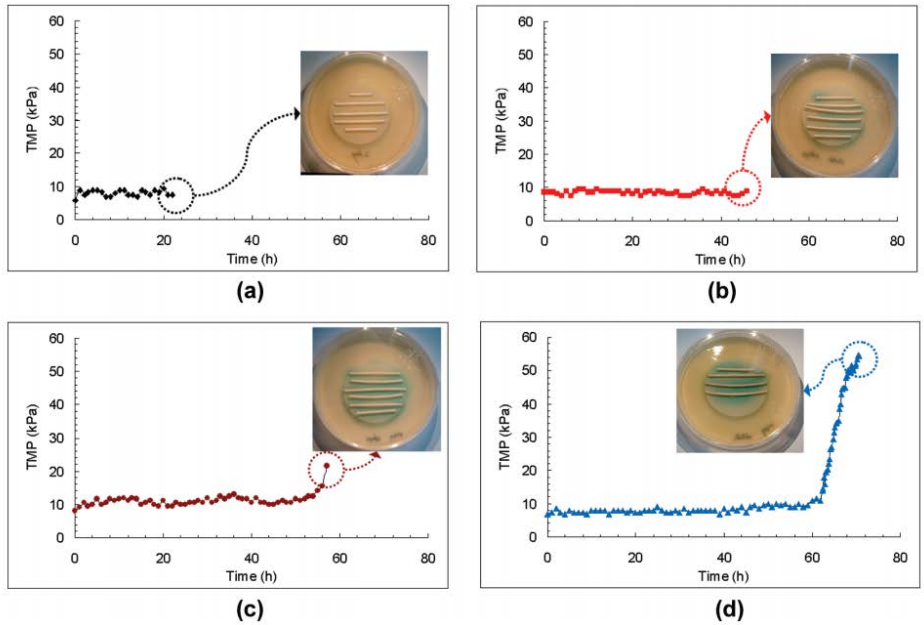

Figure II-19. Occurrence of AHL signals in biocake during continuous MBR operation: (a) 22 h, (b) 46 h, (c) 58 h, and (d) 72 h. (Yeon et al., 2009a)

II.2.4. Detection of AHL Signal Molecules

Before the detection of AHL molecules, extraction process should be required to obtain high concentration and puridity of AHL molecules. Liquid-liquid extraction (LLE) and solid-phase extraction (SPE) are commonly used to extracte AHLs. LLE is extracted with organic solvents (e.g., chloroform. ethyl acetate and hexane) and SPE used the silica or aluminum columns. After the extraction, sample can be concentrated by rotaty evaporation.

AHL detection methods can be dividied into two groups as follows:

(i) Biosensors for detection of AHLs

Bacterial sensor has been widely used to detect the presence of AHLs. Biosensors have detectable phenotypes such as light emission, expression of β-galactosidase activity or production of pigments upon the presence of exogenous AHLs (Figure II-21). The representative biosensors are *Agrobacterium tumefaciens* strains (Farrand et al., 2002) and *Chromobacterium violaceum* CV026 (McClean et al., 1997). When external AHLs were introduced, they produce indicating molecules, β-galactosidase (blue color indicating using X-gal) and pigment (purple color indicating), respectively. These techniques are convenient, fast and sensitive for detecting the presence of AHLs. However, it can be difficult to determine the concentration and structure of AHLs (Wang et al., 2011).

(ii) HPLC-MS for detection of AHLs

Although biosensor methods can detect the presence of HSLs *in situ*, they

cannot provide information for a wide or complete spectrum and of HSLs compounds (i.e., identification). Spectroscopic properties have been widely used to characterization of QS molecules structures. Most procedures have been carried out by using a combination of reversed-phase HPLC and MS for selective detection. The target molecules are usually separated in C18 silica columns by isocratic or gradient elution with water–methanol or water-ACN as mobile phases (Teplitski et al., 2003). In addition, although AHLs can be determined by GC-MS, quantification of AHLs by HPLC-MS is better than that of GC-MS due to the low volatility of AHL molecules (Wang et al., 2011).

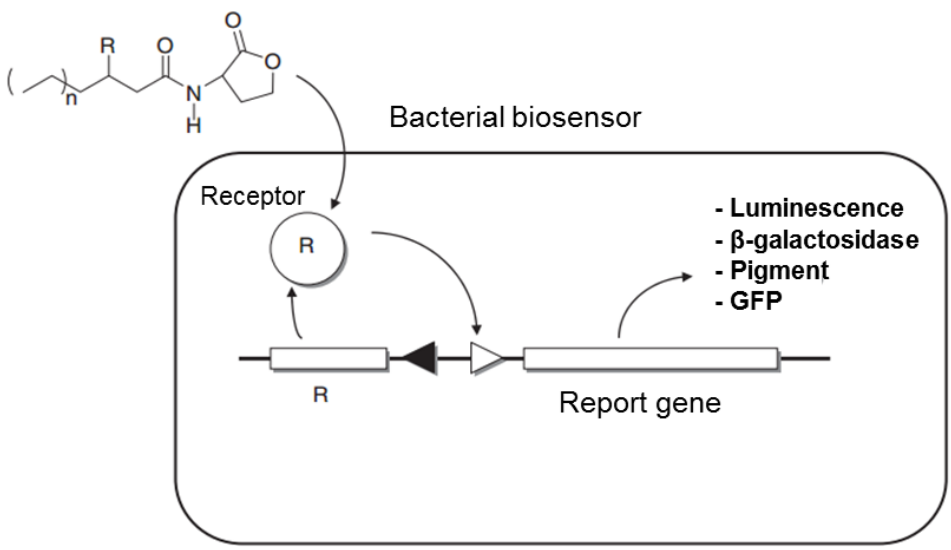

Figure II-20. Construction and use of a bacterial AHL biosensor. The exogenous AHL interacts with a LuxR family protein inside the bacterial biosensor (non-AHL producer), which results in the transcription of a reporter gene(s) from a LuxR family-AHL regulated promoter as shown by the open triangle. The LuxR family gene is usually expressed from a constitutive promoter as shown with a filled triangle. The properties of biosensor can be dependent on report gene (s) (Modified from (Steindler and Venturi, 2007)).

II.3. QS Control

II.3.1. QS Control Strategy

As mentioned in the previous section, biofilm formation is closely related to quorum sensing. Quorum sensing helps bacteria to coordinate group behavior, but it is not essential for growth or survival (Lade et al., 2014). Thus, interference with QS could lead to the inhibition of biofilm formation without negative effects for bacterial growth affecting the MBR performance. In other word, QS control can be a novel way to control the membrane biofouling without suppressing bacterial growth (Hentzer et al., 2002).

Three key factors in AHL QS are below;

[1] Signal molecule synthesis (LuxI homologue)

[2] Signal molecule receptor (LuxR homologue)

[3] Signal molecule

Therefore, AHL QS inhibition strategy can be divided into three ways (Figure II-22),

[1] Inhibition of AHL synthesis

[2] Interference with signal receptors

[3] Degradation of AHL signal molecules

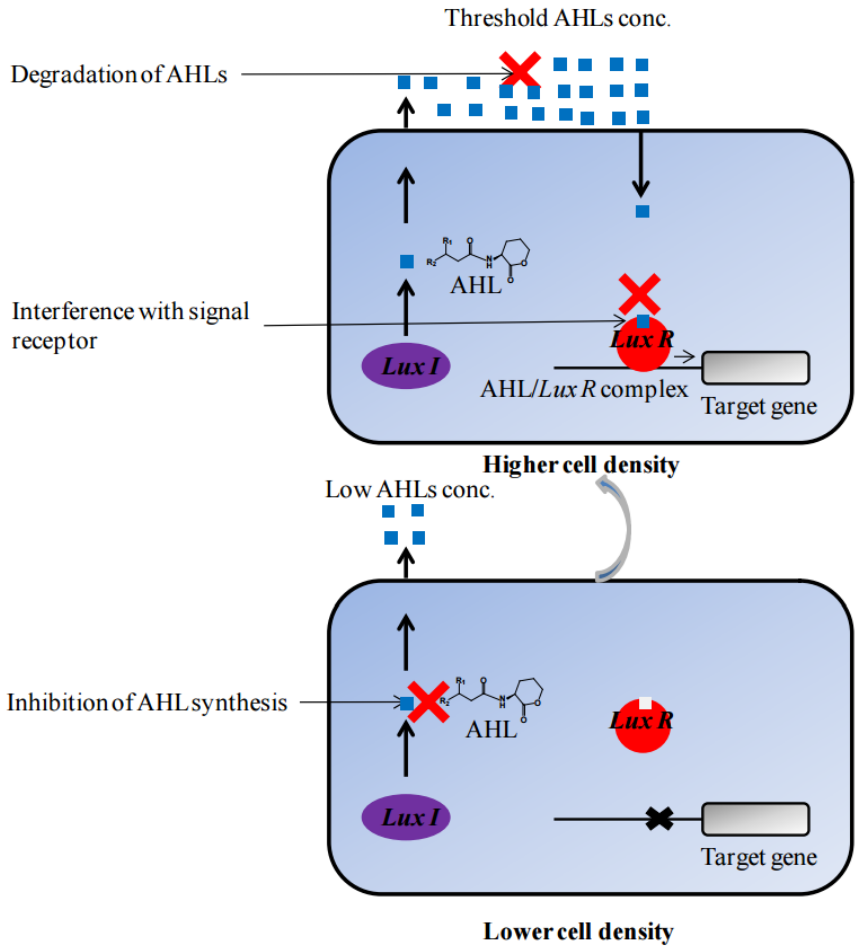

Figure II-21. Inhibition of quorum sensing in Gram-negative bacteria by various mechanism. Three quorum quenching strategies have been used for attenuating AHL-mediated phenotypes; (i) Inhibition of AHL synthesis (ii) Degradation of AHL signal molecules (ii) Interference with signal molecules. (Lade et al., 2014)

II.3.1.1. Inhibition of AHL Synthesis

Inhibition of the LuxI-like protein (AHL synthesis protein) appears to be a simple approach to hamper QS, because it is clearly impossible without signal molecules.

AHL signal molecules are synthesized from the acyl-acyl carrier protein (acly-ACP) and S-adenosylmethionine (SAM) by LuxI-type synthases (Figure II-23a). This catalytic reaction is proceeded by the two-step mechanism, 1) synthesis of intermediate acyl-SAM through transferring an acyl group from acyl-ACP to the amino group of SAM and 2) synthesis of AHL by lactonization of the methionine part, concomitant with the release of methylthioadenosine (MTA) (Parsek et al., 1999; Raychaudhuri et al., 2005). AHLs can have different length and substitution according to their respective acyl side chains, which confer them with signal specificity (Galloway et al., 2011).

Kai et al. (2014) reported that AHL analog substances inhibit the AHL synthesis (Figure II-23b). However, surprisingly, few studies have been reported concerning the target for specific synthase protein (Parsek et al., 1999; Parveen and Cornell, 2011).

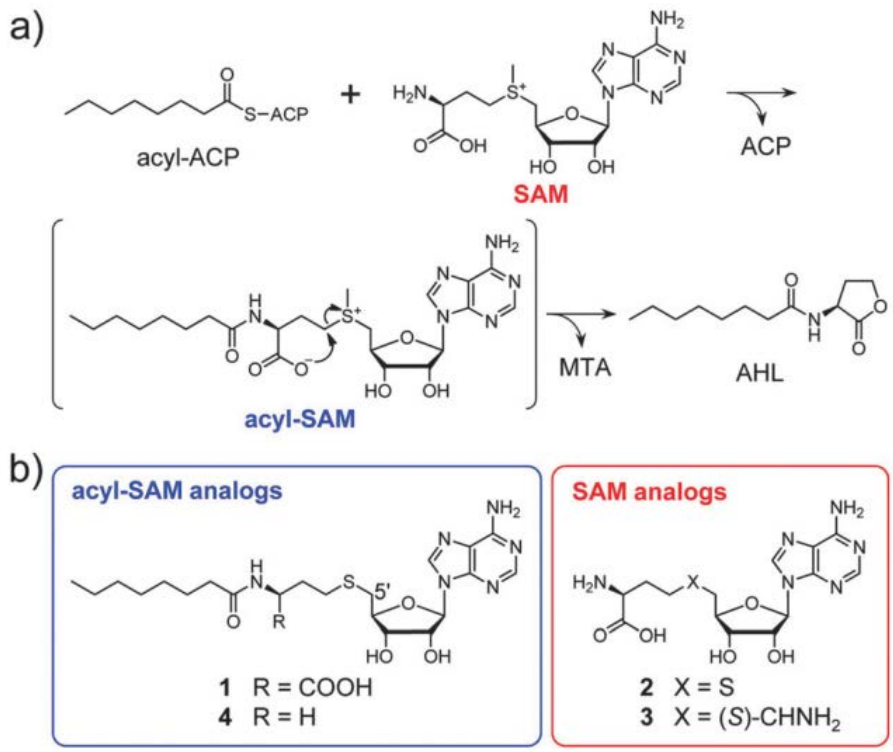

Figure II-22. (a) Mechanism of AHL production by Lux-type AHL syntheses. (b) Structure of acyl-SAM analogs and SAM analogs. (Kai et al., 2014)

II.3.1.2. Interference with Signal Receptors

The purpose of this strategy is the inhibition or blockage of biding between signal molecules and receptor proteins (Figure II-23) using antagonist, structurally similar to signal molecules. The major advantage of this strategy is to control unwanted microbial activity without side effects because the antagonist specifically interferes with expression of specific traits. Many studies have been carried out to identify synthetic analogues of AHLs that function as AHL antagonists (Chen et al., 2011; Koch et al., 2005; Olsen et al., 2002; Smith et al., 2003). In nature, algae and higher plants have been found to produce substances that inhibit AHL-regulated signalling (Bauer and Robinson, 2002; Givskov et al., 1996). In addition, it has been reported that several halogenated furanones interfering AHL based QS by specific interaction with LuxR (Manefield et al., 1999; Manefield et al., 2002).

II.3.1.3. Degradation of AHL Signal Molecules

Degradation or inactivation of AHL molecules can be achieved by quorum quenching enzymes. Although it is presumable that four potential cleavage sites in the AHL molecules (Figure II-24a), QQ enzymes degrading AHLs can be divided into only two group: one that leads to the degradation of homoserine lactone ring and another that leads to cleavage of acyl chain from AHLs (Figure II-24b). Lactonase can open the lactone ring (Dong et al., 2000; Dong et al., 2001), acylase can cleave the acyl side chain from AHL (Leadbetter and Greenberg, 2000; Lin et al., 2003). In addition, oxidoreductase can catalyze the oxidation or reduction of acyl side chain (Chowdhary et al., 2007; Uroz et al., 2005). Meanwhile, an opened ring of AHL molecule by lactonase spontaneously undergoes ring formation at the acidic pH (Camara et al., 2002).

Although various QQ enzymes have been found, the physiological function of QQ enzymes and whether AHLs are their primary substrates have not been entirely clarified. Some characterized QQ enzymes are shown with their origin and substrate specificity in Table II-4 (Chen et al., 2013; Fetzner, 2015).

Meanwhile, QQ enzymes would be affected by metal ions or chemical reagents. Chen et al. (2010) reported that Na^{+}, K^{+}, Ca^{2+}, Fe^{3+}, and Mn^{2+} exhibited positive effect while Cu^{2+}, Cr^{3+}, SDS, Hg^{2+} and Ag^{+} significantly or completely inhibited the activity of AHL-lactonase produced from recombinant $AiiA_{B546}$. In addition, AHL-lactonase was enhanced by Mg^{2+}, Zn^{2+}, EDTA at 10 mM but reduced at 1 mM. Li^{+}, Pb^{2+} and β-mercaptoethanol improved the enzyme activity at 1 mM but reduced at 10 mM. Moreover, Wang et al. (2004) reported that Mg^{2+}, Ca^{2+}, Mn^{2+}, Co^{2+}, Ni^{2+}, Zn^{2+}, and Cd^{2+} showed no effect on activity of AHL-lactonase, which was

produced from *E. coli* encoding aiiA gene, at 0.2 and 2 mM. On the other hand, AHL-lactonase was partially inhibited by Cr^{2+}, Pb^{2+}, and Fe^{2+} at 2 mM and completely inhibited by Cu^{2+} and Ag^{2+} at 0.2 mM.

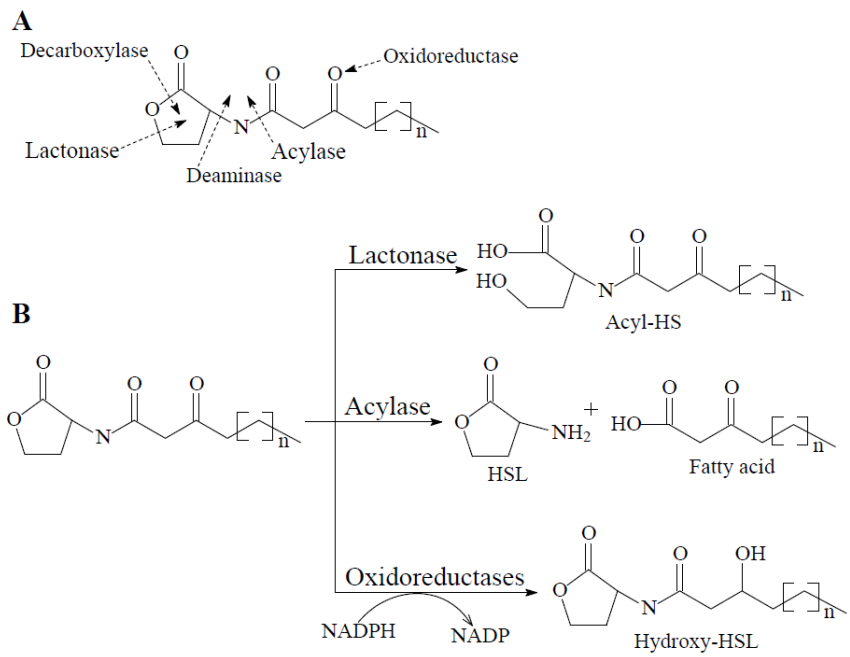

Figure II-23. Possible linkage degraded by quorum quenching enzymes in quorum sensing molecule *N*-acyl homoserine lactone (A) and corresponding degradation mechanism of quorum quenching enzymes (B). (Dong and Zhang, 2005)

Table II-4. QQ enzymes involved in the degradation of the QS signal AHLs.

Enzyme	Host	Substrate
AHL-lactonase		
AiiA	*Bacillus* sp. 240B1	C6-10-HSL
	Bacillus cereus A24	AHL
	Bacillus mycoides	AHL
	Bacillus thuringiensis	AHL
	Bacillus anthrais	C6, C8, C10-HSL
AttM	*Agrobacterium tumefaciens*	C6-HSL; 3OC8-HSL
AiiB	*Agrobacterium tumefaciens* C58	Broad
AiiS	*Agrobacterium tumefaciens* K84	Broad
AhlD	*Arthrobacter* sp. *IBN110*	Broad
AhlK	*Klebsiella pneumoniae*	C6-8-HSL
QlcA	*Acidobacteria*	C6-8-HSL
AiiM	*Microbacterium testaceum* StLB037	C6-10-HSL
QsdA	*Rhodococcus erythropolis* W2	C6-14-HSL
AhlS	*Solibacillus silvestris* StLB046	C6, C10-HSL
QsdH	*Pseudoalteromonas byunsanensis* 1A01261	C8, C14-HSL; 3OC6-HSL
AidH	*Ochrobactrum* sp. T63	C4, C6, C8, C10-HSL; 3OC6, C8, C10, C12-HSL
PON2	All mammalian tissues	C7, C12, C14-HSL; 3OC6-10,12-HSL
MCP	*M. avium* spp. *Paratuberculosis* K-10	C6, C7, C8, C10, C12-HSL; 3OC8-HSL
BpiB07	Soil metagenome	3OC8-HSL
DlhR	*Rhizobium* sp. NGR234	3OC8-HSL

Table II-4. *(Continued)*

Enzyme	**Host**	**Substrate**
AHL-acylase		
Acylase I	Porcine (Kidney)	C4, C6, C8-HSL; 3OC10, C12-HSL
AibP	*Brucella melitensis 16M*	C12-HSL; COC12-HSL
AhlM	*Streptomyces* sp. M664	C6, C8, C10-HSL; 3OC6, C8, C12- HSL
AiiD	*Ralstonia* sp. Xj12B	3OC6, C8, C10, C12-HSL
PvdQ	*P. Aeruginosa* PAO1	C7, C8, C10, C11, C12, C14-
HacA	*P. Syringae* B728a	HSL; 3OC10, C12, C14-HSL; 3OH-C14-HSL
HacB	*P. Syringae* B728a	C8, C10, C12-HSL; 3OC8-HSL
		C4, C6, C8, C10, C12-HSL; 3OC6, C8-HSL
AiiC	*Anabaena* sp. PCC7120	C4, C6, C8, C10, C12, C14-HSL; 3OC4, C6, C8, C10, C12, C14-HSL
AiiO	*Ochrobactrum* sp. A44	C4, C6, C8, C10, C12, C14-HSL; 3OC3, C6, C8, C10, C12, C14-HSL
QsdB	Soil metagenome	C6-HSL; 3OC8-HSL
Aac	*Ralstonia solanacearum* GMl1000	C7, C8, C10-HSL; 3OC8-HSL

Table II-4. *(Continued)*

Enzyme	**Host**	**Substrate**
Oxidoreductase		
CYP1041	*Bacillus megaterium*	C12-C16-HSL; 3OC12-HSL
P450BM3	*Bacillus megaterium*	C12, C14, C16 ,C20-HSL; 3OC12, C14-HSL
Not identified	*Rhodococcus erythropolis* W2	3OC8, C10, C12, C14-HSL
Not identified	*Burkholderia* sp. GG4	3OC4, C6, C8-HSL
BpiB09	Soil metagenome	3OC12-HSL

II.3.2. Application of QQ to Control Biofouling in Membrane Process

II.3.2.1. Enzymatic QQ

Yeon et al. (2009a) reported that biofouling inhibition was achieved by adding acylase into continuous lab-scale MBR. However, free enzymes can be easily lost their activities because of low stability for environmental factors such as high or low temperature and high shear stress. Therefore, many researchers applied the QQ enzymes with diverse immobilization into MBR system.

[1] Magnetic Enzyme Carrier (MEC)

Yeon et al. (2009b) developed magnetic enzyme carrier (MEC) to overcome the limitation of free enzyme application. As shown in Figure II- 25, a magnetic ion-exchange resin (MIEX), which has a net positive surface charge, was adopted as a magnetic core. And then anionic polyelectrolyte (polystyrene sulfonate, PSS) and a cationic polyelectrolyte (chitosan) were deposition by layer-by-layer (LBL). Finally, porcine kidney acylase I (EC-Number 3.5.1.14) was immobilized on MIEX-PSS-chitosan using glutaldehyde (GA) as a cross-linking agent. This MEC showed the better performance than free enzyme in terms of biofouling control and biological stability in MBR. MEC has an additional advantage for recovery due to easy separation using magnet. Another magnetic carrier based on mesoporous silica was also developed (Lee et al., 2014). In addition, Kim et al. (2013a) reported that QQ can affect the bacterial community and reduce the EPS production in biofilm.

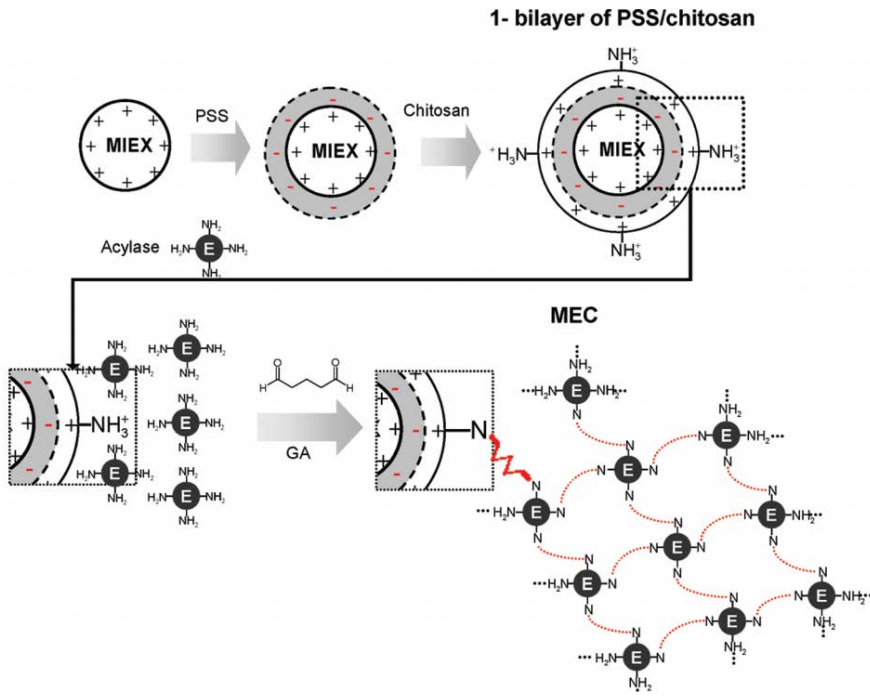

Figure II-24. Schematic diagram showing the preparation of the MEC through layer-by-layer (LBL) deposition of PSS-chitosan on MIEX resin and enzyme immobilization via glutaraldehyde treatment. (Yeon et al., 2009b)

[2] QQ Enzyme Immobilization on Membrane Surface

Kim et al. (2011) immobilized acylase onto nanofiltration (NF) membrane surface. Aggregations of chitosan and acylase can be achieved through controlling pH and then to be deposited onto membrane surface using N_2 gas. Lastly, deposited aggregates were cross-linked with glutaaldehyde (GA) (Figure II-26). The acylase-NF membrane immobilized membrane showed the higher permeability than raw NF membrane. Furthermore, they also found the dramatic decrease in cell and EPS on acylase-NF membrane surface (Figure II-27).

[3] QQ Enzyme Immobilization on Alginate Bead

Porcine Kindey acylase I was encapsulated in hydrogel matrix. The mixture of acylase and sodium alginate was dropped into calcium chloride solution to solidify and form spherical alginate beads using ion exchange reaction. Finally, this beads reacted with glutaldehyde (GA) to enhance the mechanical strength and stability (Jiang et al., 2013). They reported that acylase encapsulating beads mitigated the biofouling in MBR and reduced the EPS in both broth and biocake.

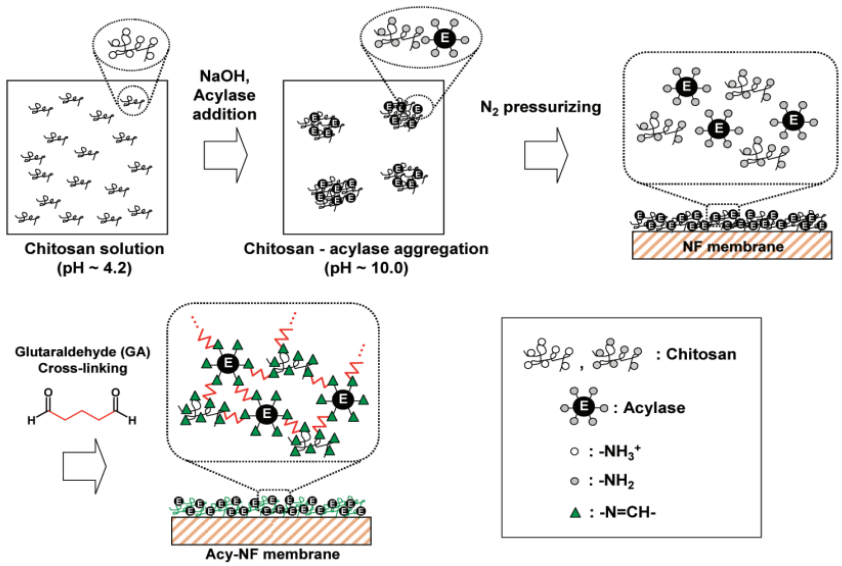

Figure II-25. Schematic diagram of acylase immobilization onto the nanofiltration membrane surface by forming a chitosan-acylase matrix. (Kim et al., 2011)

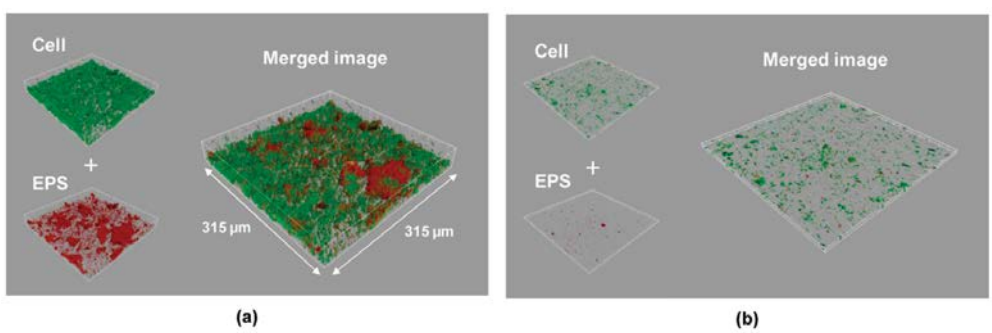

Figure II-26. Reconstructed CLSM images of biofilm formed on the (a) raw and (b) Acy-NF membranes after a 38-hour operation of the continuous NF of P. aeruginosa and then stained with SYTO 9 and ConA. Magnification 400×. Image size 315 μm × 315 μm. (Kim et al., 2011)

II.3.2.2. Bacterial QQ

II.3.2.2.1. Isolation of QQ bacteria

Although diverse application methods for QQ enzyme were developed, underlying the limitation of enzyme still remains due to its high cost and low stability. Recently, for effective QQ application, many researchers have tried to find quorum quenching bacteria which produces QQ enzyme degrading signal molecules. They usually isolated the QQ bacteria using by enrichment culture. In detail, for example, sludge samples from nature or real wastewater treatment plants were cultivated in minimal medium containing AHLs (e.g., C4-HSL, C6-HSL or oxo-C6-HSL and so on) as the sole carbon source (Christiaen et al., 2011). After three cycles of enrichment culture, the cell suspension was spread on LB agar plate, and different types of colony were isolated. Lastly, after AHL-degrading activity of each colony was analyzed and bacterium can be identified by DNA sequencing (Kim et al., 2014).

Rhodococcus sp. BH4 and *Bacillus methylotrophicus* sp. WY producing lactonase degrading a wide variety of AHL molecules were isolated (Khan et al., 2016; Oh et al., 2012). In addition, Cheong et al. (2013) isolated *Pseudomonas* sp. 1A1 which produces three types of acylase enzyme. They also found that lactonase and acylase produced from their QQ bacteria are intracellular and extracellular enzymes, respectively, using LC-MS or bioassay.

II.3.2.2.2. Application of Bacterial QQ

Although QQ bacteria are more stable than enzymes, immobilization of QQ bacteria is also required to protect them from the attack of other microorganisms co-habiting in the mixed liquor and wash out from excess sludge discharge.

[1] Microbial-vessel

Oh et al. (2012) isolated a QQ bacterium, *Rhodococcus* sp. BH4 from a real MBR plant. This QQ bacteria produce lactonase enzyme decomposing a wide range of AHL signal molecules. They developed the microbial-vessel which is porous membrane containing QQ bacteria (Figure II-28). BH4 strain was encapsulated inside the lumen of polymeric microporous hollow fiber membrane to protect them from the attack of other microorganism in mixed liquor in MBR. QQ bacteria cannot escape from microbial-vessel because the nominal pore size is 0.4 μm, smaller than size of BH4 bacterium. However, signal molecules and nutrients can freely diffuse through the porous membrane, and thus BH4 producing intracellular lactonase inside membranes can degrade signal molecules diffused in to the vessel, and intake nutrients for survive and growth of entrapped bacteria. They input and fixed microbial-vessel in submerged MBR. They reported that the microbial-vessel inhibited the biofouling in MBR and its QQ activity was maintained for 80 days. In addition, Oh et al. (2013) reported that QQ activity of microbial-vessel could be affected by materials of membranes, inner volumes of microbial-vessels and encapsulated mass of BH4. Furthermore, Jahangir et al. (2012) reported that the performance of the microbial-vessel could be enhanced by the location close to filtration membrane, and higher recirculation rate between bioreactor and membrane

tank in external submerged MBR system. There results indicates that mass transfer of microbial-vessel would be one of the important factors because location of microbial-vessel and recirculation rate could be directly related the mass transfer between signal molecules and the microbial-vessel. Furthermore, Weerasekara et al. (2014) reported that the microbial-vessel could save the energy consumption in MBR fed with synthetic wastewater by reducing the aeration intensity.

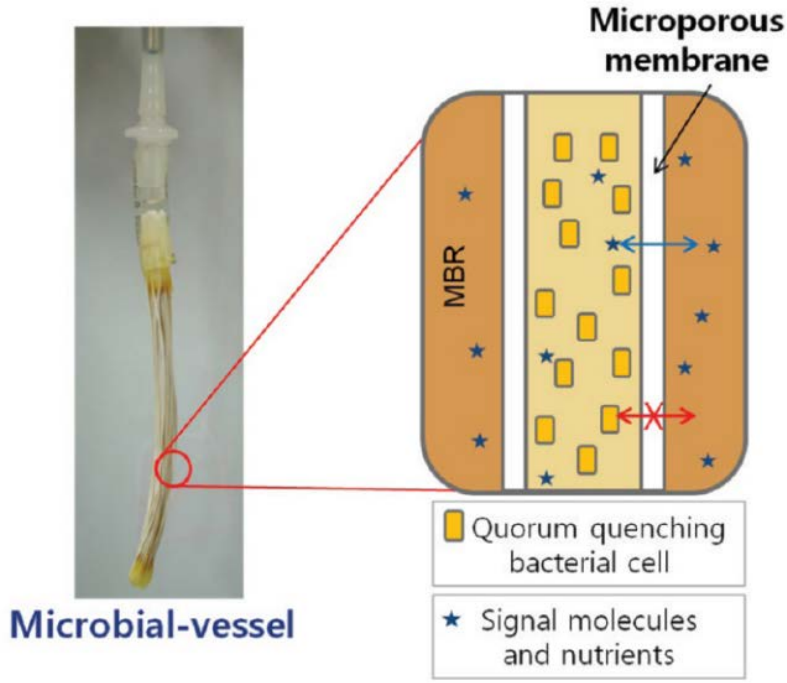

Figure II-27. Photograph and enlarged diagram of a microbial-vessel. (Oh et al., 2012)

[2] Ceramic-vessel

Cheong et al. (2014) designed the ceramic microbial-vessel (CMV) to improve activity of encapsulated QQ bacteria inside membranes using intrinsic structure of CMV. Since the much higher density of QQ bacteria was encapsulated, the F/M ratio inside the CMV could be quite low. However, the performance of CMV was improved by using inner flow feeding mode which supplies the fresh feed into lumen directly for QQ bacteria inside the CMV (Figure II-29). As shown in Figure II-30, inner flow feeding mode enhanced the viability of QQ bacteria inside the CMV. Theses result means that the high mass transfer is essential for QQ bacteria's growth and biological stability. Köse-Mutlu et al. (2015) developed the rotating microbial-vessel (called rotating microbial carrier frame, RMCF) to effectively increase its mass transfer.

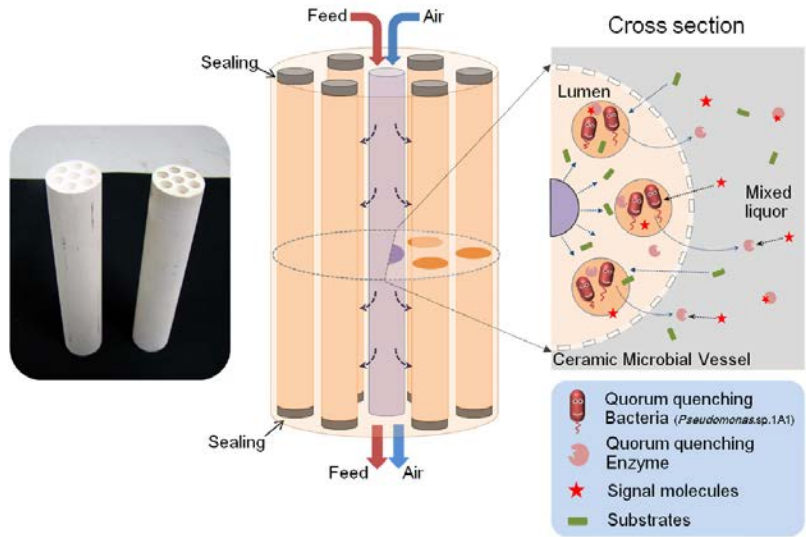

Figure II-28. Schematic diagram of the ceramic microbial-vessel under the inner flow feeding mode. (Cheong et al., 2014)

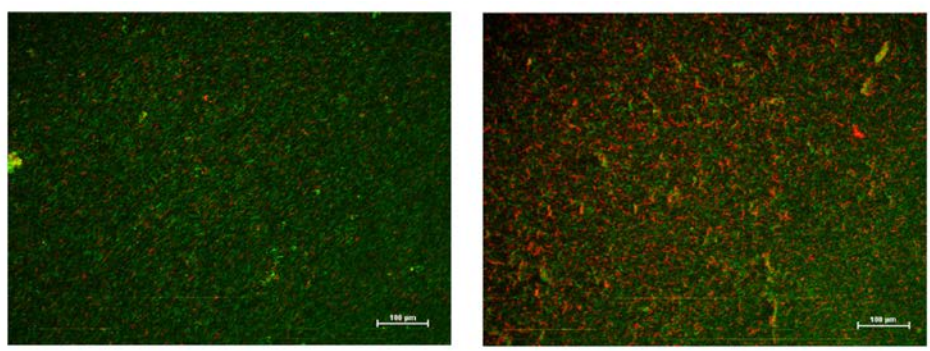

Figure II-29. Images of live/dead quorum quenching bacteria from the lumens of the used CMVs. (A) MBR-B with the CMV under the inner flow feeding mode, (B) MBR-C with the CMV under the normal feeding mode. Green color: live cell; red color: dead cell. (Cheong et al., 2014)

[3] Alginate bead

Kim et al. (2013b) developed the QQ-bead, which entrap the QQ bacteria in alginate matrix, as a first moving QQ-media. This spherical bead had porous microstructure and enough inner space, and then QQ bacteria were entrapped in both inner space and outer surface (Figure II-31). Alginate polymer is hydrogel which is well known as a high biocompatible material. In addition, Alginate bead can move freely through fluid flow in MBR because wet density of the beads is similar to that of water. Therefore, this bead can collide the membrane surface, and thus the biofilm on membrane surface can be detached by collision with beads. As a result, as shown in Figure II-32, alginate bead entrapping QQ bacteria, called QQ-bead, significantly mitigated biofouling in MBR due to its combined effect of biological QQ activity and physical washing (detachment of biofilm). Maqbool et al. (2015) reported that TMP rise-up of MBR with applied QQ-beads was quietly delayed compared to that of control MBR (without bead). They also found that concentration of AHL molecules and EPS reduced in MBR with QQ-bead compared to those of control MBR.

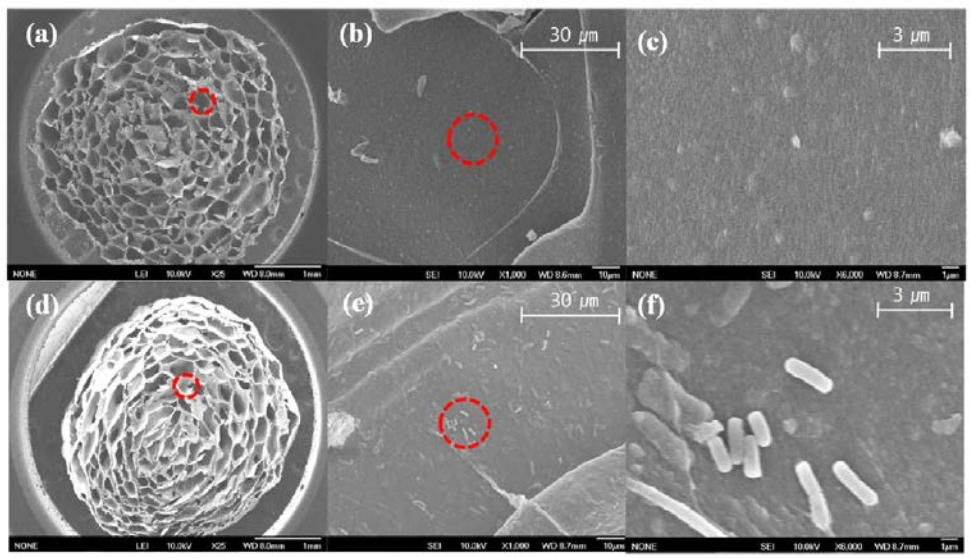

Figure II-30. SEM microphotographs of the beads: cross section of a vacant bead (a) ×25, (b) ×1000, and (c) ×6000. Cross section of a CEB (d) ×25, (e) ×1000, and (f) ×6000. (Kim et al., 2013b)

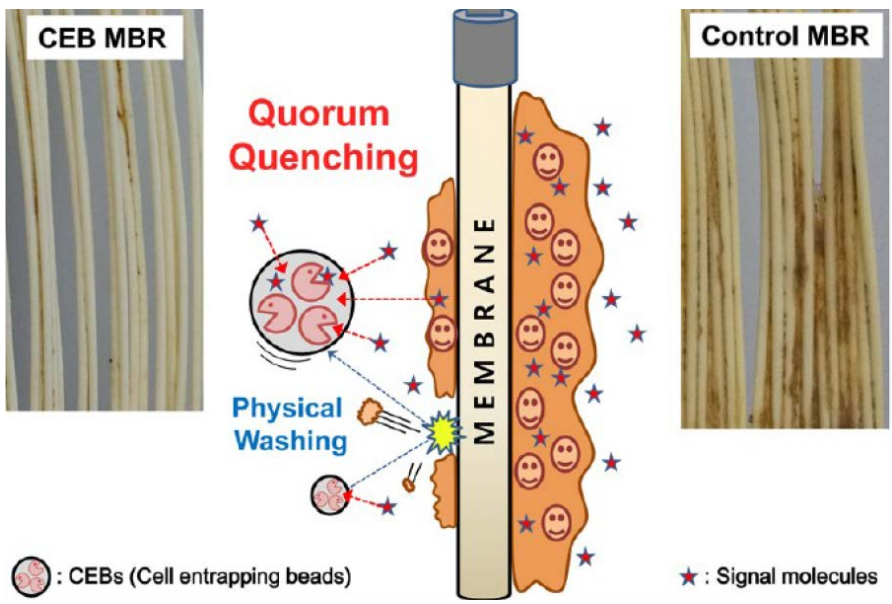

Figure II-31. Concept of QQ-bead's combined effect of both QQ and physical washing (Kim et al., 2013b).

[4] Macrocapsule

Although the alginate QQ-bead successfully mitigated biofouling in MBR fed with synthetic wastewater, the bead have not been applied into MBR fed with real wastewater. It was because alginate bead was easily decomposed in real wastewater which is usually consisted of a wide variety of component including surfactants or salts. Thus, Kim et al. (2015) reinforced alginate bead by coating synthetic polymer (called microcapsule). They used the phase inversion method (Figure II-33) to coat the alginate bead with various synthetic polymers (Figure II-34). They reported that mechanical strength of bead increased by coating. Furthermore, although QQ bacteria entrapped bead was damaged by organic solvent during preparation of macrocapsule, QQ activity and cell viability were recovered by restoration culturing in intensive nutrient medium such as LB broth. As a result, macrocapsule inhibited the membrane biofouling in lab-scale MBR fed with real wastewater.

Meanwhile, Yu et al. (2016) reported the effect of SRT on membrane fouling in MBR. They operated three MBRs with different SRT, and then analyzed bacterial communities at genus level in each MBR. They reported that as SRT increased, the abundance of QQ bacteria in mixed liquor increased, the excretion of SMP and EPS decreased, and thus membrane biofouling was alleviated. This result supports that maintaining higher concentration of QQ bacteria by any means is important to enhance QQ effect.

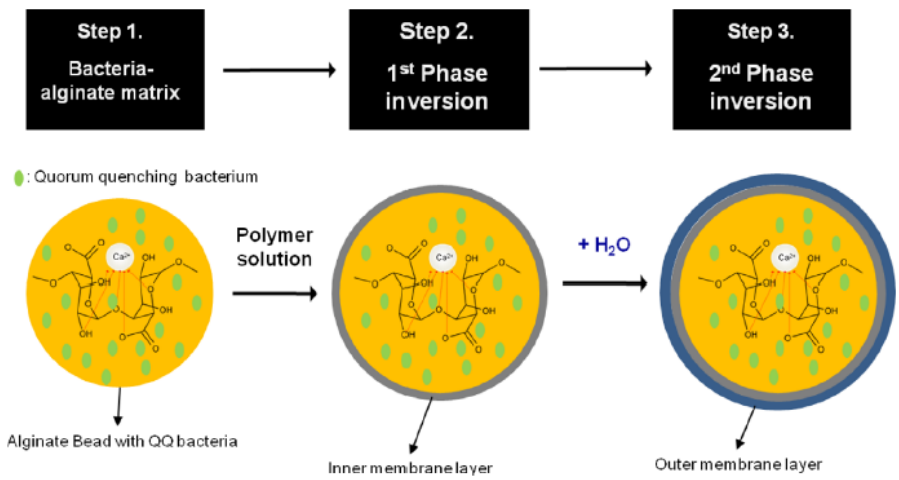

Figure II-32. Preparation scheme of a macrocapsule coated with a membrane layer through the phase inversion method. (Kim et al., 2015)

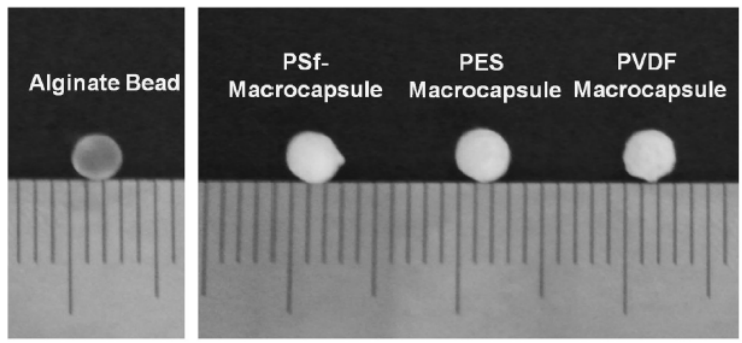

b

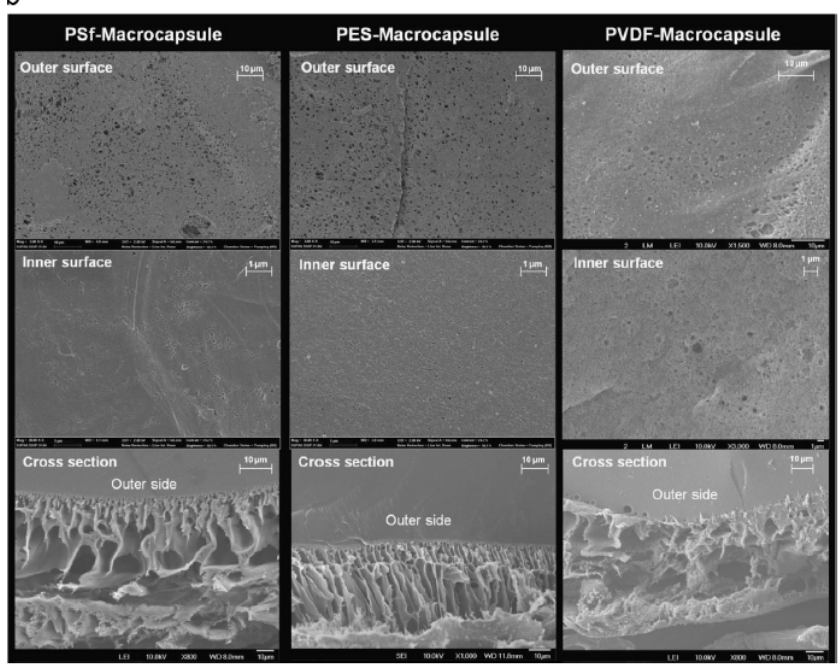

Figure II-33. (a) Photographs of an alginate bead and PSf, PES, PVDF coated macrocapsules. (b) SEM images of the outer surface, inner surface and cross-section of each macrocapsule coated with PSf, PES, and PVDF, respectively. (Kim et al., 2015)

II.4. Media for Cell Immobilization

II.4.1. Immobilization Methods

Different immobilization methods have been defined: covalent coupling/cross linking, capture behind semi-permeable membrane or encapsulation, entrapment and flocculation/adsorption (Figure II-35).

[1] Covalent bonding / cross linking

This method is based on covalent bond formation between support and cell in the presence of a crosslinking agent. Covalent bonding and crosslinking are effective and durable to enzymes while it is rarely applied for cell immobilization. It is because that cell can be damaged by toxicity of crosslinking agents (Ramakrishna and Prakasham, 1999) thus, there are few papers about covalent binding. Navarro and Durand (1977) reported a successful way of covalent binding of *Saccharomyces carlsbergensis* on porous silica beads.

[2] Entrapment

Entrapment is an irreversible method, where immobilized cells are entrapped in a support matrix. This method is extensively used for cell immobilization. The polymer matrix entrapping microorganisms has porous structure, and thus the pollutant and various metabolic products could easily diffuse through into the matrix. One of the properties of entrapment is that various porous polymers can successfully entrap microorganisms under mild conditions (Verma et al., 2006). Cell entrapment using the alginate gel is popular because of its mild preparation conditions and the

simplicity of the procedure (Kierstan and Bucke, 1977).

Although entrapment can allow high mechanical strength, there can be some disadvantages, such as, cell leakage, costs of immobilization, diffusion limitations, deactivation and abrasion of support material during usage. Furthermore, it can be low loading capacity as biocatalysts have to be incorporated into the support matrix (Gao et al., 2010; Krekeler et al., 1991; Song et al., 2005; Stolarzewicz et al., 2011).

[3] Encapsulation

Encapsulation is another irreversible immobilization method, similar to entrapment. In this process, cell are confined by the membrane walls (usually in a form of a capsule), but free-floating within the core or inner space (Górecka and Jastrzębska, 2011). The membrane itself is semi-permeable, allowing for free flow of substrates and nutrients but, keeping the cell inside. The factor determining this phenomenon is the proper pore size of the membrane, attuned to the size of core material. This structure of microencapsulation have several advantages, such as protection of immobilized cell from the harsh environmental conditions, prevention of biocatalyst leakage and increase in the process efficiency as a result (Park and Chang, 2000).

However, in encapsulation, even though high cell loading can be achieved, but the capsules can be still very weak (Song et al., 2005). In addition, The diffusion limitation is one of the inevitable drawbacks of encapsulation method (López et al., 1997).

[4] Adsorption

This technique is based on the physical interaction between the microorganism and the surface of supporting material. The properties of adsorption method are frequently reversible, cheap and effective. Contrary to cell entrapment and encapsulation having the mass transfer problem, an adsorption method provides a direct contact between nutrients (or substrates) and the immobilized cells (Braschler et al., 2005). This technique involves the transport of the cells from the bulk phase to the surface of support (porous and inert support materials), followed by the adhesion of cells, and subsequent colonization on surface of support (Kilonzo and Bergougnou, 2012). In contrast to ceramics, wood chips and straw, fibrous matrices provide good supporting surfaces for cell adsorption (Chu et al., 2009; Talabardon et al., 2000) due to their high specific surface area, void volume, mechanical and permeability, low pressure drop, diffusion problems and toxicity, maximum loading, biodegradability and durability and low cost and high availability (Huang and Yang, 1998).

In general, few points need to be considered before choosing the materials for the whole cell immobilization as follows:

1) Stable, robust and inert

2) Biocompatible against immobilized cell

3) Permeability for substrate and nutrients

4) Mass transfer (high specific surface area)

5) Available to simple, quick, inexpensive and eco-friendly process

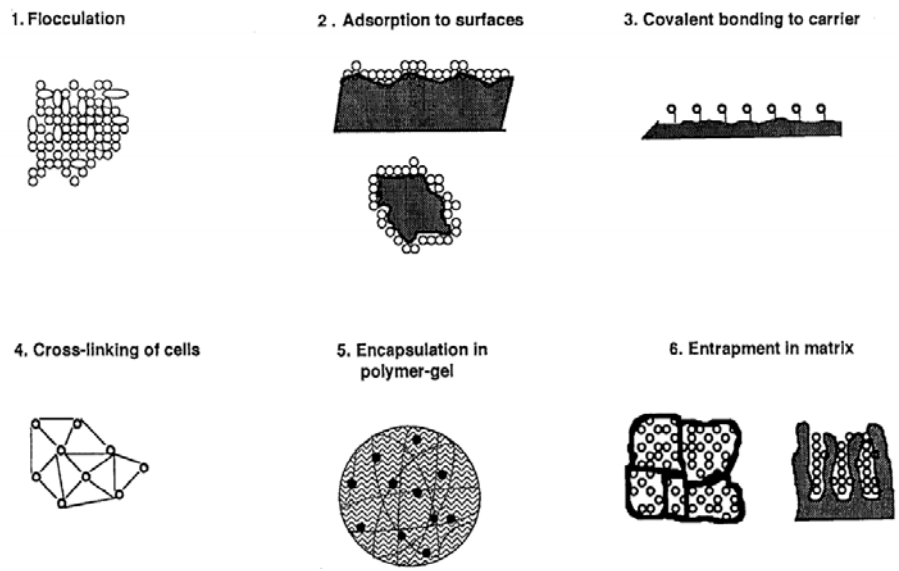

Figure II-34. Methods for immobilization of viable microbial cells. (Cassidy et al., 1996)

II.4.2. Hydrogel

Hydrogel polymers absorb water and swell readily without dissolving (i.e., insoluble polymer). Hydrogels are being used for cell immobilization in medicine and biotechnology (Cima et al., 1994). They can contain the cell chemically or physically to provide stability, structural support, or immunoisolation. For successful immobilization, the hydrogel must be biocompatible, high permeability and mass transfer. Sufficient supply of oxygen and essential nutrients and substrate through the hydrogel network, plus adequate removal of metabolic waste and phenotypic secretions are essential for sustaining the immobilized cells in the hydrogel complexes (Jen et al., 1996).

There are many kinds of hydrogel polymers (Table II-5). Especially, PVA is one of the most popular and the oldest synthetic hydrogel polymer due to its good biocompatibility (Kamoun et al., 2015). In addition, PVA hydrogel can be enhanced its properties such as, elasticity, mechanical strength, etc., by compositing other hydrogel polymers (Figure II-36).

Table II-5. Method for synthesizing physical and chemical hydrogels.

(Hoffman, 2012)

Physical gels
- Warm a polymer solution to form a gel (e.g., PEO-PPO-PEO block copolymers in H_2O)
- Cool a polymer solution to form a gel (e.g., agarose or gelatin in H_2O)
- 'Crosslink' a polymer in aqueous solution, using freeze–thaw cycles to form polymer microcrystals (e.g., freeze–thaw PVA in aqueous solution)
- Lower pH to form an H-bonded gel between two different polymers in the same aqueous solution (e.g., PEO and PAAc)
- Mix solutions of a polyanion and a polycation to form a complex coacervate gel (e.g., sodium alginate plus polylysine)
- Gel a polyelectrolyte solution with a multivalent ion of opposite charge (e.g., Na + alginate$^-$ + Ca^{2+} + 2Cl^-)
Chemical gels
- Crosslink polymers in the solid state or in solution with:
- Radiation (e.g., irradiate PEO in H_2O)
- Chemical crosslinkers (e.g., collagen with glutaraldehyde or a bis-epoxide)
- Multi-functional reactive compounds (e.g., PEG+diisocyanate = PU hydrogel)
- Copolymerize a monomer + crosslinker in solution (e.g., HEMA+EGDMA)
- Copolymerize a monomer + a multifunctional macromer (e.g., bis-methacrylate terminated PLA-PEO-PLA + photosensitizer + visible light radiation)
- Polymerize a monomer within a different solid polymer to form an IPN gel (e.g., AN + starch)
- Chemically convert a hydrophobic polymer to a hydrogel (e.g., partially hydrolyse PVAc to PVA or PAN to PAN/PAAm/PAAc)

Abbreviations: EGDMA, ethylene glycol dimethacrylate; HEMA, hydroxyethyl methacrylate; IPN, inter-penetrating network; PAAc, poly(acrylic acid); PAAm, polyacrylamide; PAN, polyacrylonitrile; PEG, poly(ethylene glycol); PEO, poly(ethylene oxide); PLA, poly(lactic acid); PVA, poly(vinyl alcohol); PVAc, poly(vinyl acetate).

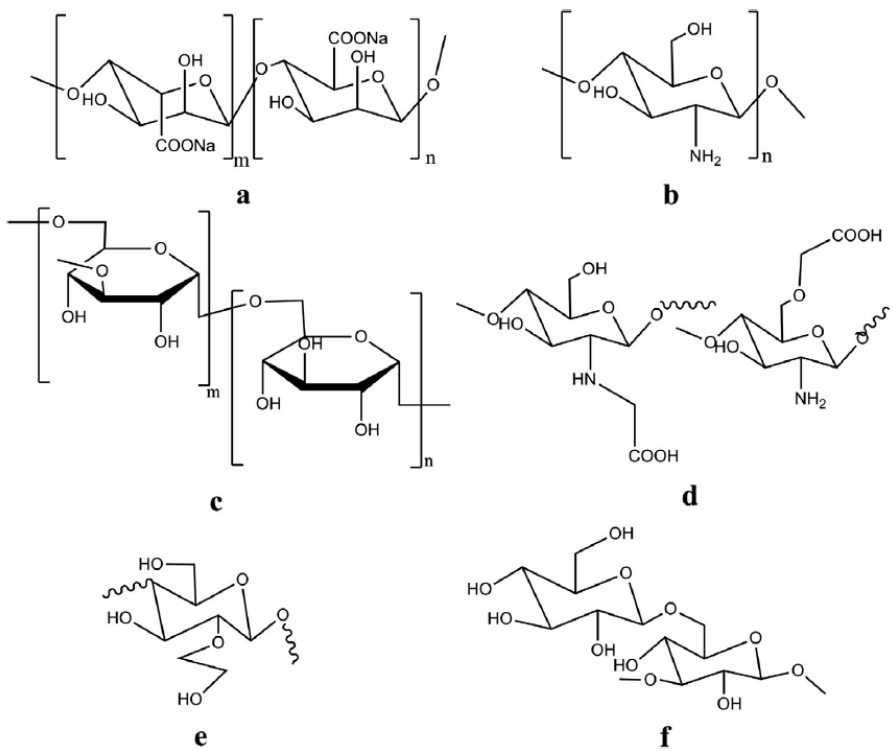

Figure II-35. Chemical structures of natural polymers and their derivatives which were blended with PVA hydrogel to form wound dressing materials, such as sodium alginate (a), chitosan (b), dextran (c), N-O-carboxymethyl chitosan (d), hydroxyethyl starch, HES (e), and (1,3), (1,6)-b-glucan (f). (Kamoun et al., 2015)

II.4.3. Nanofiber

Surface area of media is an important parameter because mass transfer is highly dependent on effective area of media as well as permeability related to surface properties (pore size, affinity, etc.). Nanofiber has been well known as a material having high specific surface area due to its ultrathin diameters or thickness (about 3 nm - 5 μm). Generally, nano-scale thickness of nanofiber can be achieved by electrospinning technology (Figure II-37). Thickness of nanofiber is controlled by variables including the flow rate, electric field strength (Zong et al., 2002), distance between tip and collector, needle tip design, and collector composition and geometry (Pham et al., 2006).

For enzyme application, high enzyme loading is always desired to reduce the size of system. The enzyme loading on nanofiber is expected to be high considering the great surface area (Jia et al., 2002). In addition, higher activity of nanofiber is also expected due to its large surface area and thin thickness enhancing the mass transfer. Recently, nanofiber has been used as a method for whole cell immobilization. Liu et al. (2009) developed the fibrous hydrogel material with encapsulated microbes (Figure II-38). Although the electrospinning process typically uses harsh organic solvents and extreme conditions that generally are harmful to bacteria, their techniques overcame these limitations. They reported that encapsulated microbes were insoluble and high stability, viability and enough permeability. In addition, their media had high biocompatibility compared to conventional nanofibers.

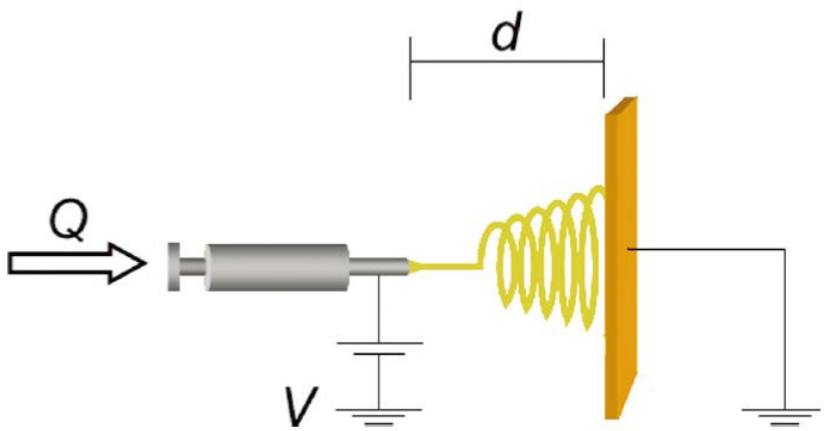

Figure II-36. Typical electrospinning setup. *Q*, flow rate; *d*, distance between plate and needle; *V*, applied voltage. (Pham et al., 2006)

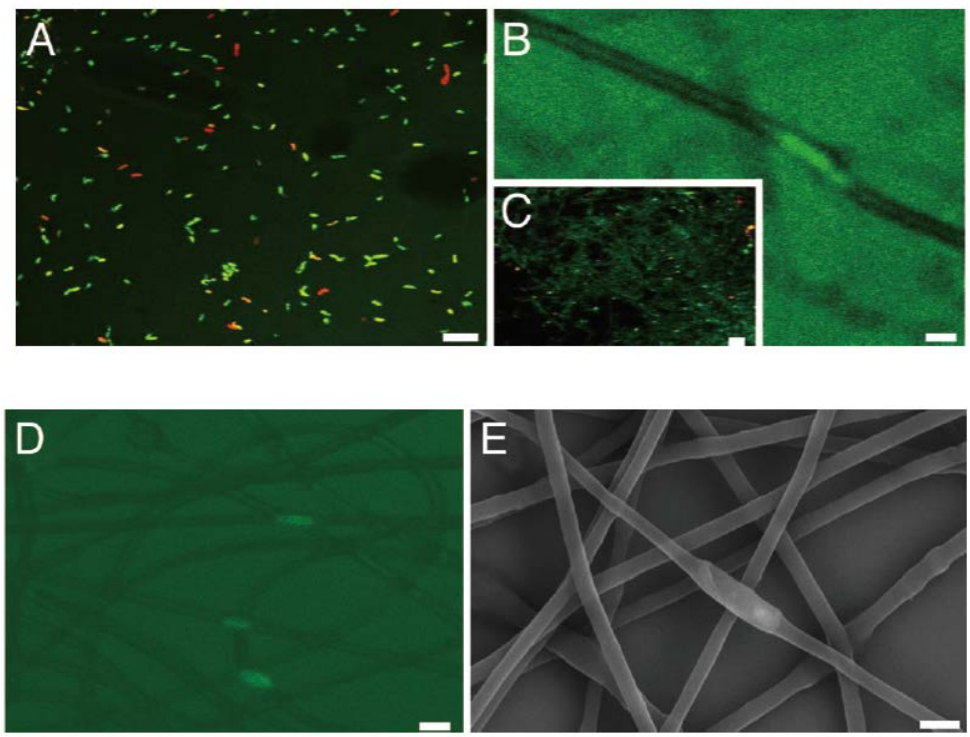

Figure II-37. Confocal images of stained and fluorescent (red, dead cells; green, live cells) cells of (*A*) *P. fluorescens* before electrospinning, (*B* and *C*) *P. fluorescens* inside the dry electrospun FDMA/PEO-blend fibers and, (*D*) *Z. mobilis* in dry electrospun FDMA/PEO-blend fibers. (*E*) SEM image of uranyl acetate-stained *P. fluorescens* cells after electrospinning. (Scale bars, 10 _m in *A*, 1 _m in *B*, 20 _m in *C*, 2 _m in *D*, and 1 _m in *E*). (Liu et al., 2009)

II.4.4. Application of Media in Wastewater Treatment

Many researchers and engineers have used various media in wastewater treatment. Especially, they have been tried to attach or entrap the activated sludge on their media (called bio-carrier) to improve the biological efficiency in wastewater treatment. In particular, bio-carriers have been used in moving bed biofilm reactor (MBBR) process for wastewater treatment process. Interestingly, bio-carriers are usually designed to be enhance its surface area as shown in Figure II-39. The principle of MBBR is to employ bio-carriers with attached-growth biomass that are able to move freely through fluid flow in the reactor induced by aeration (in aerobic reactors) or mechanical mixing (in anaerobic and anoxic reactors). Because biomass can attach and develop on the surface of bio-carriers (i.e., biofilm formation on bio-carriers), and thus wash out of the biomass could be reduced, and specific slow-growing microorganisms, such as nitrifying bacteria, could be developed (Randall and Sen, 1996). Furthermore, it is possible to obtain a higher concentration of total biomass in the reactor, but without significant increase of biomass in broth. However, biomass in broth of MBBR was reported to have difficulty with settling compared to CAS (Leiknes and Ødegaard, 2001). Meanwhile, MBR process produces the high effluent quality due to its property of perfect solid-liquid separation without the settling problem while high MLSS is one of the problems causing membrane biofouling. Therefore, MBR and MBBR processes have been employed jointly. In general, the effect of bio-carriers on membrane fouling propensity can be classified into (1) physio-chemical effects that exert on the characteristics of mixed liquor suspension; and (2) mechanical effect that exerts on membrane surfaces (Huang et al., 2008b; Jin et al., 2013). Chen et al. (2016) compared two types of moving bed

membrane bioreactors (MBMBR), MBMBR (without the scouring of bio-carriers) and $MBMBR_{sc}$ (with the scouring of membrane by bio-carriers), with a conventional MBR (Figure II-40). They reported MBMBR could reduce the membrane fouling by lowing the biopolymers compared to a conventional MBR. In addition, the scouring of the membrane surface by bio-carriers was significantly effective for membrane fouling control, and the effects of bio-carriers on mitigation of membrane fouling depended more on mechanical effect of bio-carriers souring than physio-chemical effect of mixed liquor suspended. Others used the sponge typed media for attachment of sludge (Agrawal et al., 1997; Ngo et al., 2006).

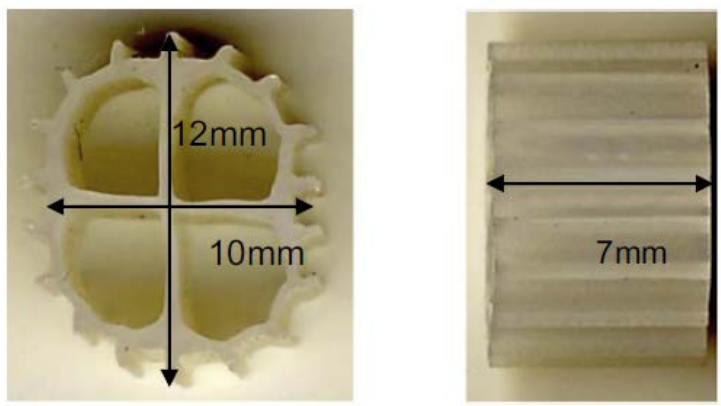

Figure II-38. Images of Bio-carriers. (Jin et al., 2013)

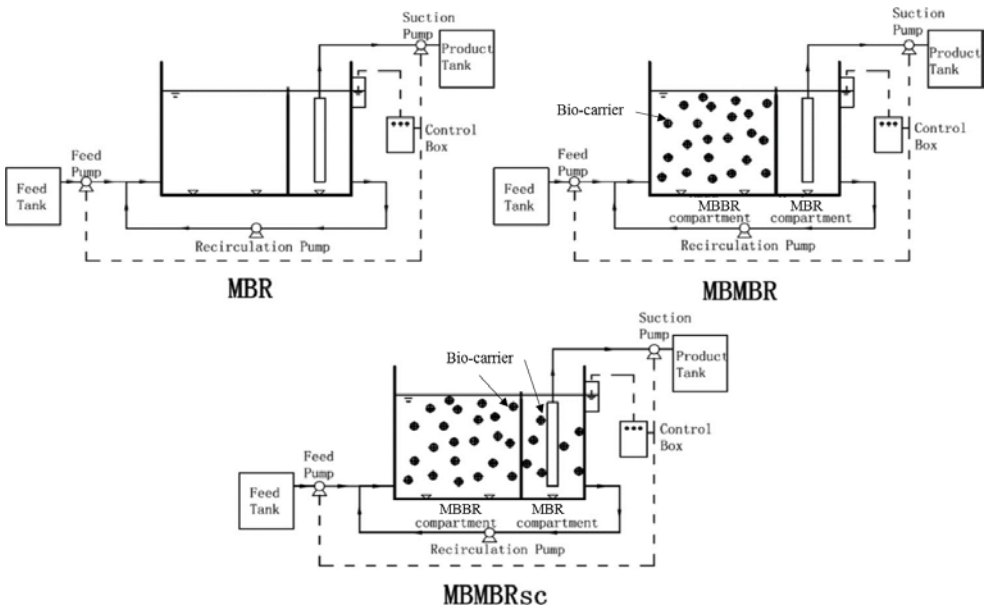

Figure II-39. Schematic diagram of the three bioreactors (a) the MBR, (b) the MBMBR, and (c) the $MBMBR_{SC}$. (Chen et al., 2016)

II.5. Motion of Particles in Fluid Flow

As previously mentioned in Fouling Control in MBR section (Chapter II.1.7), it has been well known that mechanical washing by adding media is a effective membrane fouling control because moving media could mechanically remove the foulant, such as biocake, on membrane surface without additional energy input. However, although some researchers studied the mechanical washing effect by moving particles, there is not sufficient and detail information. Shim et al. (2015) tried to find the optimum condition for effective mechanical cleaning using Box-Behnken response surface methodology which is one of the design of experiment (DOE). They found that aeration rate significantly affected the mechanical cleaning effect than other factors, such as bead diameter and bead number, because biofilm on membrane surface can be detached by not only collision of moving bead but also shear stress induced by air bubbles. Moreover, even though Rosenberger et al. (2011) showed that the circulating of particles can be affected by their density and shape in a membrane reactor however, they did not describe the relationship between effect of physical washing and motion of particles in detail. Thus, it is required that investigate the motion of particles in reactors to improve and control the mechanical cleaning effect.

It has been well known that drag is one of the important parameter to understand the motion of particle in fluid. Drag can be defined the force acting opposite to the relative motion of particles moving with respect to a surrounding fluid. Thus, in case of a particle, drag exist between the fluid and the surface of particle. Generally, drag equation can be present as follows (Becker, 1959):

$$F_D = \frac{1}{2}\rho v^2 A C_D$$

where,

F_D is the drag force,

ρ is the density of the fluid,

v is velocity of particle relative to the fluid,

A is the cross sectional area of particle, and

C_D is the drag coefficient (dimensionless number).

As shown in upper equation, the drag force is affected by density of fluid, velocity of particle, size of particle and drag coefficient (Figure II-41). In addition, drag coefficient depends on the Reynolds number ($R_e = \frac{\rho v D}{\mu}$) and on the shape of the particles. It indicates the particle motion can be affected by the shape of particle.

To predict the exact motions of particle, simulation approach can be generally effective. However, simulation of moving particles in MBR is difficult because facilities in a membrane tank (e.g., membrane module, lines, aerators and so on) are complex, and flow in the membrane tank is convoluted because of aeration. Furthermore, if particles is not sphere shape (e.g., cylinder) and flexible, the simulation to estimate the motion of flexible particles under real MBR condition becomes extremely difficult. Although it is very difficult to find the simulation results for motion of fiber-shaped particles in MBR, there are summarized some properties for motion of fiber-shaped particles in flow under limited conditions.

(i) The motion of an isolated neutrally buoyant ellipsoid in an unbounded low Reynolds number linear shear flow, assuming that the inertia of the particle and the fluid can be neglected (i.e., Newtonian fluid). The equation of motion for the ellipsoid have been theoretically and the differential equations governing the time evolution of $\emptyset$ given by (Jeffery, 1922):

$$\frac{d\emptyset}{dt} = \frac{\gamma}{r_e^2+1}(r_e^2 sin^2\emptyset + cos^2\emptyset)$$

where $\emptyset$ is angle of the fiber projection in the flow gradient plane with respect to the flow direction, γ is shear rate and r_e is the effective aspect ratio of the ellipsoid.

(ii) Some researchers have theoretically and experimentally investigated the flow induced deformation of single fiber in simple shear flow (Forgacs and Mason, 1959; Goldsmith, 1967). A cylindrical fiber in the flow/gradient plane is predicted to bend when the dimensionless group (called the bending ratio BR) is less than one.

$$BR = \frac{E_\gamma(\ln 2r_e - 1.50)}{(\mu\dot{\gamma})2r_p^4}$$

E_γ: Fiber Young's modulus

μ: Fluid viscosity

r_e: Equivalent aspect ratio

r_p: Length to diameter ratio

(iii) The fiber exhibited different apparent flexibility, which depended on the stiffness of the fiber, the strength of the flow field and the initial configuration of fiber (Wang et al., 2006). Also, flow motion of fiber can be highly affected by its flexibility (Figure II-42).

(iv) Rotation of fiber can be affected by the length of wall gap when fiber passing through the space between walls. Periodical motion of the fiber is suppressed as the length of wall gap decrease. (Ku and Lin, 2009)

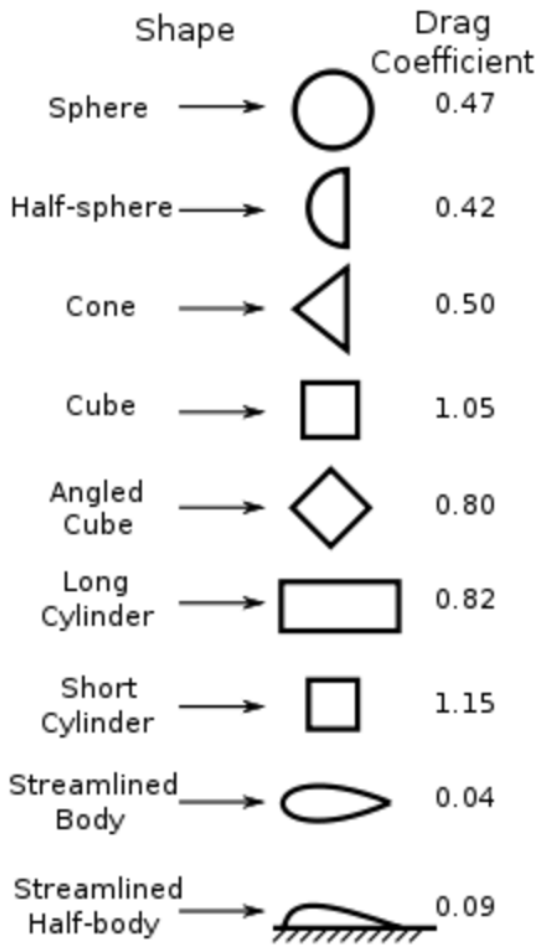

Figure II-40. Measured drag coefficients. Drag coefficients in fluids with Reynolds number approximately 10^4. (http://en.wikipedia.org)

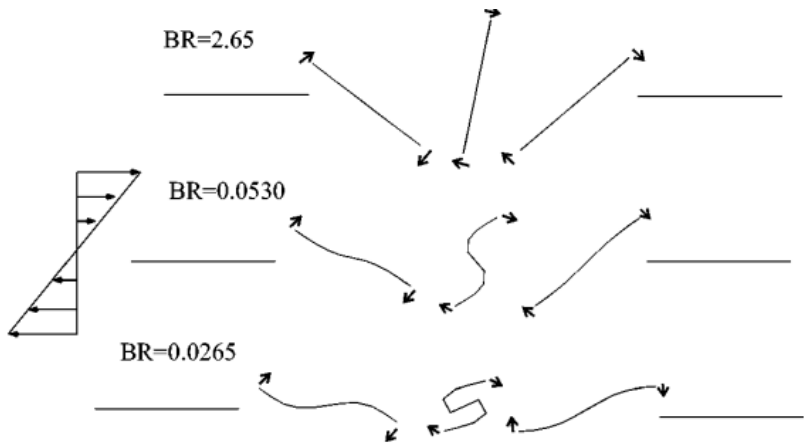

Figure II-41. Snapshots intrinsically straight, model fibers (r_p= 50, N = 10) of three different stiffness. (Schmid et al., 2000)

Chapter III

Crossing the Border between Laboratory and Field: Bacterial Quorum Quenching for Anti-Biofouling Strategy in an MBR

III.1. Introduction

As was clearly shown in the literature review section, it was experimentally observed that QS is closely associated with biofilm formation on membrane surface in MBRs. From an applicative point of view, bacterial QQ has been demonstrated a successful mitigation of biofouling in MBRs. In detail, bacteria which produce quorum quenching enzymes were isolated from a real MBR plant. Subsequently, those quorum quenching bacteria were encapsulated in a vessel (Cheong et al., 2014; Cheong et al., 2013; Jahangir et al., 2012; Oh et al., 2012) or entrapped in beads (Kim et al., 2015; Kim et al., 2013b; Maqbool et al., 2015). They proved QQ bacteria entrapping bead (QQ-bead) is very efficient in both physical and biological effects on biofouling control in MBR for wastewater treatment.

To date, however, most studies examining quorum quenching (QQ) MBR have been performed in lab-scale reactors using synthetic wastewater. Although substantial mitigation of biofouling by quorum quenching has been demonstrated, such an approach has not been fully investigated in a larger pilot-scale MBR using real wastewater. More often than not, the microbial environment in lab-scale reactors is notably different from that in real full-scale reactors due to the different scales of the technological equipment and the different raw wastewater characteristics. Especially, inhibitors affecting QQ activity (Chen et al., 2010; Wang et al., 2004) could be existing in real wastewater and the long-term survival of QQ bacteria in QQ-beads is questionable. Thus, it is required to confirm not only biofouling control by QQ but also QQ activity and viability of QQ bacteria in MBR fed with real wastewater for long-term operation.

The purpose of this study was to bring the QQ-MBR closer to potential practical application by demonstrating the QQ effects in pilot-scale MBRs installed at a municipal wastewater treatment plant and fed with real wastewater. Two MBR systems, one using a one-stage (only one aerobic tank) process, and the other using a three-stage (anaerobic/aerobic/membrane tanks) process, were operated for an extended period of more than four months. To examine the life-span of encapsulated beads containing quorum quenching bacteria under real wastewater condition, their QQ activity was monitored regularly for that period. Considering that QQ may affect microbial floc size and extracellular polymeric substance (EPS), the changes of protein, polysaccharide concentrations and floc size distribution were monitored. The energy savings through the QQ-MBR was also evaluated relative to the energy consumption of a conventional-MBR.

III.2. Materials and Methods

III.2.1. Preparation of QQ-Beads

QQ-beads were prepared using dripping method. However, the material and solidification methods were modified to reinforce their stability by mixing poly(vinyl alcohol) and sodium alginate solutions because QQ-beads made of alginate matrix are easily decomposed in real wastewater. The mixture of poly(vinyl alcohol), alginate and *Rhodococcus* sp. BH4 was dripped into $CaCl_2$-boric acid solution to form beads. Then, the beads were immersed in sodium sulfate solution and stored in water (Figure III-1). *Rhodococcus* sp. BH4, which was isolated from a real MBR plant was used as a QQ bacterium in this study because its biofouling control effect in MBR has been confirmed in a number of previous studies using synthetic wastewater (Jahangir et al., 2012; Maqbool et al., 2015; Oh et al., 2012; Weerasekara et al., 2014) as well as it was reported to be capable of degrading a wide range of AHL molecules by AHL-lactonase (Oh et al., 2013). The concentration of QQ bacteria (*Rhodococcus* sp. BH4) in beads was approximately 4-5 mg per g of beads. The average size and wet density of QQ-beads were approximately 4.3 mm and 1.05 g/mL, respectively. The average size and density of commercial plastic bead (A-bead) approximately 4.0 mm and 1.03 g/mL.

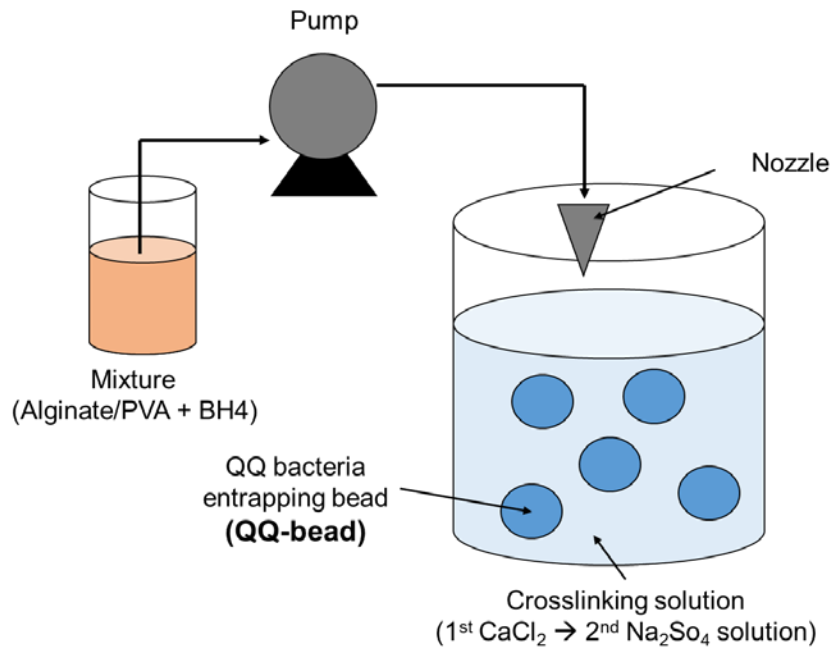

Figure III-1. Schematic diagram of the preparation of QQ-beads.

III.2.2. MBR Configurations and Operation Conditions

The two types of pilot-scale submerged MBRs, one- and three-stage MBRs, were installed at a municipal wastewater treatment plant (Daejeon, Korea), as shown in Figure III-2. The one-stage MBR, a simple MBR system, consisted of only an aerobic membrane tank. It is worth noting that the one-stage MBR was designed, installed and operated by Dr. Taewoo Yi at Hanwha Engineering and Construction. All the outputs from the one-stage MBR are originated from his work (Lee et al., 2016).

In the one-stage MBR, two types of aeration devices were equipped: one for oxygen supply to activated sludge, and the other for membrane scouring (Figure III-2a). The air supply for the microorganisms was constantly maintained at 10 L/min during the entire operation period, whereas the air scrubbing volumes for membrane cleaning were varied 0.3-0.9 SAD_m (specific aeration demand per membrane area, $m^3/m^2/h$). Two one-stage MBRs with a working volume of 80 L of each were operated in parallel. In phase 1, one reactor was used for a vacant-MBR (with vacant-beads) and the other was used for a QQ-MBR (with QQ-beads). Same intensity of membrane aeration was maintained at 0.3 SAD_m for both MBRs to confirm the QQ effect in real wastewater. In phase 2, one reactor was used for a conventional-MBR (without bead) and the other was used for a QQ-MBR. Different membrane aeration intensity was applied to investigate the potential of energy savings for QQ-MBR, that is, 0.9 SAD_m for the conventional-MBR whereas 0.3 SAD_m for QQ-MBR. For each one-stage MBR, three C-PVC membranes with a pore size of 0.4 μm (Pure-envitech, Korea) and an effective total surface area of 0.9 m^2 were used. The flux

was maintained at a constant 20 L/m^2/h (LMH) in a continuous cycle of filtration (10 min), followed by relaxation (2 min).

A real conventional MBR system is composed of biological nutrient removal processes, such as anoxic-aerobic (A/O) or anaerobic-anoxic-aerobic (A^2O) processes. To bring the QQ-MBR closer to potential practical application, the one-stage MBR was expanded to a three-stage MBR with an additional anoxic process for nutrient removal. The three-stage MBR consisted of an anoxic, an aerobic and a membrane tank. An air diffuser was equipped in each of the aerobic and membrane tanks (Figure III-2b). To confirm the competitiveness of QQ-beads having both QQ activity and physical washing effects, QQ-beads were compared with A-beads which are commercially used to control the membrane fouling by their physical washing effect. Three three-stage MBRs were operated in parallel: one was a conventional-MBR (without beads), another was an A-MBR (with commercial plastic bead, called A-bead) and the other was a QQ-MBR (with QQ-beads).

Poly(ethersulfone) membranes with a pore size of 0.04 μm (Microdyn-Nadir, Germany) were applied, giving an effective total surface area of 3.5 m^2 to each MBR. Identical diffusers were equipped in each aerobic tank for oxygen supply and in each membrane tank for membrane cleaning. The aeration rate for oxygen supply was constantly maintained at 8 L/min in an aerobic tank. The aeration rate for membrane cleaning was 0.34 or 0.46 SAD_m in a membrane tank. The flux was maintained at 15 L/m^2/h (LMH) in a continuous cycle of filtration (8 min) followed by relaxation (2 min). Influent was fed into the anoxic tank, while activated sludge in the membrane tank was continuously recirculated into anoxic tank with a recirculation rate of 2.5 Q.

In both types of MBRs, activated sludge was directly taken from the wastewater treatment plant and real wastewater, which passed sedimentation tank and screen, was fed as the influent. A mesh screen (size: about 2 mm) was placed in the membrane tank so that vacant- or QQ-beads (size: about 4.3 mm) were constantly retained in the membrane tank in each MBR. TMP is defined as the pressure difference between broth and permeate side of a membrane in a submerged MBR. The extent of biofouling in each MBR was quantitatively evaluated by monitoring the TMP which increases to compensate for the membrane-fouling under constant flux operation. When the TMP reached above 25 kPa during the MBR operation, used membrane was taken out and chemical washing with 1000 ppm of NaOCl solution was conducted, which resulted in more than 96% of permeability recovery. The operating conditions of each MBR and other important specifications are provided in Table III-1.

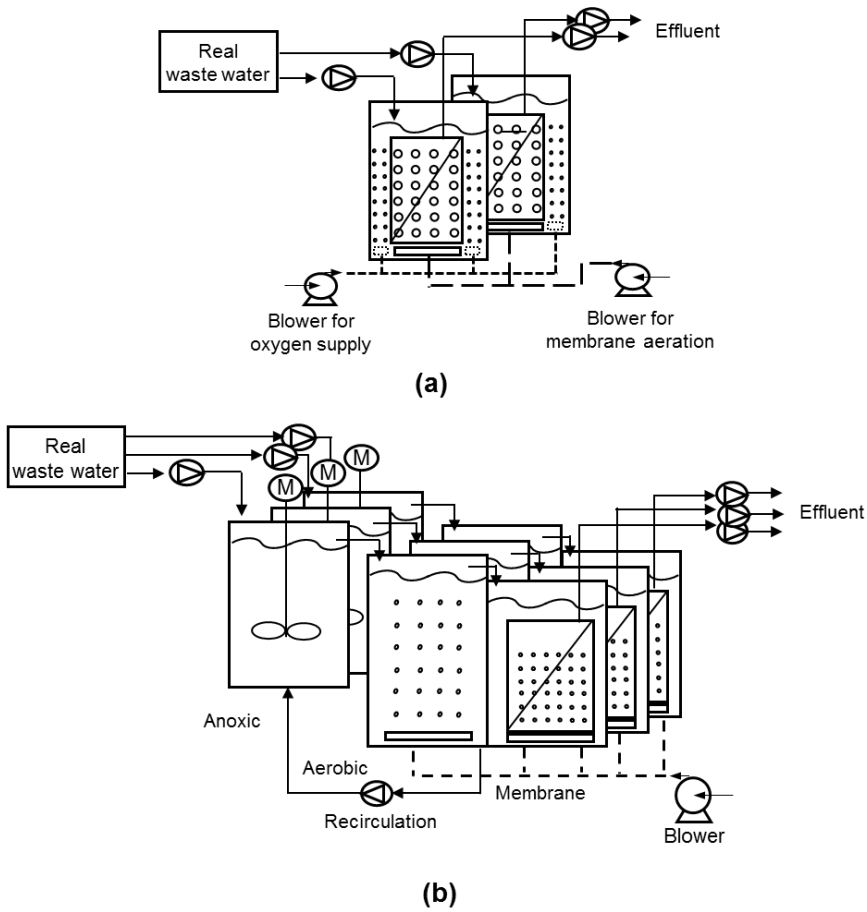

Figure III-2. MBR configurations. (a) Two one-stage MBRs in parallel, each of which consists of only a membrane tank where two types of aerations are equipped: one for oxygen supply to activated sludge, and the other for membrane scouring. (b) Three three-stage MBRs in parallel, each of which consists of an anoxic, an aerobic and a membrane tank.

Table III-1. MBR operating conditions.

	One-stage MBR (Aerobic tank)	Three-stage MBR (Anoxic/aerobic/membrane tanks)
Total working volume (L)	80	450 (150 / 150 / 150)
Total HRT (h)	5.2	10.7
SRT (day)	25 days	Nearly infinite
Membrane type	C-PVC, Flat sheet	PES, Flat sheet
Membrane area (m^2) / pore size (μm)	0.9 / 0.4	3.5 / 0.04
pH	6.5 - 7	6.5 - 7
MLSS (mg/L)	10,000 - 13,000	5,800 - 8,000
Flux (LMH)	20	15
Filtration mode (filtration/relaxation, min/min)	10 / 2	8 / 2
Aeration for oxygen supply (L/min)	10	8
Aeration for membrane scouring (SAD_m, $m^3/m^2/h$)	0.3 - 0.9	0.34
Concentration of beads (%, v(beads) / v(membrane tank))	1	0.8

SAD_m: specific aeration demand per membrane surface ($m^3/m^2/h$)

III.2.3. Bioassay for the Detection of QS bacteria Producing AHLs

LB agar covered with X-Gal (5-bromo-4-chloro-3-indolyl-β-d-galactopyranoside) was used for the bioassay. These assays consisted of streaking the AHL reporter strain, *A. tumefaciens* A136 (Fuqua and Winans, 1996), on the plate, and then placing each sample to be tested. If the sample produces or contains AHLs, then they diffuse through the agar, developing a blue color in the reporter strain as a result (Figure III-3). Positive and negative controls consisted of standard C8-HSL and distilled water, respectively.

III.2.4. Bioluminescence Assay for Measuring the AHLs

The AHL molecules were measured via a bioluminescence assay (Oh et al., 2013). First, the reporter strains of *A. tumefaciens* A136 and the AHL sample were mixed and loaded into 96-well-plate. The plate was placed on an incubator to maintain the temperature at 30 ℃ for 90 min, and then Beta-Glo Assay System (Promega) solution was added into each well. After 40 min, the luminescence intensity was measured by using a luminometer (Synergy 2, Bio-Tek). The concentration of AHL samples were determined by plotting the calibration curve of standard AHLs.

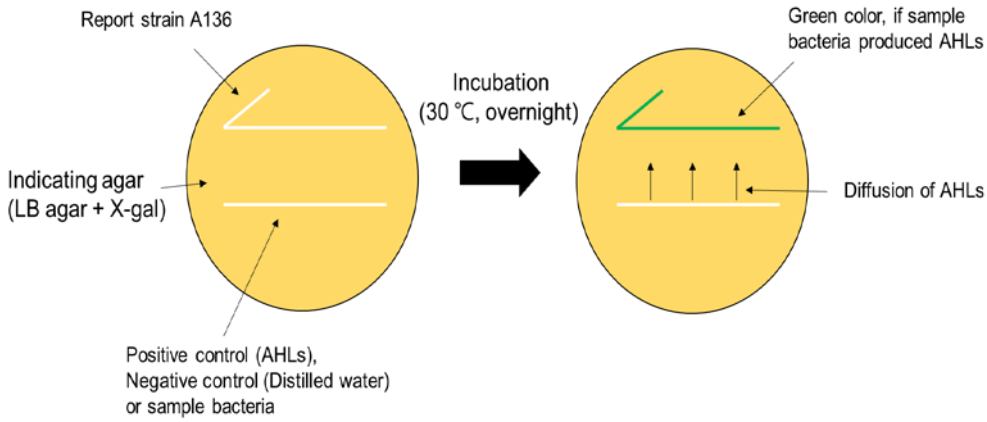

Figure III-3. Cross-feeding assay for detection of QS bacteria producing AHLs.

III.2.5. Measurement of Biological and Mechanical stability of QQ-beads

The activity of QQ-beads was determined by the degradation rate of C8-HSL (*N*-octanoyl-$_{DL}$-homoserine lactone). C8-HSL was chosen as a representative AHL molecule because it is one of the dominant AHL molecules in MBRs for wastewater treatment (Oh et al., 2012; Yeon et al., 2009a). Standard C8-HSL (Sigma-Aldrich) was dissolved in Tris-HCl buffer (50 mM, pH 7) to a final concentration of 200 nM. Next, 50 QQ-beads were added to 20 mL of the C8-HSL solution and then reacted using orbital shaker at 50 rpm at 25 °C. The residual concentration of C8-HSL was measured using a bioluminescence assay. To determine the biological stability of QQ-bead in a continuous MBR, 50 QQ-beads were withdrawn and strongly washed for measurement of the residual QQ activity. The relative QQ activity at each time point was calculated by the ratio of residual activity to initial activity.

In addition, QQ activity of QQ-beads was tested in real wastewater instead of Tris-HCl buffer solution. Real wastewater was filtered through a 0.2 μm syringe membrane.

Furthermore, the viability of the entrapped BH4 into QQ-beads was visually observed using a confocal laser scanning microscope (CLSM, C1 plus, Nikon, Japan) after staining with live/dead kit (Molecular Probes).

To investigate the mechanical stability of QQ-beads during MBR operation, compression tests were performed using a texture analyzer (CT3 4500, Brookfield) at a mobile probe (TA44) speed of 0.5 mm/s up to 50% deformation of beads. The

hardness work, a measure of energy required to compress the sample, was calculated as the area under the curve of the compression plot (Kim et al., 2015).

III.2.6. Evaluation of the Energy Savings in the QQ-MBR

To assess the energy savings of the QQ-MBR, a QQ-MBR was operated under lower aeration intensity than that of a conventional-MBR; the aeration intensity accounts for the largest portion of the specific energy consumption of an MBR. Although a full-scale MBR and a pilot-scale MBR were significantly different from each other in terms of system configuration and capacity (Table III-2), the specific energy consumption data obtained from the operation of a real full-scale MBR (Figure III-4) was used to calculate the specific energy consumption in a pilot-scale MBR (one-stage) with following assumptions and principles:

1. The energy parameters affecting the QQ-MBR are only filtration (permeation) and aeration (coarse bubble aeration).
2. The efficiency of the filtration pump and the blower is identical for both the pilot-scale and full-scale MBRs.
3. The specific filtration energy of the pilot-scale MBR (one-stage MBR) without any beads is identical to that of the full-scale MBR when the flux and filtration mode are identical. The specific filtration energy of the QQ-MBR was estimated using equation (1) because the relationship between the filtration energy and the integral area of TMP profile is linear.

Specific filtration energy of QQ-MBR (kWh/m^3)

$$= E_{f,f} \times \frac{\int_0^t TMP(QQ)dt}{\int_0^t TMP(Conventional)dt} \quad \text{-------- eqs (1)}$$

$E_{f,f}$: Specific filtration energy in the full-scale MBR, 0.071 kWh/m^3

4. Specific aeration energy of the pilot-scale MBR (one-stage MBR) was estimated using equation (2) because the relationship between aeration energy and air flow rate is linear.

$$\text{Specific aeration energy (kWh/m}^3\text{)} = E_{f,a} \times \frac{SAD_{m,p}}{SAD_{m,f}} \quad \text{----- eqs (2)}$$

$E_{f,a}$: Specific aeration energy in the full-scale MBR, 0.521 kWh/m^3

$SAD_{m,P}$: Specific aeration demand in the pilot-scale MBR (m^3/m^2/h)

$SAD_{m,f}$: Specific aeration demand in the full-scale MBR (m^3/m^2/h)

In addition, the saving cost of chemical cleaning of QQ-MBR was estimated with following assumptions procedures:

1. Chemical cleaning cost for 1 year obtained from the operation of a real full-scale MBR (17000m^3/d) was 0.125 million $. That chemical cost included the labor and chemical expenses.
2. The delay of the TMP rise-up in QQ-MBR compared to conventional-MBR will be identically occurred in full-scale MBR.
3. When QQ-beads were applied into full-scale MBR (17000m^3/d), Chemical cost for 1 year of operation in full-scale QQ-MBR was estimated using equation (3) because chemical cleaning cost could be proportional to the number of TMP rise-up.

$$\text{Chemical cost of QQ-MBR (\$)} = C_{f,c} \times \frac{Day_{TMP\ rise-up,QQ}}{Day_{\ TMP-rise-up,conventional}} \quad \text{----- eqs (3)}$$

$C_{f,c}$: Chemical cost for 1 year of operation in the full-scale MBR, 0.125 million ($)

$Day_{\ TMP\ rise\text{-}up,\ conventional}$: Day till TMP rise-up in conventional-MBR (day)

$Day_{\ TMP\ rise\text{-}up,\ QQ}$: Day till TMP rise-up in the QQ-MBR (day)

Table III-2. Operating conditions of one-stage and full-scale MBRs for the calculation of energy consumption

	QQ-MBR	Conventional-MBR	Full-scale MBR
Capacity (m^3/d)	0.3	0.3	17,000
Filtration membrane	Pure-envitech membrane (Flat, C-PVC, 0.4 μm)		
Filtration flux (LMH)	20	20	20
Filtration/relaxation mode (min/min)	10 / 2	10 / 2	10 / 2
Aeration for membrane ($SAD_{m,}$,$m^3/m^2/h$)	0.3	0.9	1.2

*Both QQ- and conventional-MBRs are one-stage MBRs, each of which consists of an aerobic membrane tank. The full-scale MBR consists of anaerobic, anoxic and aerobic membrane tanks.

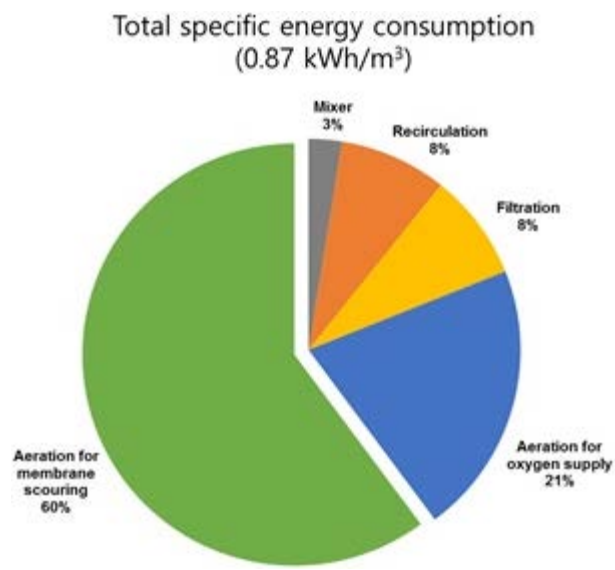

Figure III-4. Distribution of the energy consumption in the operation of the MBR (17,000 m^3/d) installed at a municipal wastewater treatment plant in Korea.

III.2.7. Analytical Methods

EPS (extracellular polymeric substances) concentrations in the mixed liquor and the biofilm were analyzed in both vacant- and QQ-MBRs. Soluble EPS were obtained by centrifuging the mixed liquor (6000 rpm, 10 min) and then filtering the supernatant through a 0.45 μm syringe filter. Bound EPS was extracted from the pellet (activated sludge floc). EPS in the biofilm was obtained as follows. First, a used membrane was taken from a membrane tank and briefly washed with tap water. Next, the biofilm was detached from the used membrane via sonication (10 min) and then extracted using the modified thermal extraction method (ZHANG et al., 2009). The proteins and polysaccharides in the EPS were quantitatively determined using the Bradford assay and the phenol-sulfuric acid method, respectively (Dubois et al., 1956).

Mixed liquor suspended solid (MLSS), chemical oxygen demand (COD), total nitrogen (TN) and ammonia-nitrogen (NH_4-N) were measured according to standard methods. The average floc size was measured using a particle size analyzer (Microtrac S3500).

III.3. Results and Discussion

III.3.1. QQ Effects on the Performance of the One-Stage MBR Fed with Real Wastewater

The pilot-scale MBR experiments were conducted to investigate the influence of real wastewater on QQ effect instead of the synthetic wastewater because the characteristics of influent wastewater should have a large impact on MBR performance (Miura et al., 2007a). Prior to applying QQ-beads into the MBRs, a bioassay test was conducted to confirm the presence of QS bacteria producing AHLs in the real wastewater. As shown in Figure III-5, it was revealed that QS bacteria existed in the feed wastewater as well as the activated sludge used for inoculum in this study. In phase 1, vacant-beads with no QQ-bacterium and QQ-beads entrapped with QQ-bacteria were placed into the first one-stage MBR (Vacant-MBR) and the second one-stage MBR (QQ-MBR), respectively. The loading rate of the beads in each one-stage MBR was 1% in v/v (volume of beads/volume of reactor), while the same intensity of membrane aeration was maintained at 0.3 $m^3/m^2/h$ (SAD_m) for both MBRs.

As shown in Figure III-6a, the rate of TMP build-up, which reflects the extent of membrane biofouling, was delayed by approximately 500% in the QQ-MBR compared with that in the vacant-MBR. Biofouling reduction in QQ-MBR could be attributed to both a biological effect due to quorum quenching of the QQ-beads and a physical effect due to friction between the beads and the membrane. Assuming that the physical cleaning effect by beads would be identical in both vacant- and QQ-MBRs because of the equal bead loading, the delay of the TMP build-up rate in QQ-

MBR can be attributed solely to the QQ activity of the QQ-beads. The characteristics of real wastewater are more variable and unsteady, unlike that of synthetic wastewater, as shown in Figure III-7. Note that biofouling control through bacterial QQ can also be achieved in an MBR, which suggests the QQ-MBR is approaching closer and closer to practical application.

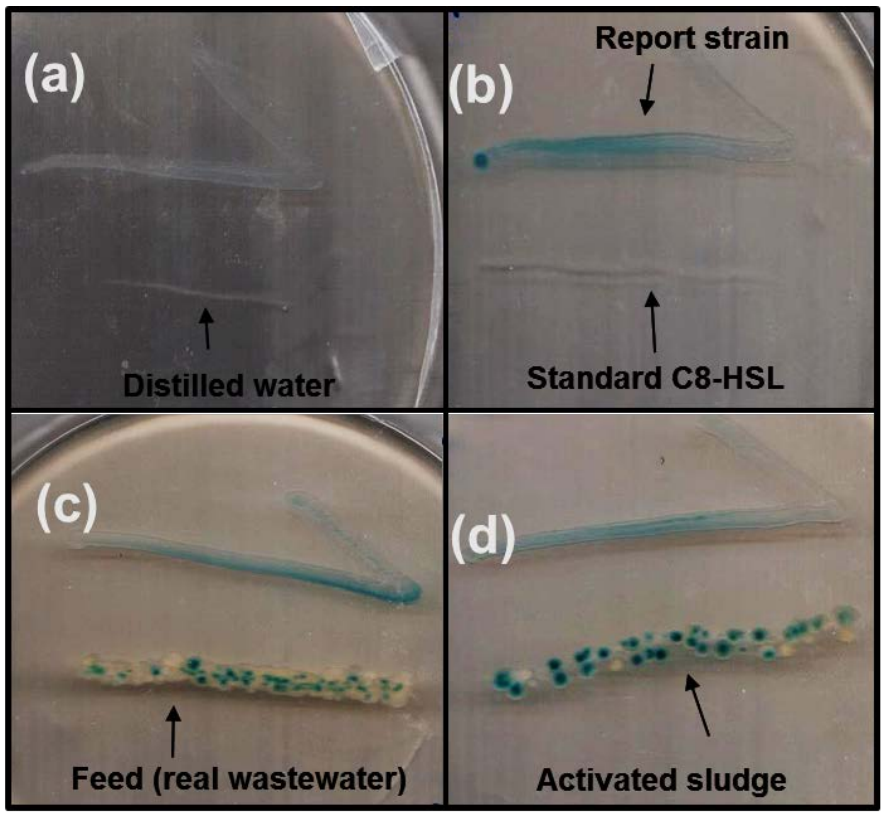

Figure III-5. Bioassay for detecting QS bacteria. Evidence for the QS bacteria producing AHLs is indicated by the expression of β-galactosidase activity (blue color) in the reporter strain, *A. tumefaciens* A136 which in each bioassay is streaked across the top half of the plate. (a) Distilled water and (b) standard C8-HSL were loaded on the lower line as negative and positive control, respectively. (c) Feed (real wastewater) and (d) activated sludge were loaded on the lower line in which blue colors indicate the presence of QS bacteria producing AHLs.

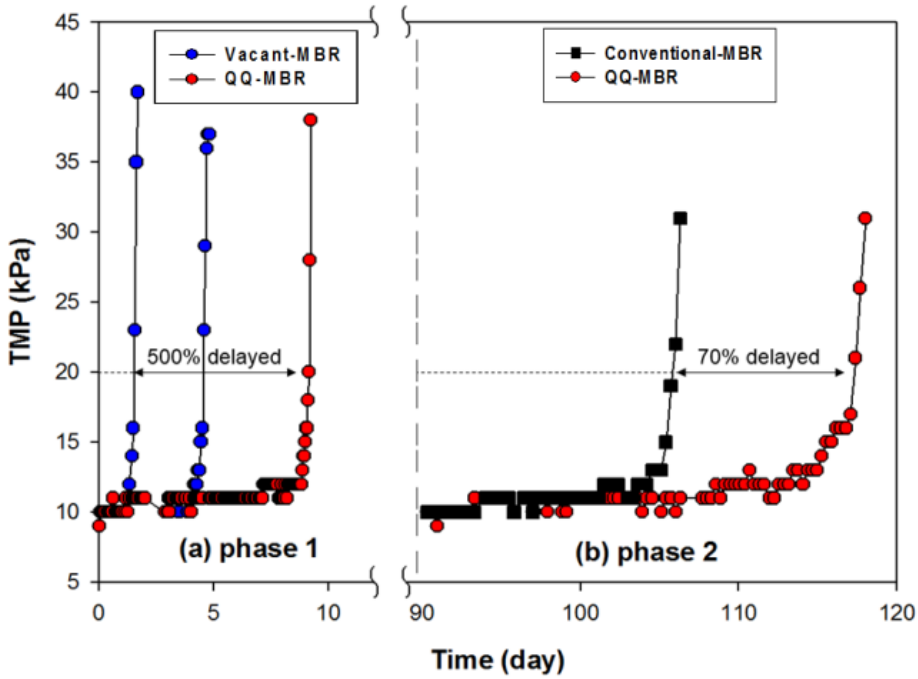

Figure III-6. TMP profiles during the operation of two one-stage MBRs in two phases. (a) phase 1; TMP rise-up in the vacant- and QQ-MBRs at the same aeration intensity (SAD_m= 0.3 $m^3/m^2/h$). (b) phase 2; TMP rise-up in the conventional-MBR (SAD_m= 0.9 $m^3/m^2/h$) and QQ-MBR (SAD_m= 0.3 $m^3/m^2/h$) at the different aeration intensity.

Figure III-7. Variation of COD and SS concentration in the feed. The feed to the MBRs was the effluent from the primary sedimentation tank of a municipal wastewater treatment plant (Daejeon, Korea). (COD: chemical oxygen demand, SS: suspended solid).

III.3.2. QQ Effects on EPS Relevant to Biofouling

Quorum sensing is known to be the cell-to-cell communication between microorganisms, which determines phenotypes, such as secretion of EPS, biofilm formation, and virulence (Dobretsov et al., 2009; Fuqua et al., 1996). Many previous studies on QQ-MBR using synthetic wastewater reported that the concentration of EPS was decreased in a QQ-MBR (Cheong et al., 2014; Kim et al., 2011; Kim et al., 2013b; Maqbool et al., 2015; Weerasekara et al., 2014). Especially, concentration of soluble EPS in broth and EPS in biofilm were significantly reduced compared with those in control MBRs by the application of *Rhodococcus* sp. BH4 into MBR fed with synthetic wastewater (Maqbool et al., 2015; Weerasekara et al., 2014). To confirm the change in EPS concentration in the QQ-MBR fed with real wastewater, EPS analysis of the mixed liquor and the biocake were conducted for both vacant- and QQ-MBRs.

After the same operating period of 14 days, the used membrane modules were taken out from both vacant- and QQ-MBRs to measure the amount of total attached biomass (TAB) and EPS in the biocake on the membrane surface. Mixed liquor in each MBR was also sampled to measure the total (i.e., polysaccharides plus protein) soluble and bound EPS (EPS in activated sludge floc). The total soluble and the total bound EPS in the mixed liquor in the QQ-MBR were reduced by approximately 60% (Figure III-8a) and 15% (Figure III-8b), respectively, compared to those in the vacant-MBR. It has been reported that the soluble EPS may have great influence on the membrane-biofouling in MBR (Jarusutthirak and Amy, 2006; Rosenberger et al., 2006; Wisniewski and Grasmick, 1998). Especially, Wisniewski et al. revealed the significant role of the soluble fraction of EPS on membrane

permeability. Thus, even though our results show that the amount of soluble EPS was much smaller than that of bound EPS in the mixed liquor, the 60% reduction of soluble EPS through QQ-beads could substantially mitigate the biofouling in QQ-MBR. The TAB per unit area of membrane in the vacant-MBR (420 mg/m^2) was much greater than that in the QQ-MBR (60 mg/m^2), indicating much lower biomass was accumulated on the membrane surface in QQ-MBR after the same operation period. Moreover, the concentration of polysaccharide per unit membrane surface was significantly reduced in the QQ-MBR (Figure III-8c). It has been reported that EPS plays a great role in biofilm formation and is also a key foulant of membrane-biofouling in an MBR (Jarusutthirak and Amy, 2006; Kim et al., 2001; Nagaoka et al., 1996; Wang et al., 2009). Thus, one of the main reasons why QQ-beads mitigate biofouling in MBR fed with real wastewater could be a reduction of soluble EPS in the mixed liquor as well as the reduction of EPS in the biocake. It seems that the reduction of EPS in QQ-MBR in this study using real wastewater is similar to previous studies using synthetic wastewater (Maqbool et al., 2015; Weerasekara et al., 2014).

Two methods, bioassay-luminescence assay and HPLC, were performed to analyze the concentration of AHLs and to monitor their changes in pilot-scale MBR fed with real wastewater along with the operation of QQ-MBR. First, the reproducible and credible analysis data were not obtained by a bioassay-luminescence method because the luminescence from the sample taken from the MBRs fed with real wastewater exhibited unreliable standard error. Second, concentrations of AHLs were not detected by HPLC because the concentrations of AHLs in MBR were below the detection limits of HPLC. However, previous studies

showed that the concentrations of AHLs were reduced in QQ-MBR (*Rhdococcus* sp. BH4 applied) fed with synthetic wastewater (Maqbool et al., 2015; Oh et al., 2012). Also, as shown in Figure III-9, QQ-beads also decomposed standard C8-HSL dissolved in real wastewater. Thus, although the concentration of AHLs could not be measured, we speculated that the decrease in EPS in the QQ-MBR was caused by QQ-beads decomposing AHL molecules.

Meanwhile, although TMP rise-up rate was delayed, membrane-fouling still occurred in QQ-MBR. It may be related to other membrane-fouling mechanisms such as pore blocking, sludge accumulation, and other types of quorum sensing.

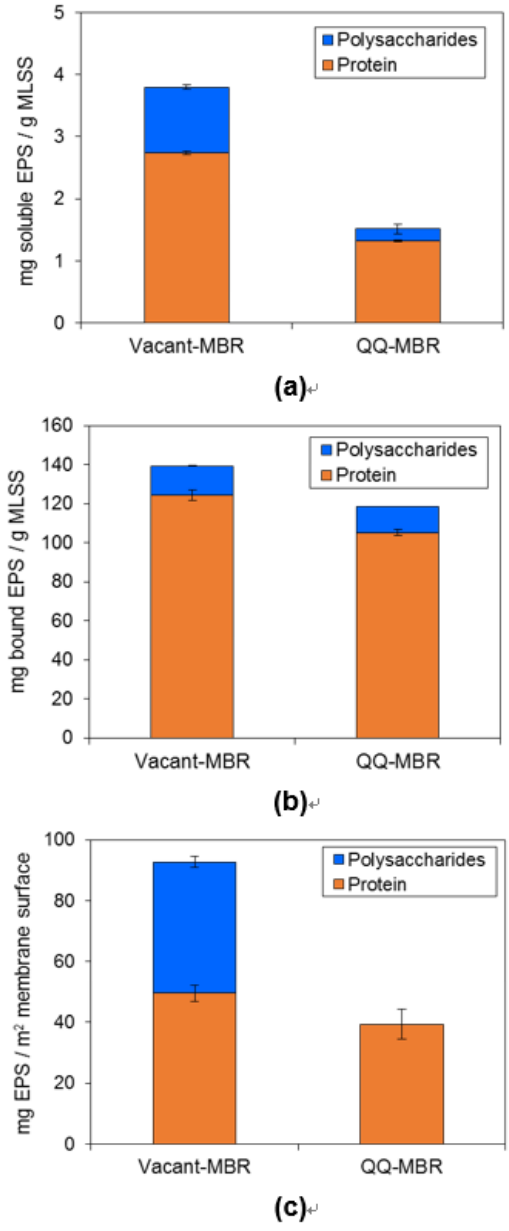

Figure III-8. EPS analysis in one-stage vacant- and QQ-MBRs. (a) Soluble EPS. (b) Bound EPS (EPS in activated sludge floc). (c) EPS in biocake. *Concentration of polysaccharides in biocakes in QQ-MBR was below the detection limit. Each bar represents the average value of duplicate measurements. Error bar: standard deviation (n=2).

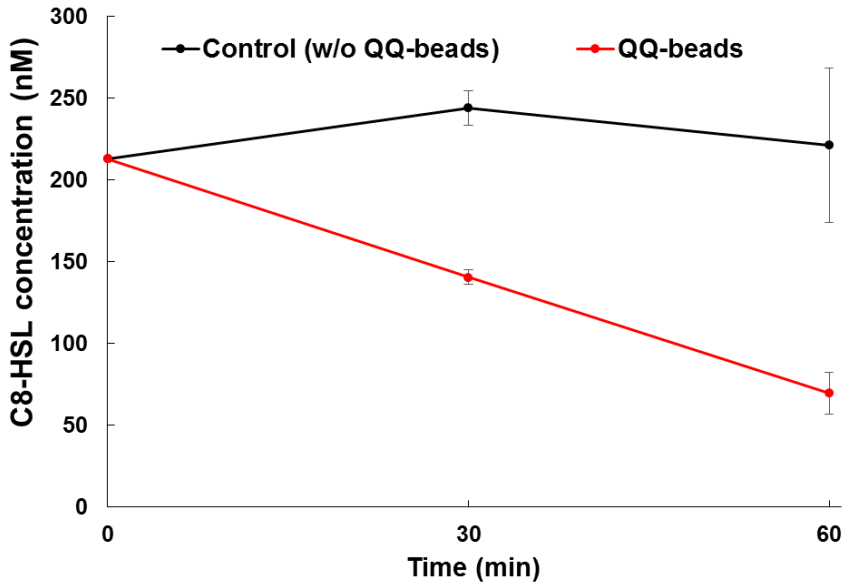

Figure III-9. QQ activity of QQ-beads in real wastewater solution. Error bar: standard deviation (n=2).

III.3.3. Comparison of the Energy Consumption Between Conventional- and QQ-MBRs

In submerged MBR systems, coarse bubble aeration for membrane scouring is a major energy consumer, often exceeding 50% share of the total energy consumption (Figure III-4). Consequently, many efforts have been made and reported to reduce the energy consumed for membrane scouring (Siembida et al., 2010; Wu and He, 2012). As the rate of TMP rise-up was substantially delayed in the QQ-MBR, it was attempted to quantitatively evaluate how much energy savings would be achieved by the addition of QQ-beads. For that purpose, the conventional- and QQ-MBRs were run in parallel, applying the same aeration intensity for the oxygen supply, but with different coarse bubble aeration conditions for membrane cleaning. The specific aeration demand per membrane surface area (SAD_m) was 0.9 $m^3/m^2/h$ for the conventional-MBR, whereas it was 0.3 $m^3/m^2/h$ for the QQ-MBR. In other words, the membrane aeration intensity in the QQ-MBR was reduced to one-third of that in the conventional-MBR. As shown in Figure III-6b, even though the conventional-MBR was operated at 3-fold greater air scrubbing intensity, the TMP rise-up rate in the conventional-MBR was faster than that in the QQ-MBR.

Based on Figure III-6b, the specific filtration energy required for permeate suction and specific aeration energy for membrane cleaning in one-stage MBRs were estimated using eqs (1) and (2), which were derived with some assumptions described in experimental section. Figure III-10 shows a comparison of the specific energy consumed for filtration (permeate suction) and air scrubbing between the conventional- and QQ-MBRs. The difference in the filtration energy consumption was not as high as that in air scrubbing for membrane cleaning. Note that the specific

energy consumption for membrane scouring in the conventional-MBR was approximately three-times greater than that in the QQ-MBR. The specific energy consumption for both items was approximately 0.46 kWh/m^3 in the conventional-MBR, whereas the amount was 0.20 kWh/m^3 in the QQ-MBR. As a result, QQ-MBR could reduce the biofouling related energy consumption by about 60%.

Moreover, comparison of full operating cost between conventional- and QQ-MBRs was conducted. The mixer, recirculation, biological aeration, chemical cleaning were considered as additional operating cost. Furthermore, cost of QQ-beads was included for the operation cost of QQ-MBR. Thus, cost of QQ-bead and total saving cost by adding the QQ-bead were estimated and compared when it was assumed that QQ-beads (18 m^3, 1% volume of beads volume/volume of membrane tank) were applied into full-scale MBR (17,000 m^3/d). To estimate the cost of QQ-bead, cost of BH4 production, polymers and salt solutions were considered. Chemical cleaning cost included labor and chemical expenses. Mixer, recirculation and biological aeration cost were obtained by converting values from Figure III-4 to electricity cost.

Energy saving by QQ-beads in full-scale MBR was estimated based on the result of Figure III-6b: about 70% delayed TMP rise-up and about 67% reduced membrane aeration compared to conventional-MBR. As shown in Figure III-11, even though addition of QQ-bead requires additional cost, about 34% of reduced total cost was estimated in QQ-MBR by reducing the membrane aeration and chemical cleaning cost, 67% and 41%, respectively. This result indicates that QQ-MBR could be highly competitive in terms of economic benefits.

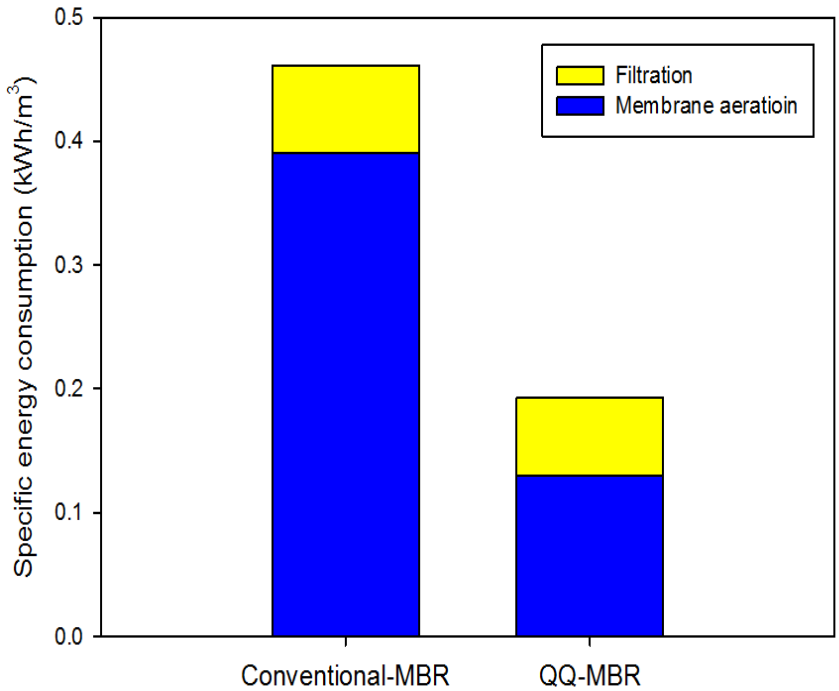

Figure III-10. Comparison of energy consumption related to biofouling between one-stage conventional- and QQ-MBRs. It was assumed that only two parameters, membrane aeration and filtration energy were affected by biofouling control of QQ.

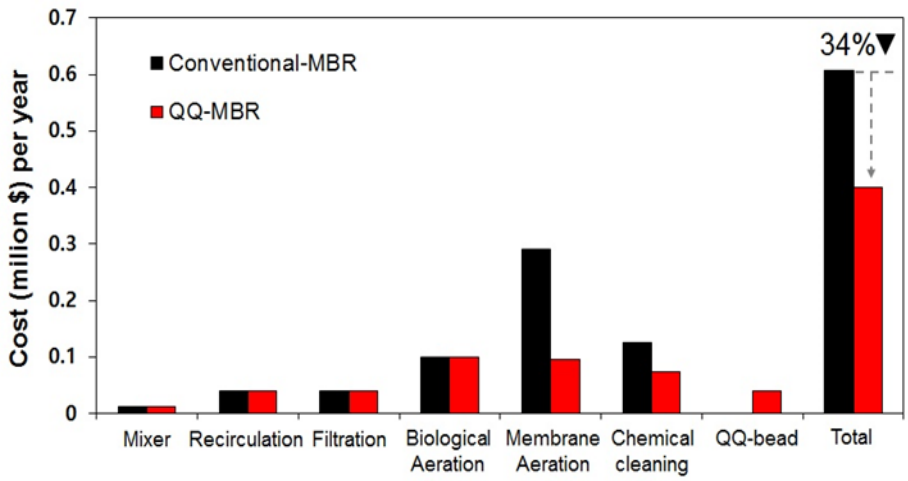

Figure III-11. Comparison of full operating cost per year in conventional- and QQ-MBRs. It was calculated based on a full–scale MBR with 17,000 m^3 of wastewater treatment /day. The volume of membrane tank: 1,800 m^3. The volume of beads in the membrane tank: 1.0% (v/v)

III.3.4. QQ Effect in the Three-stage MBR Fed with Real Wastewater

The efficiency of the QQ-MBR for biofouling control was confirmed in the one-stage MBR system. However, a conventional real MBR system has anoxic processes. To bring the QQ-MBR closer to potential practical application, the one-stage MBR was expanded to a three-stage MBR with an additional anoxic process. In addition, QQ-beads which have both QQ activity and physical washing effects were compared with A-beads which are commercially available and are to mitigate membrane fouling only by their physical washing effect.

Figure III-12 shows the profiles of TMP rise-up in the conventional-, A- and QQ-MBRs operated at the same aeration intensity (0.34 $m^3/m^2/h$). QQ-beads and commercial A-beads of 0.8% v/v were applied into QQ-MBR and A-MBR, respectively. It took approximately 18 days in both conventional- and A-MBRs, whereas it took 35 days in the QQ-MBR, to reach the TMP of 20 kPa. In other words, the rate of TMP rise-up was delayed by approximately 100% in the QQ-MBR through the addition of QQ-beads to the membrane tank. This result indicates that the QQ effect on the membrane fouling is also valid in the three-stage MBR system with an anoxic process. In addition, it was confirmed that the performance of QQ-beads was better than commercial A-beads under same aeration intensity (0.34 $m^3/m^2/h$). Interestingly, TMP rise-up between conventional- and A-MBRs was not significantly different at aeration intensity of 0.34 $m^3/m^2/h$ while TMP-rise-up in A-MBR was about 95% delayed than that in conventional-MBR at aeration intensity of 0.46 $m^3/m^2/h$ (Figure III-13). It indicates that the physical washing effect of A-beads was valuable at the higher intensity of aeration while it was inadequate at lower intensity of aeration. This phenomenon might have caused by the fact that A-beads

have only physical washing effect which can be affected by hydrodynamics in MBRs. In addition, even though the aeration intensity of QQ-MBR was 35% lower than that of A-MBR, the TMP rise-up rates of QQ-MBR and A-MBR were similar. In other words, QQ-MBR could reduce the aeration energy 35% compared to A-MBR. Thus, it can be concluded that the biological QQ is an effective energy saving approach for biofouling control in MBRs compared to physical approach.

Meanwhile, the extent of the delay of TMP rise-up decreased from 500% (Figure III-6a) for the one-stage MBR to 100% (Figure III-12) in the three-stage MBR. This reduced performance might be attributed to the activated sludge recycle throughout the three tanks and/or the considerably smaller loading volume of the QQ-beads (v/v) in the three-stage MBR [0.27% (v/v)], which was approximately one-third of that in the one-stage MBR [1% (v/v)]. Further research should be performed to determine the best operating conditions that are able to optimize the use of the QQ-beads in the QQ-MBR. In addition, the difference of MBR process between the one- and three-stage MBRs could give rise to the change of microbial community, which might be another cause of reduced performance.

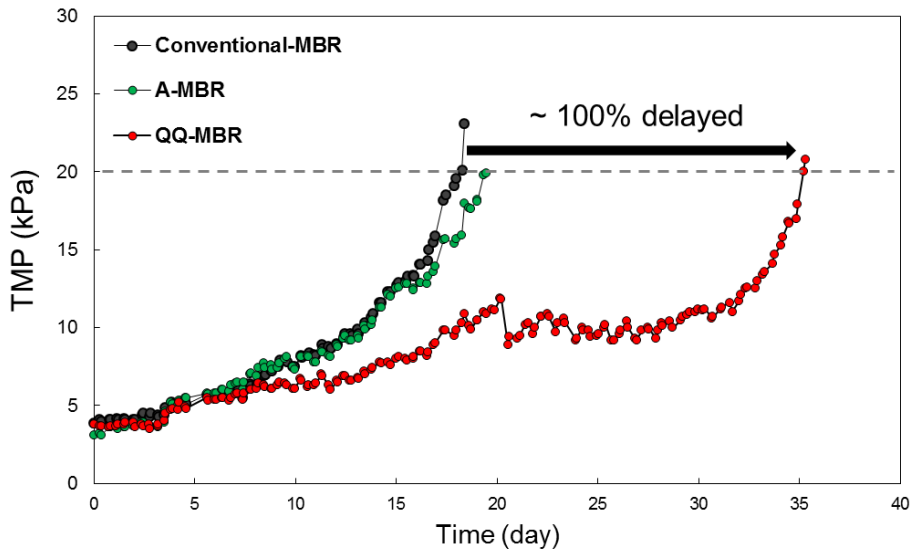

Figure III-12. TMP profile of three-stage conventional-, A- and QQ-MBRs at the same membrane aeration intensity (SAD_m= 0.34 $m^3/m^2/h$).

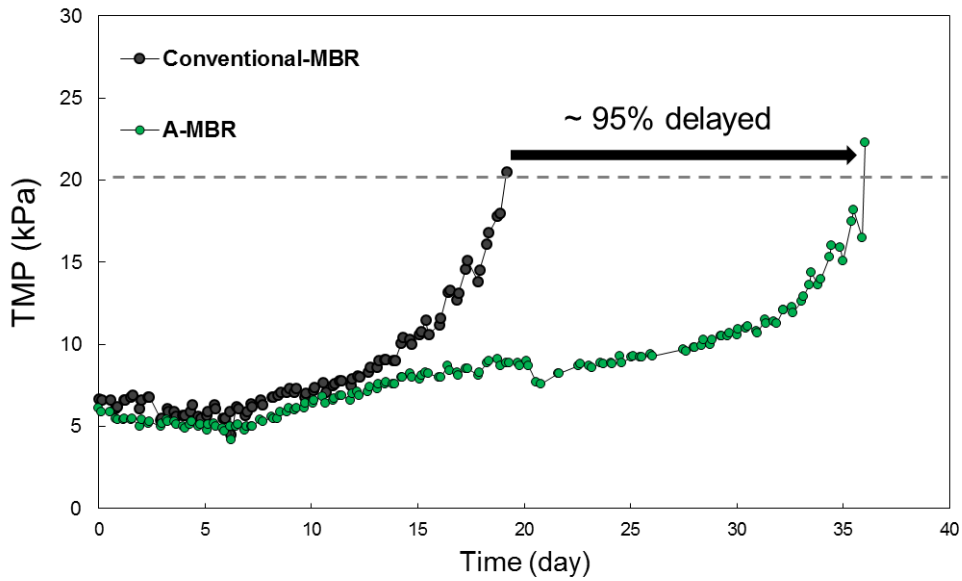

Figure III-13. TMP profile of three-stage conventional- and A-MBRs at the same membrane aeration intensity (SAD_m= 0.46 $m^3/m^2/h$).

III.3.5. QQ Effect on the Floc Size of the Activated Sludge

Microbial floc size is one of the important factors of the floc characteristics and is related to membrane-biofouling (Kang et al., 2003; Le-Clech et al., 2006). However, some reports on the QS/QQ effects on floc size are contradictory to each other. It was reported that the granule formation and size is closely related to AHL-based QS (Li et al., 2014; Tan et al., 2014). Jiang et al. (2013) found that the size of the activated sludge floc decreased by quorum quenching. However, Weerasekara et al. (2014) reported the change of microbial floc size could be attributed to microbial adaptation when seeded into a new reactor, instead of the effect of QQ.

In this work, in the one-stage MBR, the average floc size in the vacant-MBR was 106 μm, but that in the QQ-MBR was 88 μm (approximately 20% reduction), as shown in Figure III-14. In the three-stage MBR, however, the floc size in all three tanks became much smaller than that in one-stage MBRs. Moreover, no significant difference of the average floc size was observed, not only between three tanks but also between the conventional- and QQ-MBRs in each tank. Kim et al. (2001) and McMillan et al. (2003) mentioned that activated sludge can be mechanically broken by the pumping device. In the three-stage MBR, microbial flocs are continuously recirculated via the high flow rate of the recirculation pump (2.5Q, 1.7 L/min), so that they could be broken mechanically by pumping shear, which may be more powerful than the QQ effect. Consequently, the microbial floc size would be equalized, regardless of the tank types.

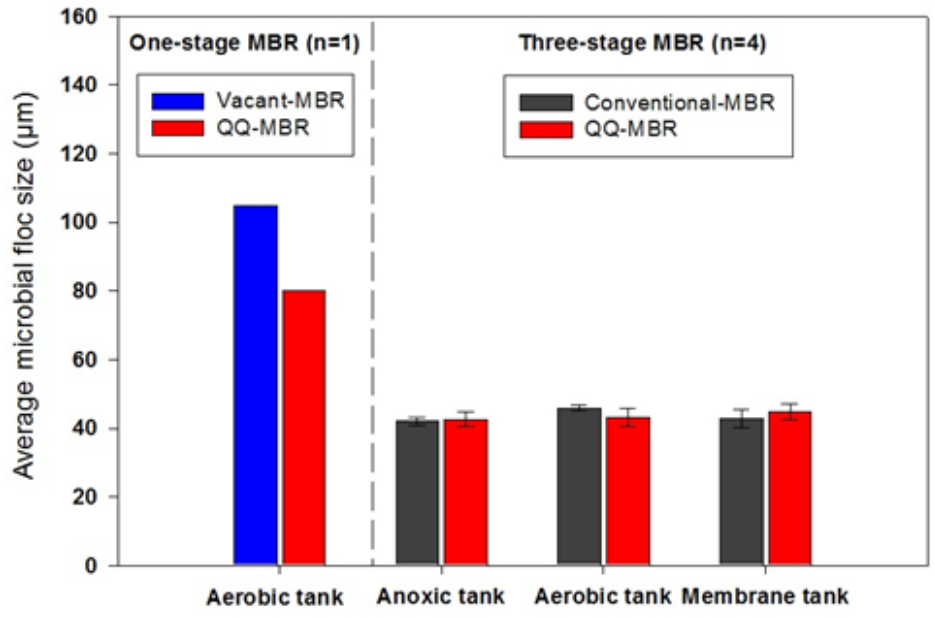

Figure III-14. Average microbial floc size in one-stage and three-stage MBRs. Error bar: standard deviation (n=4).

III.3.6. QQ Effect on the Effluent Quality

QQ-MBR inhibited biofouling and thus could substantially reduce the energy consumption of the MBR. However, this study cannot go further without verifying the effluent water quality in the QQ-MBR because it must be one of the main factors in the evaluation of MBR performance. It has been reported that certain nitrifying, denitrifying and nitrogen fixation bacteria were involved in quorum sensing (Batchelor et al., 1997; Burton et al., 2005; De Clippeleir et al., 2011; Toyofuku et al., 2007). In addition, QQ could affect the metabolism of QS bacteria in the activated sludge.

The removal efficiencies of some pollutants was monitored, such as COD, T-N, NH_4-N and NO_3-N for one-stage and three-stage MBRs. However, there was no significant difference between conventional- and QQ-MBRs in both one-stage and three-stage MBRs (Figure III-15 and Table III-3). This result indicates that quorum quenching has no adverse effect on the effluent water quality in QQ-MBR fed with real wastewater.

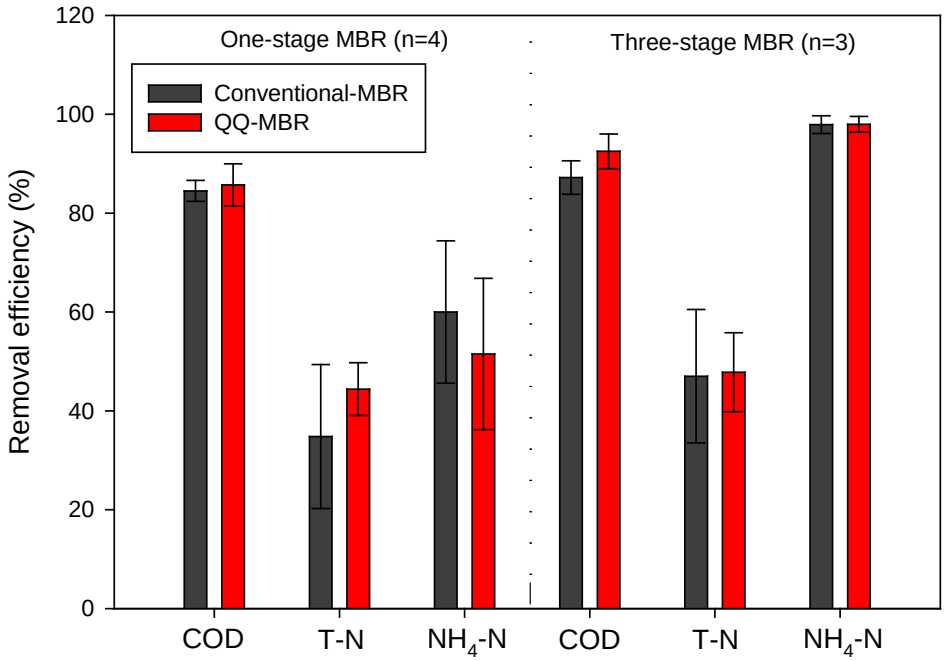

Figure III-15. Effluent water quality of one-stage and three-stage MBRs. (COD: chemical oxygen demand, T-N: total nitrogen, NH_4-N: ammonia-nitrogen). Error bar: standard deviation. (n=4 for one-stage MBR, n=3 for three-stage MBR).

Table III-3. Soluble COD, total nitrogen (T-N), ammonia (NH_4-N) and nitrate (NO_3-N) in MBRs (n=4 for one-stage MBR, n=3 for three-stage MBR). Range and [average (standard deviation)] of values are presented in the table.

	One-stage Conventional-MBR	One-stage QQ-MBR	Three-stage conventional-MBR	Three-stage QQ-MBR
Influent soluble COD	66 ~ 88 mg/L [79 (±8)] mg/L	66 ~ 88 mg/L [79 (±8)] mg/L	88 ~ 130 mg/L [104 (±19)] mg/L	88 ~ 130 mg/L [104 (±19)] mg/L
Effluent soluble COD	11 ~ 13 mg/L [12 (±1)] mg/L	6 ~ 14 mg/L [11 (±3)] mg/L	9 ~ 23 mg/L [14 (±6)] mg/L	4 ~ 16 mg/L [8 (±5)] mg/L
COD removal	82 ~ 88% [85 (±2)]%	83 ~ 93% [86 (±4)]%	82 ~ 90% [87 (±3)]%	88 ~ 96% [93 (±4)]%
Influent T-N	31.2 ~ 41.0 mg/L [34.0 (±4.1)] mg/L	31.2 ~ 41.0 mg/L [34.0 (±4.1)] mg/L	29.4 ~ 33.0 mg/L [31.0 (±1.5)] mg/L	29.4 ~ 33.0 mg/L [31.0 (±1.5)] mg/L
Effluent T-N	15.6 ~ 28.2 mg/L [22.1 (±4.8)] mg/L	15.6 ~ 21.4 mg/L [18.9 (±2.3)] mg/L	10.4 ~ 22.5 mg/L [16.6 (±4.9)] mg/L	14.0 ~ 21.0 mg/L [16.3 (±3.3)] mg/L
Denitrification	10.8 ~ 50.0% [34.8 (±14.6)]%	36.0 ~ 50.0% [44.4 (±5.3)]%	31.8 ~ 64.6% [47.0 (±13.5)]%	36.4 ~ 54.2% [47.8 (±8.1)]%
Influent NH4-N	22.4 ~ 29.0 mg/L [25.9 (±2.8)] mg/L	22.4 ~ 29.0 mg/L [25.9 (±2.8)] mg/L	29.4 ~ 31.4 mg/L [30.3 (±0.8)] mg/L	29.4 ~ 31.4 mg/L [30.3 (±0.8)] mg/L
Effluent NH_4-N	4.0 ~ 14.0 mg/L [10.5 (±3.8)] mg/L	6.0 ~ 20.2 mg/L [12.9 (±5.0)] mg/L	0.0 ~ 1.3 mg/L [1.0 (±0.5)] mg/L	0.0 ~ 1.2 mg/L [1.0 (±0.5)] mg/L
Nitrification	41.7 ~ 82.1% [60.0 (±14.4)]%	30.3 ~ 73.2% [51.5 (±15.3)]%	95.7 ~ 100.0% [97.9 (±1.8)]%	96.0 ~ 100.0% [97.9 (±1.6)]%
Influent NO_3-N	0.0 ~ 1.7 mg/L [0.5 (±0.7)] mg/L	0.0 ~ 1.7 mg/L [0.5 (±0.7)] mg/L	0.0 ~ 1.2 mg/L [0.4 (±0.6)] mg/L	0.0 ~ 1.2 mg/L [0.4 (±0.6)] mg/L
Effluent NO_3-N	2.2 ~ 22.3 mg/L [11.9 (±7.1)] mg/L	0.1 ~ 10.9 mg/L [5.4 (±4.9)] mg/L	9.8 ~ 22.6 mg/L [14.5 (±5.8)] mg/L	13.0 ~ 21.5 mg/L [15.9 (±4.0)] mg/L

*Denitrification (%) = $[(T\text{-}N_{Influent} - T\text{-}N_{effluent})/ T\text{-}N_{Influent}] \times 100$

*Nitrification (%) = $[(NH_4\text{-}N_{Influent} - NH_4\text{-}N_{effluent})/ NH_4\text{-}N_{Influent}] \times 100$

III.3.7. Stability of the QQ-Beads in the Long-Term Operation of the QQ-MBR

On the path toward the practical application of a QQ-MBR, long-term stability of the QQ-beads is required because a short life span of QQ-beads would require their frequent replacement, which would increase the operational cost of the QQ-MBR. Thus, the stability of QQ-beads in terms of the QQ activity, viability and mechanical strength were tested during the long-term (100-140 days) operation of both QQ-MBRs.

The used QQ-beads were intermittently removed from the aerobic tank (one-stage MBR) or the membrane tank (three-stage MBR). Next, the relative QQ-activity, defined by the degradation ratio of standard C8-HSL for 120 min in the presence of used QQ-beads, was monitored and plotted against the operating time (Figure III-16). In the one-stage QQ-MBR, the relative activity of QQ-beads decreased by 40% of their initial activity during 25 days, but increased slowly up to the initial QQ activity level after approximately 60 days. In the three-stage MBR, the relative activity of QQ-beads decreased by approximately 10-20% of the initial activity during 100 days of operation. A possible explanation for the initial decrease of the QQ activities might be that the QQ bacteria were adapting themselves to the new environment when they were exposed to the real wastewater.

In parallel with the relative QQ activity of the QQ-beads, live/dead cells in the QQ-beads were also observed intermittently in the three-stage QQ-MBR to monitor the survival of the QQ bacteria. Because it is nearly impossible for bacteria outside the beads to migrate into the beads as shown in Figure III-17, it had been concluded that cells shown in Figure III-18 were *Rhodococucs* sp. BH4 which were initially

entrapped into the QQ-beads. The population of live cells (Figure III-18a) appeared to be much higher than that of the dead cells (Figure III-18b), that is, the viability of QQ bacteria was well maintained at least for 100 days. Consequently, it is believed that QQ bacteria could live on the substrates and nutrients in real wastewater. In addition, the relative mechanical strength of the QQ-beads, defined by the ratio of residual mechanical strength to its initial value, was measured intermittently during 100 days operation. As shown in Figure III-19, the change of the mechanical strength appeared to be negligible.

All these results showed that the biological and mechanical stabilities of the QQ-beads were well maintained, even in the harsh environment of real wastewater during the relatively long-term operation of the QQ-MBR.

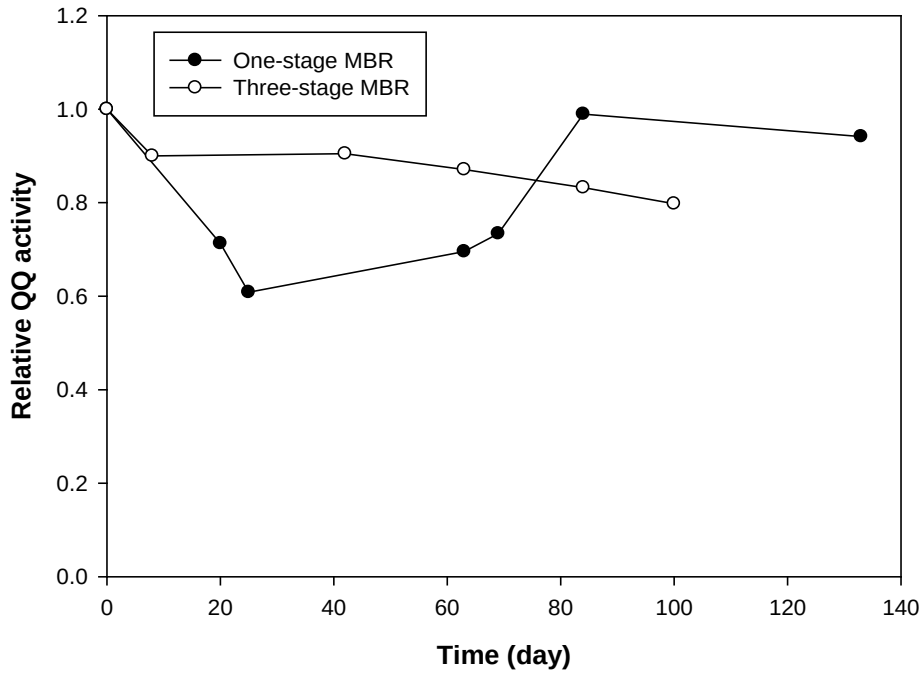

Figure III-16. Variation of the relative QQ activity of the QQ-beads during the operation of one-stage and three-stage MBRs. QQ activity: degradation ratio of standard C8-HSL for 120 min in the presence of QQ-beads.

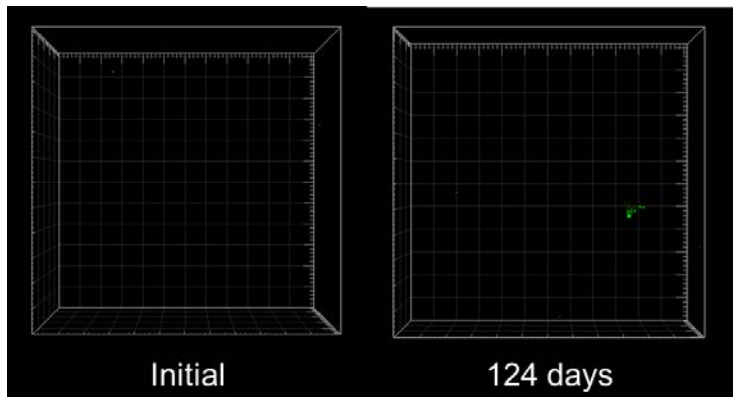

Figure III-17. Cross-sectional CLSM images of the vacant-beads sampled from one-stage vacant-MBR. (a) Initial vacant-bead. (b) Used vacant-bead for 124 days. Live and dead cell stained with a LIVE/DEAD *Bac*Light bacterial viability kit. Magnification 100×. Image size: 1212 μm × 1212 μm.

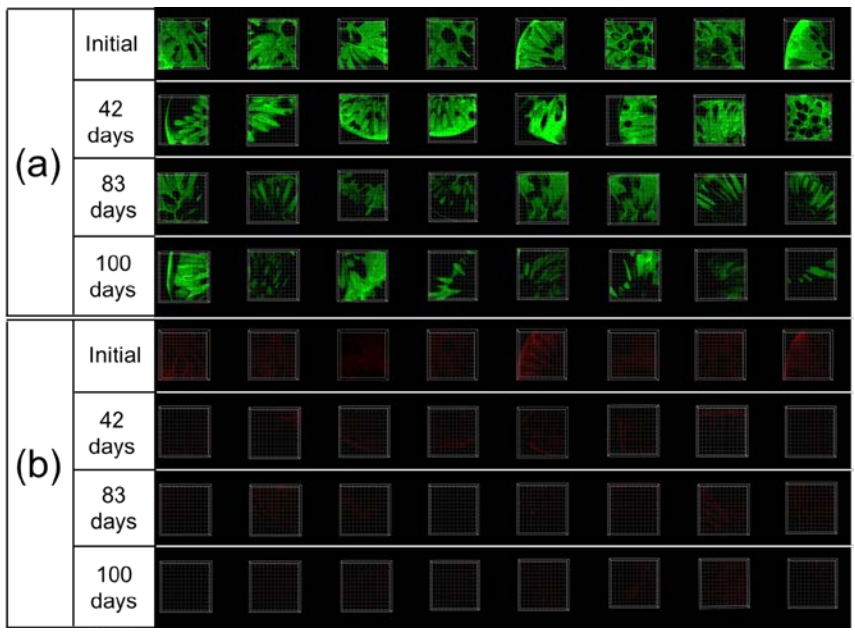

Figure III-18. Cross-sectional CLSM images of the QQ-beads sampled from the three-stage QQ-MBR; (a) live cell and (b) dead cell stained with a LIVE/DEAD *Bac*Light bacterial viability kit. Magnification 100×. Image size: 1212 μm × 1212 μm.

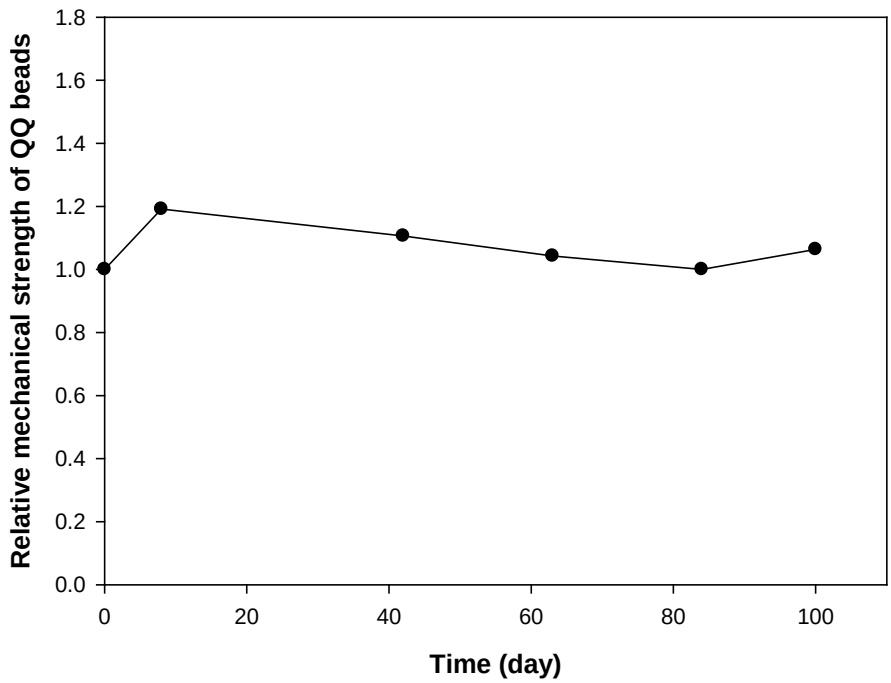

Figure III-19. Relative mechanical strength of the QQ-beads sampled from the three-stage QQ-MBR.

III.4. Conclusions

The purpose of this chapter is to demonstrate the effectiveness of QQ for biofouling control in two types of pilot-scale MBRs fed with real municipal wastewater. Based on the results of this study, the following conclusions were made:

- QQ-MBR with QQ bacteria entrapping beads could alleviate membrane fouling and thus could significantly reduce energy consumption by reducing the aeration intensity required for membrane cleaning compared with that in a conventional-MBR.

- Bacterial QQ was determined to have no influence on the effluent water quality of the pilot-scale MBRs fed with real wastewater.

- The QQ activity and mechanical stability of QQ-beads were found to be well-maintained in MBR fed with real wastewater during the four months of operation.

Chapter IV

Effect of Shape and Size of Quorum Quenching Media on Biofouling Control in MBR for Wastewater Treatment

IV.1. Introduction

Recently, Yeon et al. (2009a) reported that quorum sensing (QS), the bacterial cell-to-cell communication, plays a key role in biofilm formation on the membrane surface in MBRs and that biofouling could be inhibited by enzymatic quorum quenching (QQ), which decomposes the signal molecules such as *N*-acyl homoserine lactones (AHLs). To overcome the limitations of enzymatic QQ (e.g., high cost and low stability of enzymes), Oh et al. (2012) isolated a QQ bacterium, *Rhodococcus* sp. BH4, from a real MBR plant. BH4 produces QQ enzymes, which are capable of decomposing a wide range of AHLs, leading to the mitigation of membrane biofouling in MBRs. After that, many researchers isolated some other QQ bacteria and developed different media for entrapping QQ microorganisms more effectively. Some researchers encapsulated QQ bacteria inside the lumen of microporous membranes, as fixed QQ-media, having only a biological QQ effect (Cheong et al., 2014; Cheong et al., 2013; Jahangir et al., 2012; Köse-Mutlu et al., 2015; Oh et al., 2013; Oh et al., 2012; Weerasekara et al., 2014). Others entrapped QQ bacteria into spherical beads, as moving QQ-media (Khan et al., 2016; Kim et al., 2015; Kim et al., 2013b; Lee et al., 2016; Maqbool et al., 2015).

In particular, spherical QQ-beads have been favored because they have not only a biological (QQ) effect but also a physical washing effect through collisions between the moving beads and the surface of the filtration membrane. Moreover, the QQ-spherical bead proved to mitigate biofouling under harsh environment in a pilot MBR fed with real wastewater (Lee et al., 2016). However, there has been no report on the effect of geometrical changes in the moving QQ-media on their physical washing and/or biological QQ performance.

In this study, a cylinder-type medium (QQ-cylinder), as a new shape of moving medium, was prepared to improve the performance of the QQ-MBR. QQ-cylinders with various sizes were prepared and compared with spherical QQ-beads in batch testes in terms of QQ activity and the physical washing effect under identical loading volumes of each medium. The anti-biofouling capability of the QQ-cylinders was also evaluated in a continuous laboratory-scale MBR with a flat sheet membrane module. Based on those results, the effects of the shape and size on the performance of the QQ medium were investigated to determine the dominant parameters affecting its performance in QQ-MBRs.

IV.2. Material and Methods

IV.2.1. Preparation of QQ-Beads and QQ-Cylinders

Rhodococcus sp. BH4 was used as a QQ bacterium for both QQ-beads and QQ-cylinders because it is capable of degrading a wide variety of signal molecules of AHLs by producing AHL-lactonase (Oh et al., 2013). Its biofouling control by QQ in MBRs for wastewater treatment has been demonstrated in a number of previous studies (Jahangir et al., 2012; Kim et al., 2015; Lee et al., 2016; Maqbool et al., 2015; Oh et al., 2013; Oh et al., 2012; Weerasekara et al., 2014). Spherical QQ-beads were prepared as described in previous work (Lee et al., 2016). QQ-cylinders and cylinders without QQ bacteria (i.e., vacant-cylinder) were prepared from the polymeric mixture of polyvinyl alcohol and sodium alginate. BH4 was mixed with the polymeric mixture for the QQ-cylinders. For the vacant-cylinders, an equivalent volume of distilled water was added to the polymeric mixture instead. Cross-linking of the polymer mixture was achieved by extruding it through a nozzle into a $CaCl_2$-boric acid solution. Using various sizes of nozzles (inner diameter of 0.8 - 3.5 mm), beads and cylinders with various diameters and lengths were prepared as shown in Figure IV-1. The average densities of the QQ-beads and the QQ-cylinders were approximately 1.06 and 1.05 g/ml, respectively. As shown in Figure IV-2, QQ bacteria (BH4) were entrapped on both surface of and inside the QQ-media.

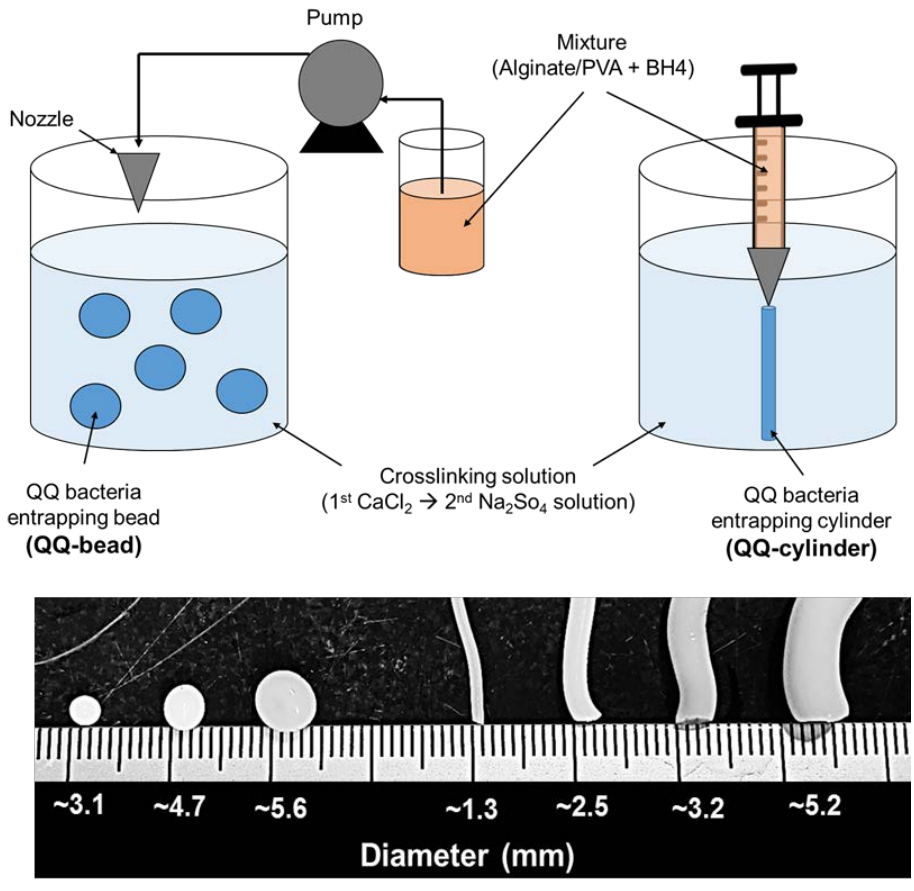

Figure IV-1. Preparation of QQ-beads and QQ-cylinders of various sizes.

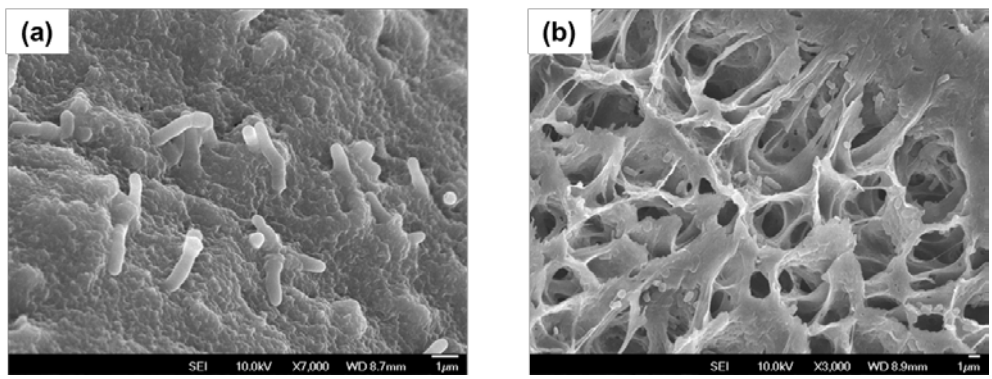

Figure IV-2. SEM images of QQ-cylinder. (a) Surface. (b) Cross-section.

IV.2.2. Assessment of Quorum Quenching Activity

The quorum quenching activities of various QQ-media were evaluated by measuring the degradation rate of standard C8-HSL (Sigma Aldrich), one of the dominant AHL molecules in MBR (Maqbool et al., 2015; Oh et al., 2012), by an *A. tumefaciens* A136 bio-luminescence assay as described in previous studies (Fuqua and Winans, 1996; Oh et al., 2013). Standard C8-HSL (Sigma-Aldrich) was dissolved in Tris-HCl buffer (50 mM, pH 7) to make a final concentration of 1 μM. The prepared medium with a total volume of 1 mL were inserted in 30 mL of C8-HSL solution in a conical tube, and then the mixture was placed on an orbital shaker at 50 rpm and 25 °C. Periodically, 1 mL of solution was taken out of the tube to measure the residual C8-HSL concentration through the A136 bio-luminescence assay. The QQ activity was presented as the amount of degraded C8-HSL (nmol) in 60 min in the presence of QQ-media.

IV.2.3. Visualization of the Trace of AHL Molecules in QQ-cylinder

To visualize signal molecules within the QQ-cylinders, *E. coli* JB525, which produces a green fluorescence protein (GFP) upon intake of a range of AHLs (Wu et al., 2000), was used. The JB525 strain was cultured in Luria-Bertani (LB) broth supplemented with tetracycline. QQ-cylinders entrapped with both BH4 and JB525 were prepared. Then, the QQ-cylinders were exposed to 1 μM C8-HSL in Tris-HCl buffer (pH 7) with 1/20 diluted LB for 2 hours, and their cross section was visualized through a confocal laser scanning microscope (CLSM, SP8 X, Leica, Germany).

IV.2.4. Assessment of the Physical Washing Effect

The physical washing effect of the media was assessed in a batch reactor with a working volume of 1.1 L. A polycarbonate (PC) plate was vertically inserted into the reactor in which the interval between the PC plate and the nearest wall of the reactor was 10 mm. Then, each batch reactor was filled with concentrated synthetic wastewater, and 5 mL of activated sludge was inoculated. The batch reactors were then operated with or without vacant-media (0.5%, v/v) at an aeration rate of 0.5 L/min. After 24 hours, the cell density in the broth of each reactor was measured by spectrophotometer at 600 nm. Simultaneously, the biofouled PC plate was taken out of each reactor and the upstream side of PC plate was stained with crystal violet. Crystal violet on the PC plate was rinsed with 100 mL ethanol solution and the concentration of crystal violet was measured by a spectrophotometer at 570 nm. The physical washing effect was defined as the ratio of the amount of normalized detached biofilm (OD_{570}/OD_{600}) in a reactor with vacant-cylinders to that in the control reactor without media. Procedures of assessment for physical washing effect of media were described in Figure IV-3.

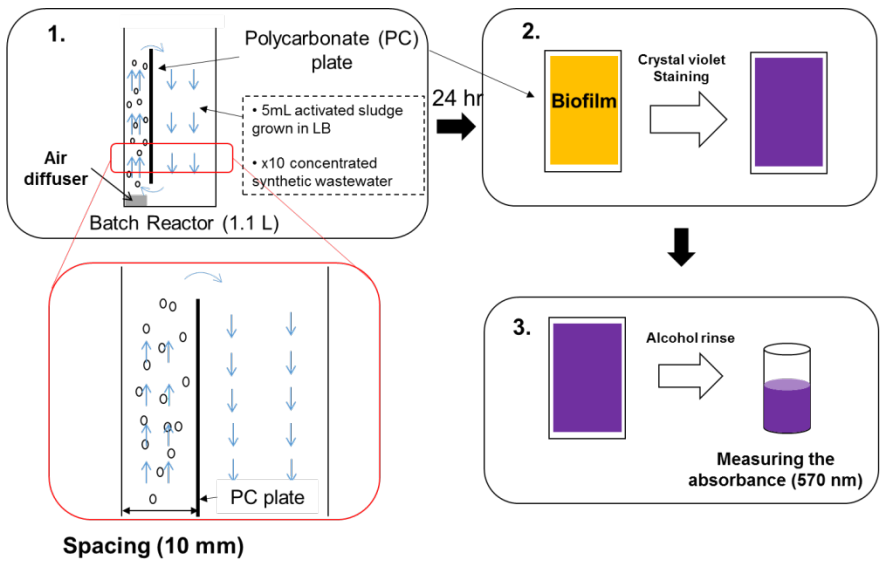

Figure IV-3. Procedures of assessment for physical washing effect of media.

IV.2.5. Trajectory of Circulating Media in a Reactor

Vacant media with different shapes were stained with Congo red (Sigma Aldrich) to clearly observe the motion and to monitor the trajectory of each medium when passing through the space between the PC plate and the reactor wall. They were stained to more clearly distinguish media from air bubbles. The snap shot images, consecutively taken every 0.1 seconds, were combined into a time-lapse composite image by a free image processing program (Startrails).

IV.2.6. MBR Configurations and Operation Conditions

Two continuous MBRs with a working volume of 2 L were operated in parallel. A flat sheet membrane (C-PVC, Pure-envitech, Korea) with a pore size of 0.4 μm and an effective surface area of 152 cm^2 was used for filtration. The distance between the membrane and the reactor wall was 10 mm (Figure IV-4). Activated sludge was taken from a wastewater treatment plant (Tancheon, Korea) and was acclimated to the synthetic wastewater before starting experiments. The composition of the synthetic wastewater in this study was as follows (mg/L) (Oh et al., 2012): glucose, 200; yeast extract, 7; bactopeptone, 57.5; $(NH_4)_2SO_4$, 52.4; KH_2PO_4, 10.9; $MgSO4{\cdot}7H_2O$, 16; $FeCl_3{\cdot}3H_2O$, 0.06; $CaCl_22H_2O$, 1.6; $MnSO_45H_2O$, 1.4; and $NaHCO_3$, 127.8. The filtration flux was fixed at 20 $L/m^2/h$ (LMH) without relaxation. The aeration rate for both air supply and membrane scouring was 0.8 or 1.0 L/min. The concentration of media applied to each reactor was 0.5% v/v (volume of media / volume of reactor). Trans-membrane pressure (TMP) was continuously monitored to evaluate the extent of biofouling during the operation of each MBR.

IV.2.7. Analytical Methods

Mixed liquor suspended solids (MLSS) and chemical oxygen demand (COD) were measured according to standard methods (Keith, 1996).

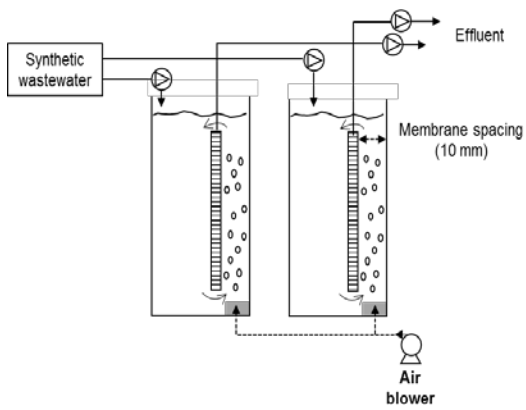

Working volume	2 L
SRT	50 days
HRT	10 hrs
Membrane	C-PVC (Pure-envitech) 152 cm^2 (0.4 ㎛)
Membrane spacing	10 mm
Flux	20 $L/m^2/h$
Air flow rate	0.8, 1.0 L/min
MLSS	3000 - 4000 mg/L
Feed COD	~250 mg/L
Broth COD (Removal efficiency)	12-20 mg/L (92-95%)

Figure IV-4. Scheme and operating conditions of the continuous laboratory-scale MBRs.

IV.3. Results and Discussion

IV.3.1. Effect of the Shape and Size of QQ-Media on QQ Activity

Three sizes of QQ-beads (diameter: 3.1-5.6 mm) and four sizes of QQ-cylinders (diameter: 1.3-5.2 mm; length: 4.7-75.4 cm) were prepared to investigate the effect of the shape and size of the media on the QQ activity. Having a total volume of QQ-media fixed at 1 mL (i.e., the total mass of QQ-media including polymeric substances and BH_4 was fixed), the degradation rates (nmol/min) of standard C8-HSL by those media were measured in a conical test tube containing 30 mL of C8-HSL solution and compared with one another (Figure IV-5). Under an identical loading volume of QQ-media (1 mL), the QQ activities of the beads increased as the number of beads increased, but their diameters decreased. In contrast, the QQ activities of the cylinders increased as their diameters decreased, but their lengths increased even though the number of cylinders was the same (i.e., N=1 for all types of cylinders).

Based on the results of Figure IV-5, the correlation between the QQ activity and total surface area of the media was analyzed. Regardless of the shape of the QQ-media, the QQ activity of the media was proportional to their total surface area (R^2 = 0.95), as shown in Figure IV-6. This indicates that the net QQ activity of QQ-media, excluding physical washing effect, was not dependent on the shape of the media (beads or cylinders) under the identical loading volume of QQ-media. However, total surface area was found to be important for the biological QQ activity under the identical loading volume. In other words, QQ activity would be proportional to the surface area to volume ratio of QQ-media. It is because the mass

transfer rate of signal molecules through QQ-media would be significantly dependent on their effective surface area (Welty et al., 2009). To confirm and elucidate this finding more clearly, the interaction between the QQ-media and quorum sensing (QS) signal molecules was investigated using a reporter strain, JB525, which produces green fluorescence protein (GFP) upon intake of a range of AHL signal molecules.

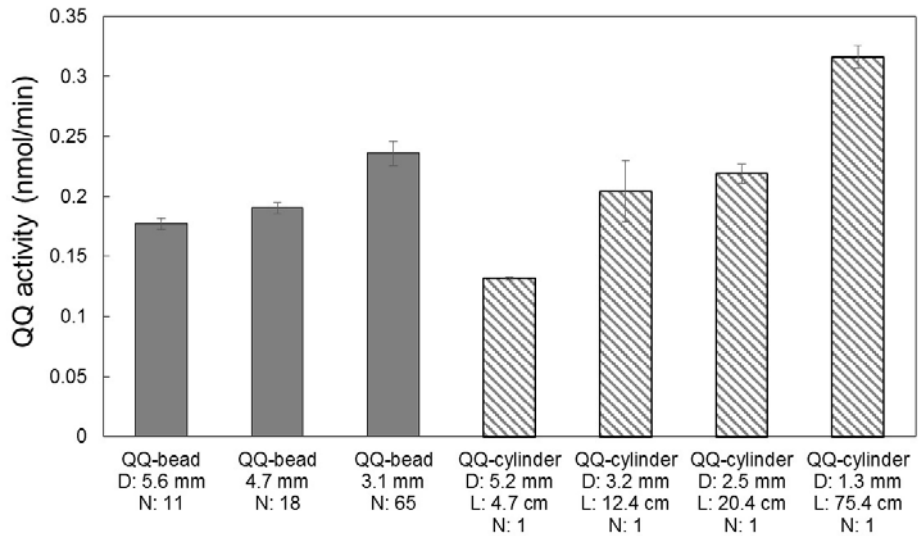

Figure IV-5. QQ activities of three QQ-beads and four QQ-cylinders having the same total volume of 1.0 ml. D, L and N represent the average diameter, length and the number of media. Error bar: standard deviation (n = 3).

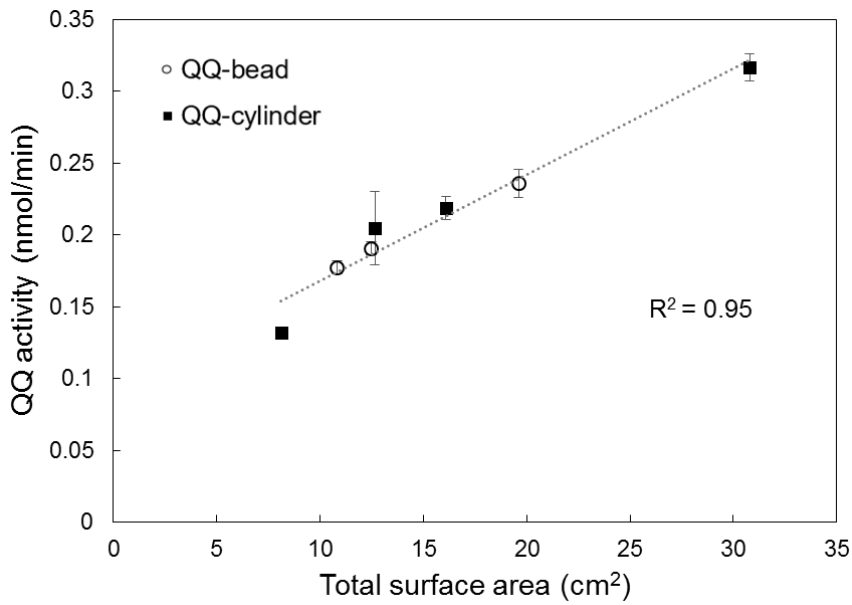

Figure IV-6. The relationship between the QQ activity and total surface area of QQ-media. Error bar: standard deviation (n = 3).

IV.3.2. Effective Region in a QQ-Medium for Quorum Quenching

To elucidate the interaction mechanism between QS signal molecules and QQ media when they come into contact with each other, two types of cylinders were prepared: 1) cylinders entrapped with only JB525 (an AHL report strain) and 2) cylinders entrapped with both JB525 and BH4 (QQ bacteria). The two types of cylinders were exposed to 1 μM C8-HSL in 30 mL Tris-HCl buffer (pH 7) with 1/20 diluted LB for 2 hours and their cross sections were visualized by fluorescence microscopy.

In a cylinder entrapped with only JB525, green fluorescence indicating the presence of QS signal molecules (C8-HSL) was observed across the cylinder (Figure IV-7a). This means that free diffusion of C8-HSL occurred within the cylinder. In contrast, in a cylinder entrapped with both JB525 and BH4, green fluorescence was observed only along the surface of the cylinder, and it faded out toward the center (Figure IV-7b). Note that the entrapped BH4 produced the endo-enzyme (Oh et al., 2013), which is capable of decomposing AHL signal molecules only if they diffuse into the cell.

Based on the contradictory results from observing the two different cylinders, it had been concluded that the presence of QQ-bacteria (BH4) limits the diffusion of signal molecules toward the center of the medium because the most AHLs were degraded by the BH4 located near the surface of the medium. Consequently, QQ-bacteria at the inner part of a medium may be deprived of opportunities to encounter and decompose signal molecules.

In summary, the surface area of a QQ medium is the more dominant parameter in terms of biological QQ activity than total mass of entrapped QQ-bacteria in a medium.

Meanwhile, in the practical application of QQ-media to real MBR for wastewater treatment, the QQ-media should be easily separated from the excess sludge and be retained in a membrane tank. In general, the greater QQ activity of QQ-bead, the smaller the diameter of QQ-bead becomes. However, it would be harder to the separate the smaller QQ-bead from the excess sludge. Fortunately, QQ-cylinder with small diameter can be easily separated due to its long length. However, when QQ-cylinder becomes too long, it would be caught in an apparatus like an aeration device or a membrane module inside the membrane tank.

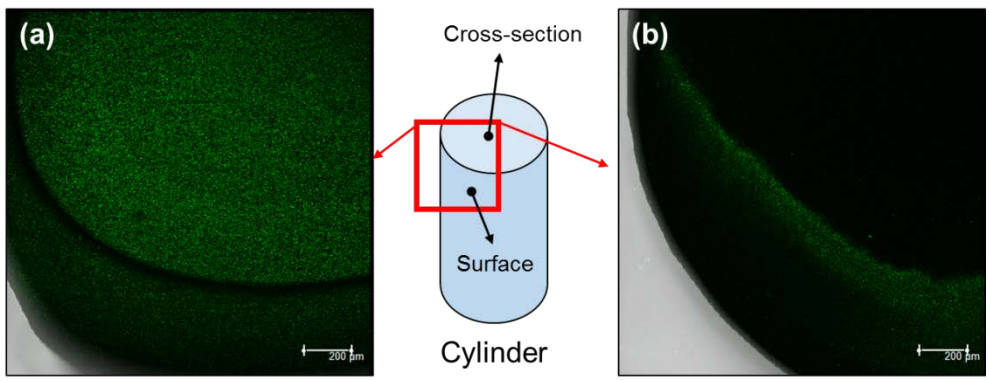

Figure IV-7. CLSM images of cylinders entrapped with (a) only JB525 and (b) both JB 525 and BH4.

IV.3.3. Comparison of the Physical Washing Effect of the QQ-Media (Bead vs. Cylinder)

To compare the physical washing effect of various media shapes, different shapes of vacant media (without QQ bacteria) were prepared and their physical washing capabilities were tested in a batch reactor (1.1 L). The interval between the PC plate and the wall of batch reactors (10 mm) was designed to be identical to the membrane spacing (10 mm) of laboratory-scale MBRs. As the loading volume of each medium was fixed at 0.5% v/v (total media volume/reactor volume), the number of media tested varied depending on the size of the medium. In Figure IV-8, the physical washing effect of bead B with a smaller diameter (3.1 mm) but a higher number (N=355) was approximately 30% greater than that of bead A, with a larger diameter (4.3 mm) but a lower number (N=131). However, when the shape was changed from bead to cylinder (diameter: 1.5 mm, length: 2.4 cm), with nearly same number (N=130), the effect of cylinder was approximately 170% greater than that of bead A. It turned out that the physical washing was greatly affected by media shape, and the cylinder shape is more desirable than the bead shape.

To deeply investigate the effect of media shape on physical washing, the circulation of bead A and the cylinder (Fig. 8) was monitored when passing through a confined space between the reactor wall and the PC plate in a batch reactor, between which the interval is 10 mm, as shown in Figure IV-9. Each medium was stained with Congo red for clear observation. During their movement snapshots were taken every 0.1 seconds for each medium passing through the confined space and then converged to make time lapse images. As each medium passed once through the channel, bead A contacted the PC plate two times (Figure IV-9a), whereas the

cylinder contacted four times (Figure IV-9b). To quantify the contact frequency for a longer period, all of the number of contacts were counted and cumulated during 24 repeated passes of each single medium through the space (Figure IV-10). The single cylinder contacted the PC plate a total of 68 times, and the average contact number per cycle was 2.8 (±2.1), whereas bead A contacted the PC plate a total of 26 times, and the average per cycle was 1.1 (±1.3). The higher contact frequency of the cylinder than that of the spherical bead may be attributed to its geometric structure, as the length of the cylinder was longer than the channel spacing. In summary, substances attached to the PC plate could be expected to be detached, at least partly by collisions between the PC plate and the media. Consequently, the QQ-cylinders are expected to have a greater physical washing effect than the QQ-beads due to their higher contact frequency.

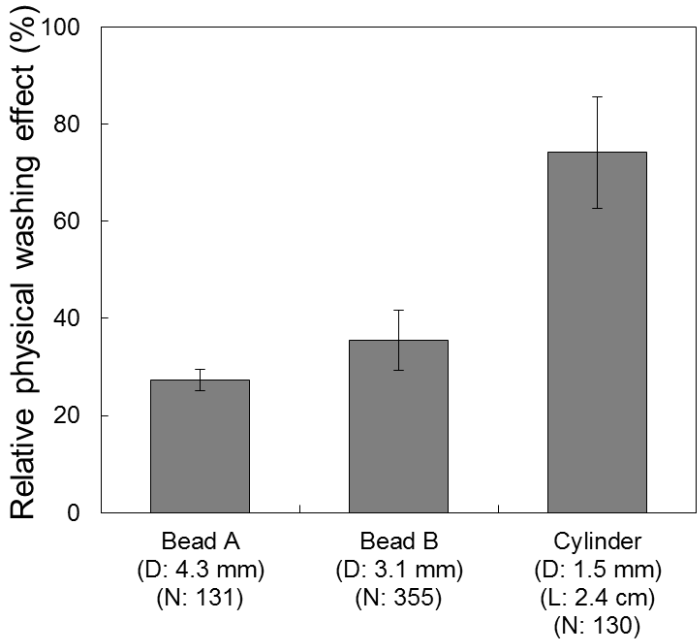

Figure IV-8. Comparison of the physical washing effect between bead A, bead B and the cylinder. D, L and N represent the average diameter, length and number of the media. Error bar: standard deviation (n = 3).

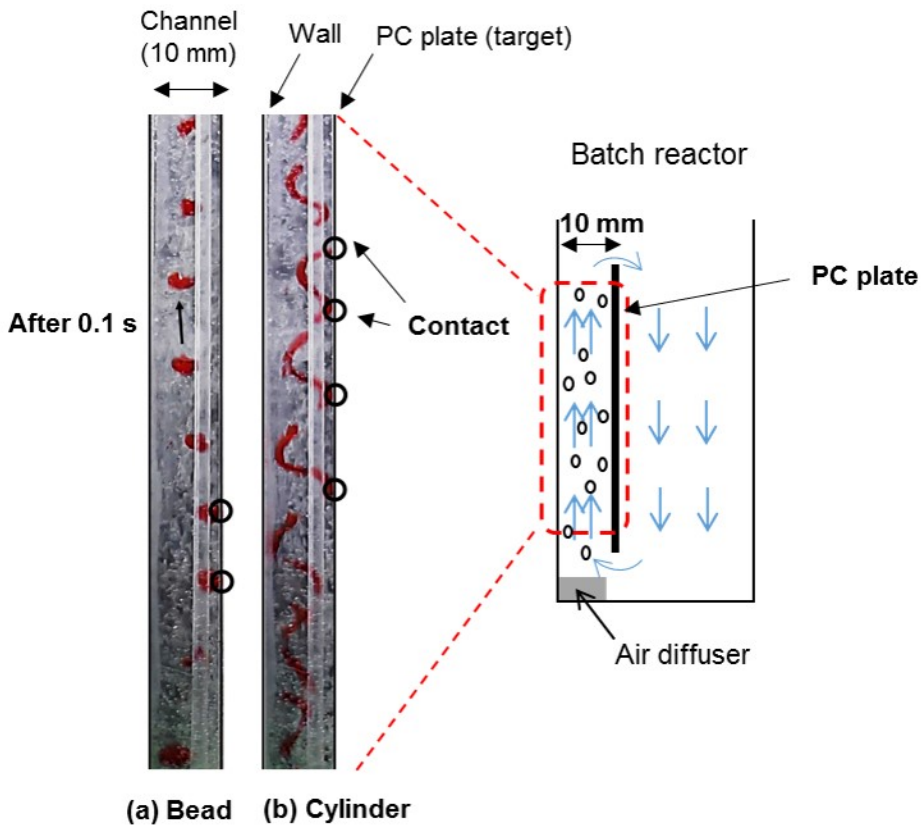

Figure IV-9. Time lapse (snap shot time = 0.1 sec) images of media passing through the channel. (a) Bead with a diameter of 4.3 mm. (b) Cylinder with a diameter of 1.5 mm and a length of 2.4 cm.

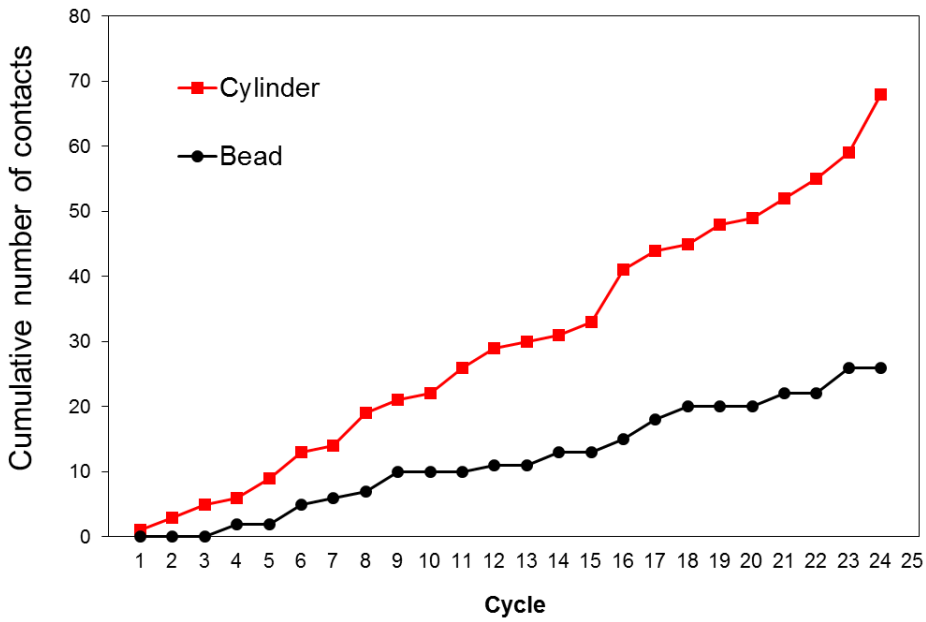

Figure IV-10. Cumulative number of contacts for a bead with a diameter of 4.3 mm and a cylinder with a diameter of 1.5 mm and a length of 2.4 cm.

IV.3.4. Correlation of Cylinder Size with the Physical Washing Effect

It has been reported that the motion of flexible fiber in shear flows can be affected by its geometry, such as the length and aspect ratio (length/diameter) (Skjetne et al., 1997; Wang et al., 2006). First, under the same loading volume (0.5 % v/v), cylinders with identical diameter but different length and number were compared to each other in terms of their physical washing effect. The physical washing effect of the cylinders increased with the increase in their length despite a decrease in number (Figure IV-11a), indicating that the length of the cylinder is more important than the number in terms of the physical washing effect. Next, under the same loading volume (0.5 % v/v), cylinders with similar lengths but different diameters and numbers were compared with each other. The cylinder with greater numbers and smaller diameters showed better physical washing (Figure IV-11b). The two parameters (length and diameter) were combined into one parameter, i.e., the aspect ratio (ratio of length to diameter), and then the physical washing effect was plotted vs. the aspect ratio. It was found that the physical washing effect of the cylinders tended to show a positive relationship with the aspect ratio (Figure IV-12).

In this study, the effects of the shape and size of QQ-medium on QQ activity and physical washing effect were separately investigated in different batch tests. However, there might be the synergistic effect between the QQ activity and the physical washing in that the efficiency of QQ activity would be improved due to detachment of biofilm by physical washing.

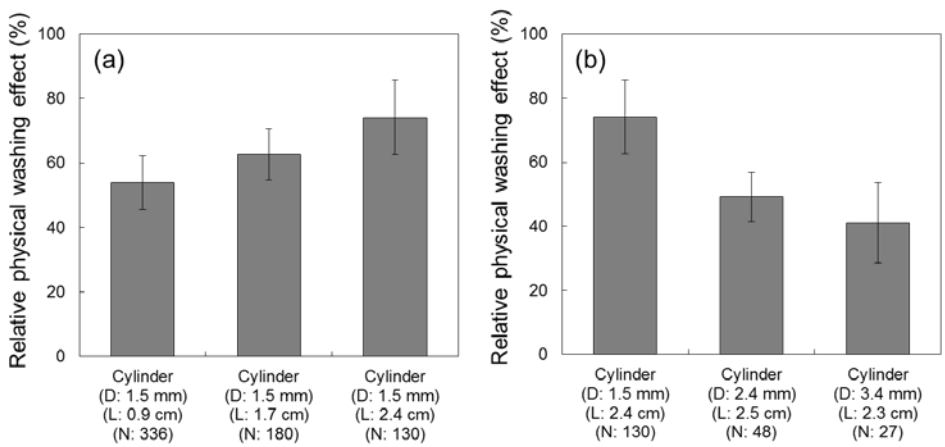

Figure IV-11. Comparison of the physical washing effect of various vacant media. (a) Cylinders with the same diameter but different lengths. (b) Cylinder with different diameters but the same length. D, L and N represent the average diameter, length and number of the media. Error bar: standard deviation (n = 3).

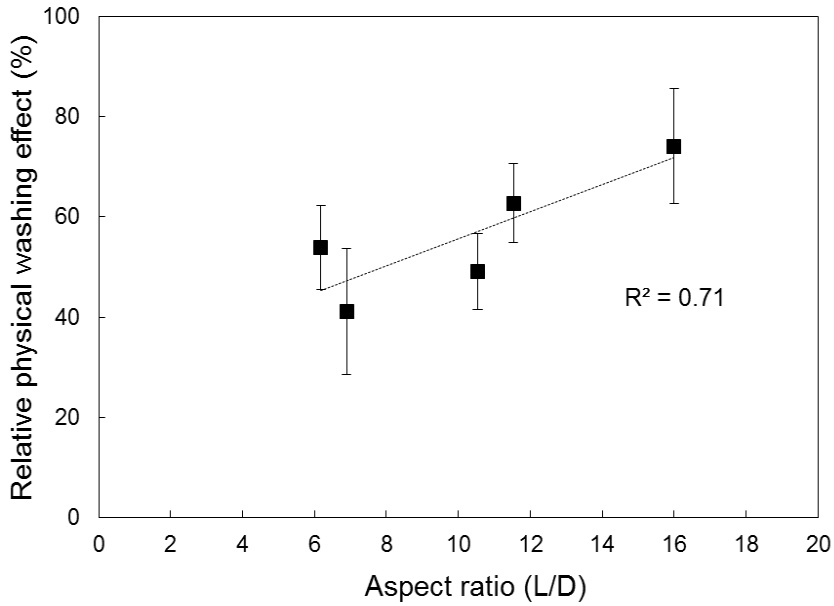

Figure IV-12. The relationship between the physical washing effect and the aspect ratio of each QQ-medium. Error bar: standard deviation (n = 3).

IV.3.5. Assessment of Biofouling Mitigation with Various QQ-Media in Continuous MBRs

Four different phases of MBR sets were operated in a continuous mode to compare biofouling mitigation between various vacant- or QQ-media configurations. TMP rise-up was monitored and their profiles are shown in Fig. IV-13. In addition, for quantitative comparison, T_{TMP}, the average number of days taken to reach a TMP of 20 kPa was calculated in each phase.

In phase 1, conventional- (without media) and QQ-cylinder MBRs were run in parallel at air flow rate of 1.0 L/min (Figure IV-13a). T_{TMP} was approximately 1.3 days in the conventional-MBR, while it was 5.2 days in the QQ-cylinder MBR. In other words, the rate of TMP rise-up, which reflects the extent of membrane biofouling, was delayed by approximately 300% with the insertion of the QQ-cylinder. In Figure IV-13b, the T_{TMP} in the vacant-cylinder- and QQ-cylinder-MBRs were 0.9 days and 2.3 days, respectively, resulting in a ratio of T_{TMP} values of 2.5. Because the physical washing effects was the same with vacant-cylinders and QQ-cylinders, the delay of TMP rise-up in the QQ-cylinder MBR could be attributed to the biological QQ activity of the QQ-cylinders. In phase 3, the vacant-cylinder MBR was compared with vacant-bead MBR (Figure IV-13c). The ratio of T_{TMP} was 2.5, indicating that the rate of TMP rise-up in the vacant-cylinder-MBR was delayed approximately 150% longer than that in the vacant-bead-MBR. Consequently, the better physical washing effect of the cylinders compared with the beads was confirmed in continuous MBR. Finally, the QQ-cylinder MBR and the QQ-bead MBR were operated in parallel at an air flow rate of 0.8 L/min. The ratio of T_{TMP} value of the QQ-cylinder MBR to that of the QQ-bead MBR was calculated to be

1.6, which indicates that the TMP rise-up of the QQ-cylinder MBR was delayed by 60% more than that of the QQ-bead MBR (Figure IV-13d). As demonstrated in batch studies, the improved inhibition of biofouling in the QQ-cylinder MBR may be attributed to the higher QQ activity and physical washing effect of the QQ-cylinders compared with the QQ-beads.

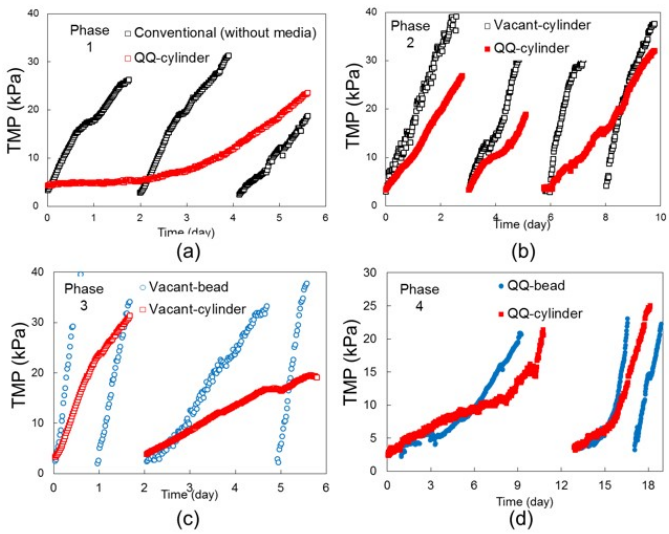

Average days till one TMP-jump to 20 kPa

	MBR A	MBR B	Ratio (B/A)
Phase 1	Conventional (1.3 days)	QQ-cylinder (5.2 days)	4.1
Phase 2	Vacant-cylinder (0.9 days)	QQ-cylinder (2.3 days)	2.5
Phase 3	Vacant-bead (0.6 days)	Vacant-cylinder (1.5 days)	2.5
Phase 4	QQ-bead (4.8 days)	QQ-cylinder (7.6 days)	1.6

Figure IV-13. Comparison of transmembrane pressure profiles in MBRs at four different phases. (a) Control and QQ-cylinder (D: 1.6 mm; L: 3 cm; N: 168). (b) Vacant-cylinder (D: 1.7 mm; L: 3.1 cm; N: 140) and QQ-cylinder (D: 1.7 mm; L: 3cm; N: 146). (c) Vacant-bead (D: 3.4 mm; N: 517) and vacant-cylinder (D: 1.6 mm; L: 3cm; N: 168). (d) QQ-bead (D: 3.4 mm; N: 490) and QQ-cylinder (D: 1.7 mm; L: 3 cm; N: 147). D, L and N represent the average diameter, length and number of the media

IV.4. Conclusions

The purpose of this chapter was to investigate the effect of the shape and size on QQ-media. A new shape of moving medium, cylinder-typed medium (QQ-cylinder) was developed, and compared to previous spherical bead (QQ-bead) in terms of QQ activity and physical washing effect. Based on the results of this study, the following conclusions were made:

- QQ activity was highly dependent on total surface area of media regardless of shape of media. Additionally, it was found that surface of medium is more effective for QQ activity than inner space of medium.

- Physical washing effect was greatly affected by medium shape. Especially, it was found that physical washing effect of cylinder was higher than that of bead due to its higher contact frequency. Moreover, the physical washing effect of cylinders is in close association with the aspect ratio.

- The enhanced performances of QQ-cylinder was confirmed in laboratory-scale continuous MBR with a flat sheet membrane module.

Chapter V

Conclusions

V. Conclusions

The effectiveness of QQ for biofouling control was demonstrated in pilot-scale MBRs fed with real municipal wastewater. In addition, effects of shape and size of media were investigated to enhance the performance of QQ-MBR. Based on the experimental results, the following conclusions were made:

- QQ bacteria entrapping beads (QQ-beads) effectively inhibited the biofouling in pilot-scale MBR fed with real wastewater.
- QQ-MBR could reduce the operating cost by reducing the aeration intensity.
- Bacterial QQ was determined to have no influence on the effluent water quality of the pilot-scale MBRs fed with real wastewater.
- QQ activity and mechanical stability of QQ-beads were well-maintained in MBR fed with real wastewater during the four months of operation.
- QQ activity was highly dependent on total surface area of media regardless of shape of media.
- Surface of medium is more effective for QQ activity than inner space of medium.
- Physical washing effect of cylinder was higher than that of bead due to its higher contact frequency.
- Physical washing effect of cylinders is in close association with the aspect ratio.
- The enhanced performances of QQ-cylinder was confirmed in laboratory-scale continuous MBR with a flat sheet membrane module.

국문초록

분리막 생물반응기(Membrane bioreactor)는 고도 하·폐수처리 공정으로 각광받고 있지만, 분리막 표면위의 생물막형성으로 인해 투수도 감소, 분리막 수명 단축, 운전비 증가 등의 공정 효율성이 떨어지는 문제점이 발생하게 된다. 최근에 정족수감지(Quorum sensing)가 생물막형성에 중요한 역할을 한다는 것이 밝혀졌고, 정족수감지 억제(Quorum quenching) 미생물을 이용하여 분리막 생물반응기의 생물막오염을 저감을 시킨 연구결과들이 보고되고 있다. 특히, 정족수감지 억제 구형담체(QQ-bead)는 고정된 정족수감지 억제 미생물에 의한 생물학적인 정족수감지 억제 효과와 구형담체의 유동에 의한 물리세정 효과를 동시에 가져 생물막형성 억제 효과가 뛰어난 것으로 보고되었다. 하지만 이전의 연구결과들은 실험실에서 제조한 합성폐수를 이용하였고, 대부분 작은 규모의 반응기에서 진행되어 실제 분리막 생물반응기 운전조건과는 거리가 멀었다. 또한, 정족수감지 억제 담체의 성능(정족수감지 억제와 물리세정 효과)을 향상시키기 위한 중요인자가 무엇인지 제시하지 못하였다. 따라서, 본 연구에서는 보다 실증적인 연구를 위해 실폐수를 처리하는 파일럿 규모의 분리막 생물반응기에 정족수감지 억제 구형담체를 적용해 실용화 가능성을 확인하였다. 또한, 정족수감지 억제 담체의 성능에 영향을 미치는 중요인자들을 확인하였고, 이를 통해 기존보다 성능이 뛰어난 새로운 형태의 정족수감지 억제 담체를 개발하였다.

첫째, 실폐수 처리용 분리막 생물반응기를 안정적으로 운전하기 위해 실제 하폐수 처리장에 파일럿 규모 (~1 m^3/d)의 반응기를 설치하였고, 정족수감지 억제 구형담체를 적용하였다. 정족수감지 억제 구형담체가 파일럿 규모의 실폐수 처리용 분리막 생물반응기에서도 생물막오염을 효과적으로 억제하였고, 처리수의 수질에는 부정적인 영향을 주지 않는 것으로 확인되었다. 정족수감지 억제 구형담체의 생물막오염 억제 효과로 인해 분리막 세정용 폭기량을 줄일 수 있었고, 경제성 분석을 통해 운전비용 저감률이 평가되었다. 추가적으로, 산업용 플라스틱 담체와 생물막오염 억제 효과를 비교해, 정족수감지 억제 구형담체의 경쟁력을 확인하였다. 그밖에 체외고분자물질과 미생물 플럭 크기에 미치는 영향을 확인하였다. 또한, 정족수감지 억제 구형담체의 성능이 약 4개월간 유지됨이 확인되었다.

둘째, 새로운 모양의 정족수감지 억제 원기둥담체(QQ-cylinder)를 개발하였고, 기존의 구형담체와 비교 하였다. 또한 원기둥담체와 구형담체의 크기를 변화시켜 담체의 모양과 크기가 정족수감지 억제활성과 물리세정 효과에 각각 어떤 영향을 주는지 확인하였다. 모든 비교실험은 담체의 총 부피가 동일한 조건에서 진행되었고, 정족수감지 억제 활성은 담체의 모양과 상관없이 담체의 표면적에 비례하는 것이 확인되었다. 반면, 물리세정 효과는 담체의 모양과 크기에 따라 크게 변하였고, 원기둥담체가 구형담체에 비해 물리세정 효과가 뛰어났다. 이는 원기둥담체가 구형담체에 비해 분리막 표면과의 접촉확률이 높기 때문으로 판단된다.

또한, 원기둥담체의 물리세정 효과와 원기둥의 종횡비의 관련성이 확인되었다. 최종적으로, 새롭게 개발된 원기둥담체를 연구실 규모 분리막 생물반응기에 적용 시, 기존의 정족수감지 억제 담체인 구형담체에 비해 생물막형성 억제효과가 뛰어남이 확인되었다.

주요어: 분리막 생물반응기, 생물막오염 억제, 정족수감지 억제, 담체, 구형, 원기둥

학번: 2011-21059

References

Agrawal, L. K., Ohashi, Y., Mochida, E., Okui, H., Ueki, Y., Harada, H., and Ohashi, A. (1997). Treatment of raw sewage in a temperate climate using a UASB reactor and the hanging sponge cubes process. *Water Science and Technology*, 36, 433-440.

Aidan, A., Abdel-Jabbar, N., Ibrahim, T. H., Nenov, V., and Mjalli, F. (2007). Neural network modeling and optimization of scheduling backwash for membrane bioreactor. *Clean Technologies and Environmental Policy*, 10, 389-395.

Amini, E., Mehrnia, M. R., Mousavi, S. M., and Mostoufi, N. (2013). Experimental Study and Computational Fluid Dynamics Simulation of a Full-Scale Membrane Bioreactor for Municipal Wastewater Treatment Application. *Industrial & Engineering Chemistry Research*, 52, 9930-9939.

Annop, S., Sridang, P., Puetpaiboon, U., and Grasmick, A. (2014). Influence of relaxation frequency on membrane fouling control in submerged anaerobic membrane bioreactor (SAnMBR). *Desalination and Water Treatment*, 52, 4102-4110.

Bassler, B. L. (1999). How bacteria talk to each other: regulation of gene expression by quorum sensing. *Current Opinion in Microbiology*, 2, 582-587.

Batchelor, S., Cooper, M., Chhabra, S., Glover, L., Stewart, G., Williams, P., and Prosser, J. (1997). Cell density-regulated recovery of starved biofilm populations of ammonia-oxidizing bacteria. *Applied and Environmental Microbiology*, 63, 2281-2286.

Bauer, W. D., and Robinson, J. B. (2002). Disruption of bacterial quorum sensing by other organisms. *Current Opinion in Biotechnology*, 13, 234-237.

Becker, H. A. (1959). The effects of shape and reynolds number on drag in the motion of a freely oriented body in an infinite fluid. *The Canadian Journal of Chemical Engineering*, 37, 85-91.

Brackman, G., Cos, P., Maes, L., Nelis, H. J., and Coenye, T. (2011). Quorum sensing inhibitors increase the susceptibility of bacterial biofilms to antibiotics in vitro and in vivo. *Antimicrobial Agents and Chemotheraphy*, 55, 2655-2661.

Braschler, T., Johann, R., Heule, M., Metref, L., and Renaud, P. (2005). Gentle cell trapping and release on a microfluidic chip by in situ alginate hydrogel formation. *Lab on a Chip*, 5, 553-559.

Burton, E., Read, H., Pellitteri, M., and Hickey, W. (2005). Identification of acyl-

homoserine lactone signal molecules produced by Nitrosomonas europaea strain Schmidt. *Applied and environmental microbiology*, 71, 4906-4909.

Camara, M., Williams, P., and Hardman, A. (2002). Controlling infection by tuning in and turning down the volume of bacterial small-talk. *The Lancet Infectious Diseases*, 2, 667-676.

Cassidy, M. B., Lee, H., and Trevors, J. T. (1996). Environmental applications of immobilized microbial cells: A review. *Journal of Industrial Microbiology*, 16, 79-101.

Chaignon, P., Sadovskaya, I., Ragunah, C., Ramasubbu, N., Kaplan, J. B., and Jabbouri, S. (2007). Susceptibility of staphylococcal biofilms to enzymatic treatments depends on their chemical composition. *Applied Microbiology and Biotechnology*, 75, 125-132.

Chen, F., Bi, X., and Ng, H. Y. (2016). Effects of bio-carriers on membrane fouling mitigation in moving bed membrane bioreactor. *Journal of Membrane Science*, 499, 134-142.

Chen, F., Gao, Y., Chen, X., Yu, Z., and Li, X. (2013). Quorum quenching enzymes and their application in degrading signal molecules to block quorum sensing-dependent infection. *International journal of molecular sciences*, 14, 17477-17500.

Chen, G., Swem, L. R., Swem, D. L., Stauff, D. L., O'Loughlin, C. T., Jeffrey, P. D., Bassler, B. L., and Hughson, F. M. (2011). A strategy for antagonizing quorum sensing. *Molecular Cell*, 42, 199-209.

Chen, R., Zhou, Z., Cao, Y., Bai, Y., and Yao, B. (2010). High yield expression of an AHL-lactonase from Bacillus sp. B546 in Pichia pastoris and its application to reduce Aeromonas hydrophila mortality in aquaculture. *Microbial cell factories*, 9, 1.

Chen, X., Schauder, S., Potier, N., Van Dorsselaer, A., Pelczer, I., Bassler, B. L., and Hughson, F. M. (2002). Structural identification of a bacterial quorum-sensing signal containing boron. *Nature*, 415, 545-549.

Cheong, W.-S., Kim, S.-R., Oh, H.-S., Lee, S. H., Yeon, K.-M., Lee, C.-H., and Lee, J.-K. (2014). Design of quorum quenching microbial vessel to enhance cell viability for biofouling control in membrane bioreactor. *Journal of Microbiology and Biotechnology*, 24, 97-105.

Cheong, W.-S., Lee, C.-H., Moon, Y.-H., Oh, H.-S., Kim, S.-R., Lee, S. H., Lee, C.-H., and Lee, J.-K. (2013). Isolation and Identification of Indigenous Quorum Quenching Bacteria, Pseudomonas sp. 1A1, for Biofouling Control in MBR. *Industrial & Engineering Chemistry Research*, 52, 10554-10560.

Choudhary, S., and Schmidt-Dannert, C. (2010). Applications of quorum sensing in biotechnology. *Applied Microbiology and Biotechnology*, 86, 1267-1279.

Chowdhary, P. K., Keshavan, N., Nguyen, H. Q., Peterson, J. A., Gonzalez, J. E., and Haines, D. C. (2007). Bacillus megaterium CYP102A1 oxidation of acyl homoserine lactones and acyl homoserines. *Biochemistry*, 46, 14429-14437.

Christiaen, S. E. A., Brackman, G., Nelis, H. J., and Coenye, T. (2011). Isolation and identification of quorum quenching bacteria from environmental samples. *Journal of Microbiological Methods*, 87, 213-219.

Chu, Y.-F., Hsu, C.-H., Soma, P. K., and Lo, Y. M. (2009). Immobilization of bioluminescent Escherichia coli cells using natural and artificial fibers treated with polyethyleneimine. *Bioresource technology*, 100, 3167-3174.

Churchouse, S., and Wildgoose, D. (1999). Membrane bioreactors progress from the laboratory to full-scale use. *Membrane Technology*, 1999, 4-8.

Cima, L., Lopina, S., and Merrill, E. (1994). Ligand-modified PEO-based materials for cell transplantation. *Annals of Biomedical Engineering*, 22, 184.

Cvitkovitch, D. G., Li, Y.-H., and Ellen, R. P. Quorum sensing and biofilm formation in Streptococcal infections. *The Journal of Clinical Investigation*, 112, 1626-1632.

Davies, D. G., Parsek, M. R., Pearson, J. P., Iglewski, B. H., Costerton, J. W., and Greenberg, E. P. (1998). The involvement of cell-to-cell signals in the development of a bacterial biofilm. *Science*, 280, 295-298.

De Clippeleir, H., Defoirdt, T., Vanhaecke, L., Vlaeminck, S. E., Carballa, M., Verstraete, W., and Boon, N. (2011). Long-chain acylhomoserine lactones increase the anoxic ammonium oxidation rate in an OLAND biofilm. *Applied microbiology and biotechnology*, 90, 1511-1519.

Dobretsov, S., Teplitski, M., and Paul, V. (2009). Mini-review: quorum sensing in the marine environment and its relationship to biofouling. *Biofouling*, 25, 413-427.

Dong, Y.-H., Xu, J.-L., Li, X.-Z., and Zhang, L.-H. (2000). AiiA, an enzyme that inactivates the acylhomoserine lactone quorum-sensing signal and attenuates the virulence of Erwinia carotovora. *Proceedings of the National Academy of Sciences*, 97, 3526-3531.

Dong, Y.-H., and Zhang, L.-H. (2005). Quorum sensing and quorum-quenching enzymes. *Journal of Microbiology*, 43, 101-109.

Dong, Y. H., Wang, L. H., Xu, J. L., Zhang, H. B., Zhang, X. F., and Zhang, L. H. (2001). Quenching quorum-sensing-dependent bacterial infection by an N-acyl homoserine lactonase. *Nature*, 411, 813-817.

Drews, A. (2010). Membrane fouling in membrane bioreactors—Characterisation, contradictions, cause and cures. *Journal of Membrane Science*, 363, 1-28.

Dubois, M., Gilles, K. A., Hamilton, J. K., Rebers, P., and Smith, F. (1956). Colorimetric method for determination of sugars and related substances. *Analytical chemistry*, 28, 350-356.

Farrand, S. K., Qin, Y., and Oger, P. (2002). Quorum-sensing system of Agrobacterium plasmids: analysis and utility. *Methods in Enzymology*, 358, 452-484.

Federle, M. J., and Bassler, B. L. (2003). Interspecies communication in bacteria. *Journal of Clinical Investigation*, 112, 1291-1299.

Fetzner, S. (2015). Quorum quenching enzymes. *Journal of Biotechnology*, 201, 2-14.

Forgacs, O., and Mason, S. (1959). Particle motions in sheared suspensions: IX. Spin and deformation of threadlike particles. *Journal of colloid science*, 14, 457-472.

Frost&Sullivan (2013). Global Membrane Bioreactor (MBR) Market.

Fuqua, C., Parsek, M. R., and Greenberg, E. P. (2001). Regulation of gene expression by cell-to-cell communication: acyl-homoserine lactone quorum sensing. *Annual review of genetics*, 35, 439-468.

Fuqua, C., and Winans, S. C. (1996). Conserved cis-acting promoter elements are required for density-dependent transcription of Agrobacterium tumefaciens conjugal transfer genes. *Journal of Bacteriology*, 178, 435-440.

Fuqua, C., Winans, S. C., and Greenberg, E. P. (1996). Census and consensus in bacterial ecosystems: the LuxR-LuxI family of quorum-sensing transcriptional regulators. *Annual Reviews in Microbiology*, 50, 727-751.

Górecka, E., and Jastrzębska, M. (2011). Immobilization techniques and biopolymer carriers. *Biotechnology and Food Science*, 75, 65-86.

Galloway, W. R. J. D., Hodgkinson, J. T., Bowden, S. D., Welch, M., and Spring, D. R. (2011). Quorum Sensing in Gram-Negative Bacteria: Small-Molecule Modulation of AHL and AI-2 Quorum Sensing Pathways. *Chemical Reviews*, 111, 28-67.

Gao, S., Wang, Y., Diao, X., Luo, G., and Dai, Y. (2010). Effect of pore diameter and cross-linking method on the immobilization efficiency of Candida rugosa lipase in SBA-15. *Bioresource technology*, 101, 3830-3837.

Givskov, M., de Nys, R., Manefield, M., Gram, L., Maximilien, R., Eberl, L., Molin, S., Steinberg, P. D., and Kjelleberg, S. (1996). Eukaryotic interference with

homoserine lactone-mediated prokaryotic signalling. *Journal of Bacteriology*, 178, 6618-6622.

Goldsmith, H. L. (1967). The microrheology of dispersions. *Rheology*, 4.

Guezennec, J., Herry, J. M., Kouzayha, A., Bachere, E., Mittelman, M. W., and Fontaine, M. N. B. (2012). Exopolysaccharides from unusual marine environments inhibit early stages of biofouling. *International Biodeterioration & Biodegradation*, 66, 1-7.

Guo, W., Ngo, H.-H., and Li, J. (2012). A mini-review on membrane fouling. *Bioresource Technology*, 122, 27-34.

Hai, F. I., Yamamoto, K., and Lee, C.-H. (2013). Membrane Biological Reactors: Theory, Modeling, Design, Management and Applications to Wastewater Reuse: IWA Publishing).

Hazlett, J. D. (1995). Membranes in bioprocessing: Theory and applications, Edited by J.A. Howell, V. Sanchez and R. W. Field, 1993, 336 + VIII pages, Chapman & Hall, London, ISBN 07514 0419 8. Price: US $65.00. *The Canadian Journal of Chemical Engineering*, 73, 272-272.

Hentzer, M., Givskov, M., and Parsek, M. R. (2002). Targeting Quorum Sensing for Treatment of Chronic Bacterial Biofilm Infections. *Laboratory Medicine*, 33, 295-306.

Hiraishi, A., Ueda, Y., and Ishihara, J. (1998). Quinone Profiling of Bacterial Communities in Natural and Synthetic Sewage Activated Sludge for Enhanced Phosphate Removal. *Applied and Environmental Microbiology*, 64, 992-998.

Hoffman, A. S. (2012). Hydrogels for biomedical applications. *Advanced Drug Delivery Reviews*, 64, Supplement, 18-23.

Hu, A. a. S., D. (2007). Activated Carbon Addition to a Submerged Anaerobic Membrane Bioreactor: Effect on Performance, Transmembrane Pressure, and Flux. *Journal of Environmental Engineering*, 133, 73-80.

Huang, L. N., De Wever, H., and Diels, L. (2008a). Diverse and distinct bacterial communities induced biofilm fouling in membrane bioreactors operated under different conditions. *Environental Science & Technology*, 42, 8360-8366.

Huang, X., Wei, C.-H., and Yu, K.-C. (2008b). Mechanism of membrane fouling control by suspended carriers in a submerged membrane bioreactor. *Journal of membrane science*, 309, 7-16.

Huang, Y., and Yang, S. T. (1998). Acetate production from whey lactose using co-

immobilized cells of homolactic and homoacetic bacteria in a fibrous-bed bioreactor. *Biotechnology and bioengineering*, 60, 498-507.

Jahangir, D., Oh, H.-S., Kim, S.-R., Park, P.-K., Lee, C.-H., and Lee, J.-K. (2012). Specific location of encapsulated quorum quenching bacteria for biofouling control in an external submerged membrane bioreactor. *Journal of Membrane Science*, 411, 130-136.

Jarusutthirak, C., and Amy, G. (2006). Role of soluble microbial products (SMP) in membrane fouling and flux decline. *Environmental science & technology*, 40, 969-974.

Jeffery, G. B. (1922). The Motion of Ellipsoidal Particles Immersed in a Viscous Fluid. *Proceedings of the Royal Society of London A: Mathematical, Physical and Engineering Sciences*, 102, 161-179.

Jen, A. C., Wake, M. C., and Mikos, A. G. (1996). Review: Hydrogels for cell immobilization. *Biotechnology and bioengineering*, 50, 357-364.

Jia, H., Zhu, G., Vugrinovich, B., Kataphinan, W., Reneker, D. H., and Wang, P. (2002). Enzyme-Carrying Polymeric Nanofibers Prepared via Electrospinning for Use as Unique Biocatalysts. *Biotechnology Progress*, 18, 1027-1032.

Jiang, W., Xia, S., Liang, J., Zhang, Z., and Hermanowicz, S. W. (2013). Effect of quorum quenching on the reactor performance, biofouling and biomass characteristics in membrane bioreactors. *Water Research*, 47, 187-196.

Jin, L., Ong, S. L., and Ng, H. Y. (2013). Fouling control mechanism by suspended biofilm carriers addition in submerged ceramic membrane bioreactors. *Journal of Membrane Science*, 427, 250-258.

Johir, M. A. H., Aryal, R., Vigneswaran, S., Kandasamy, J., and Grasmick, A. (2011). Influence of supporting media in suspension on membrane fouling reduction in submerged membrane bioreactor (SMBR). *Journal of Membrane Science*, 374, 121-128.

Judd, C. (2006). Preface. In The MBR Book, (Oxford: Elsevier Science), pp. ix-xi.

Judd, S. (2004). A review of fouling of membrane bioreactors in sewage treatment. *Water Science and Technology*, 49, 229-235.

Judd, S. (2008). The status of membrane bioreactor technology. Trends Biotechnol 26, 109-116.

Judd, S. (2010). The MBR book: principles and applications of membrane bioreactors for water and wastewater treatment: Elsevier).

Judd, S. J. (2015). The status of industrial and municipal effluent treatment with

membrane bioreactor technology. *Chemical Engineering Journal*.

Köse-Mutlu, B., Ergön-Can, T., Koyuncu, İ., and Lee, C.-H. (2015). Quorum quenching MBR operations for biofouling control under different operation conditions and using different immobilization media. *Desalination and Water Treatment*, 1-11.

Kai, K., Fujii, H., Ikenaka, R., Akagawa, M., and Hayashi, H. (2014). An acyl-SAM analog as an affinity ligand for identifying quorum sensing signal synthases. *Chemical Communications*, 50, 8586-8589.

Kamoun, E. A., Chen, X., Mohy Eldin, M. S., and Kenawy, E.-R. S. (2015). Crosslinked poly(vinyl alcohol) hydrogels for wound dressing applications: A review of remarkably blended polymers. *Arabian Journal of Chemistry*, 8, 1-14.

Kang, I.-J., Lee, C.-H., and Kim, K.-J. (2003). Characteristics of microfiltration membranes in a membrane coupled sequencing batch reactor system. *Water Research*, 37, 1192-1197.

Keith, L. H. (1996). Compilation of EPA's sampling and analysis methods: CRC Press).

Khan, R., Shen, F., Khan, K., Liu, L. X., Wu, H. H., Luo, J. Q., and Wan, Y. H. (2016). Biofouling control in a membrane filtration system by a newly isolated novel quorum quenching bacterium, Bacillus methylotrophicus sp. WY. *RSC Advances*, 6, 28895-28903.

Kierstan, M., and Bucke, C. (1977). The immobilization of microbial cells, subcellular organelles, and enzymes in calcium alginate gels. *Biotechnology and Bioengineering*, 19, 387-397.

Kilonzo, P., and Bergougnou, M. (2012). Surface modifications for controlled and optimized cell immobilization by adsorption: applications in fibrous bed bioreactors containing recombinant cells. *Journal of Microbial & Biochemical Technology*, S 8, 18-21.

Kim, A. L., Park, S. Y., Lee, C. H., Lee, C. H., and Lee, J. K. (2014). Quorum quenching bacteria isolated from the sludge of a wastewater treatment plant and their application for controlling biofilm formation. *Journal of Microbiology and Biotechnology*, 24, 1574-1582.

Kim, H.-W., Oh, H.-S., Kim, S.-R., Lee, K.-B., Yeon, K.-M., Lee, C.-H., Kim, S., and Lee, J.-K. (2013a). Microbial population dynamics and proteomics in membrane bioreactors with enzymatic quorum quenching. *Applied microbiology and biotechnology*, 97, 4665-4675.

Kim, J.-H., Choi, D.-C., Yeon, K.-M., Kim, S.-R., and Lee, C.-H. (2011). Enzyme-

Immobilized Nanofiltration Membrane To Mitigate Biofouling Based on Quorum Quenching. *Environmental Science & Technology*, 45, 1601-1607.

Kim, J.-S., Lee, C.-H., and Chang, I.-S. (2001). Effect of pump shear on the performance of a crossflow membrane bioreactor. *Water research*, 35, 2137-2144.

Kim, S.-R., Lee, K.-B., Kim, J.-E., Won, Y.-J., Yeon, K.-M., Lee, C.-H., and Lim, D.-J. (2015). Macroencapsulation of quorum quenching bacteria by polymeric membrane layer and its application to MBR for biofouling control. *Journal of Membrane Science*, 473, 109-117.

Kim, S.-R., Oh, H.-S., Jo, S.-J., Yeon, K.-M., Lee, C.-H., Lim, D.-J., Lee, C.-H., and Lee, J.-K. (2013b). Biofouling Control with Bead-Entrapped Quorum Quenching Bacteria in Membrane Bioreactors: Physical and Biological Effects. *Environmental Science & Technology*, 47, 836-842.

Kleerebezem, M., Quadri, L. E., Kuipers, O. P., and de Vos, W. M. (1997). Quorum sensing by peptide pheromones and two-component signal-transduction systems in Gram-positive bacteria. *Molecular Microbiology*, 24, 895-904.

Knoblock, M. D., Sutton, P. M., Mishra, P. N., Gupta, K., and Janson, A. (1994). Membrane Biological Reactor System for Treatment of Oily Wastewaters. *Water Environment Research*, 66, 133-139.

Koch, B., Liljefors, T., Persson, T., Nielsen, J., Kjelleberg, S., and Givskov, M. (2005). The LuxR receptor: the sites of interaction with quorum-sensing signals and inhibitors. *Microbiology*, 151, 3589-3602.

Krekeler, C., Ziehr, H., and Klein, J. (1991). Influence of physicochemical bacterial surface properties on adsorption to inorganic porous supports. *Applied microbiology and biotechnology*, 35, 484-490.

Krzeminski, P., van der Graaf, J. H., and van Lier, J. B. (2012). Specific energy consumption of membrane bioreactor (MBR) for sewage treatment. *Water Science and Technology*, 65, 380.

Ku, X., and Lin, J. (2009). Effect of two bounding walls on the rotational motion of a fiber in the simple shear flow. *Fibers and Polymers*, 10, 302-309.

Kurita, T., Kimura, K., and Watanabe, Y. (2014). The influence of granular materials on the operation and membrane fouling characteristics of submerged MBRs. *Journal of Membrane Science*, 469, 292-299.

López, A., Lázaro, N., and Marqués, A. M. (1997). The interphase technique: a simple method of cell immobilization in gel-beads. *Journal of microbiological methods*, 30, 231-234.

Lade, H., Paul, D., and Kweon, J. H. (2014). Quorum quenching mediated

approaches for control of membrane biofouling. *International Journal of Biological Sciences*, 10, 550-565.

Le-Clech, P., Chen, V., and Fane, T. A. (2006). Fouling in membrane bioreactors used in wastewater treatment. *Journal of Membrane Science*, 284, 17-53.

Leadbetter, J. R., and Greenberg, E. P. (2000). Metabolism of acyl-homoserine lactone quorum-sensing signals by Variovorax paradoxus. *Journal of Bacteriology*, 182, 6921-6926.

Lee, B., Yeon, K.-M., Shim, J., Kim, S.-R., Lee, C.-H., Lee, J., and Kim, J. (2014). Effective Antifouling Using Quorum-Quenching Acylase Stabilized in Magnetically-Separable Mesoporous Silica. *Biomacromolecules*, 15, 1153-1159.

Lee, S., Park, S.-K., Kwon, H., Lee, S. H., Lee, K., Nahm, C. H., Jo, S. J., Oh, H.-S., Park, P.-K., Choo, K.-H., et al. (2016). Crossing the Border between Laboratory and Field: Bacterial Quorum Quenching for Anti-Biofouling Strategy in an MBR. *Environmental Science & Technology*, 50, 1788-1795.

Lee, W.-N., Kang, I.-J., and Lee, C.-H. (2006). Factors affecting filtration characteristics in membrane-coupled moving bed biofilm reactor. *Water research*, 40, 1827-1835.

Leiknes, T., and Ødegaard, H. (2001). Moving bed biofilm membrane reactor (MBB-MR): characteristics and potentials of a hybrid process design for compact wastewater treatment plants. Paper presented at: Proceedings of Engineering with Membranes.

Li, Q., and Elimelech, M. (2004). Organic Fouling and Chemical Cleaning of Nanofiltration Membranes: Measurements and Mechanisms. *Environmental Science & Technology*, 38, 4683-4693.

Li, Y., Lv, J., Zhong, C., Hao, W., Wang, Y., and Zhu, J. (2014). Performance and role of N-acyl-homoserine lactone (AHL)-based quorum sensing (QS) in aerobic granules. *Journal of Environmental Sciences*, 26, 1615-1621.

Lim, B. R., Ahn, K. H., Songprasert, P., Cho, J. W., and Lee, S. H. (2004). Microbial community structure of membrane fouling film in an intermittently and continuously aerated submerged membrane bioreactor treating domestic wastewater. *Water Science and Technology*, 49, 255-261.

Lin, Y. H., Xu, J. L., Hu, J., Wang, L. H., Ong, S. L., Leadbetter, J. R., and Zhang, L. H. (2003). Acyl-homoserine lactone acylase from Ralstonia strain XJ12B represents a novel and potent class of quorum-quenching enzymes. *Molecular Microbiology*, 47, 849-860.

Liu, Y., Rafailovich, M. H., Malal, R., Cohn, D., and Chidambaram, D. (2009).

Engineering of bio-hybrid materials by electrospinning polymer-microbe fibers. *Proceedings of the National Academy of Sciences*, 106, 14201-14206.

Ludwig, T., Kern, P., Bongards, M., and Wolf, C. (2011). Simulation and optimization of an experimental membrane wastewater treatment plant using computational intelligence methods. *Water Science and Technology*, 63, 2255-2260.

Malaeb, L., Le-Clech, P., Vrouwenvelder, J. S., Ayoub, G. M., and Saikaly, P. E. (2013). Do biological-based strategies hold promise to biofouling control in MBRs? *Water Research*, 47, 5447-5463.

Manefield, M., de Nys, R., Kumar, N., Read, R., Givskov, M., Steinberg, P., and Kjelleberg, S. (1999). Evidence that halogenated furanones from Delisea pulchra inhibit acylated homoserine lactone (AHL)-mediated gene expression by displacing the AHL signal from its receptor protein. *Microbiology*, 145 (Pt 2), 283-291.

Manefield, M., Rasmussen, T. B., Henzter, M., Andersen, J. B., Steinberg, P., Kjelleberg, S., and Givskov, M. (2002). Halogenated furanones inhibit quorum sensing through accelerated LuxR turnover. *Microbiology*, 148, 1119-1127.

Maqbool, T., Khan, S. J., Waheed, H., Lee, C.-H., Hashmi, I., and Iqbal, H. (2015). Membrane biofouling retardation and improved sludge characteristics using quorum quenching bacteria in submerged membrane bioreactor. *Journal of Membrane Science*, 483, 75-83.

McClean, K. H., Winson, M. K., Fish, L., Taylor, A., Chhabra, S. R., Camara, M., Daykin, M., Lamb, J. H., Swift, S., Bycroft, B. W., et al. (1997). Quorum sensing and Chromobacterium violaceum: exploitation of violacein production and inhibition for the detection of N-acylhomoserine lactones. *Microbiology*, 143 (Pt 12), 3703-3711.

McMillan, J., Wheaton, F., Hochheimer, J., and Soares, J. (2003). Pumping effect on particle sizes in a recirculating aquaculture system. *Aquacultural Engineering*, 27, 53-59.

Meng, F., Wang, Z., and Li, Y. (2012). Cure of Filament-Caused MBR Fouling in the Presence of Antibiotics: Taking Ciprofloxacin Exposure As an Example. *Industrial & Engineering Chemistry Research*, 51, 13784-13791.

Miller, D. J., Araujo, P. A., Correia, P. B., Ramsey, M. M., Kruithof, J. C., van Loosdrecht, M. C., Freeman, B. D., Paul, D. R., Whiteley, M., and Vrouwenvelder, J. S. (2012). Short-term adhesion and long-term biofouling testing of polydopamine and poly(ethylene glycol) surface modifications of membranes and feed spacers for biofouling control. *Water Research*, 46, 3737-3753.

Miller, M. B., and Bassler, B. L. (2001). Quorum Sensing in Bacteria. *Annual Review of Microbiology,* 55, 165-199.

Miura, Y., Hiraiwa, M. N., Ito, T., Itonaga, T., Watanabe, Y., and Okabe, S. (2007a). Bacterial community structures in MBRs treating municipal wastewater: relationship between community stability and reactor performance. *Water Research,* 41, 627-637.

Miura, Y., Watanabe, Y., and Okabe, S. (2007b). Membrane Biofouling in Pilot-Scale Membrane Bioreactors (MBRs) Treating Municipal Wastewater: Impact of Biofilm Formation. *Environmental Science & Technology*, 41, 632-638.

Monclus, H., Zacharias, S., Santos, A., Pidou, M., and Judd, S. (2010). Criticality of Flux and Aeration for a Hollow Fiber Membrane Bioreactor. *Separation Science and Technology,* 45, 956-961.

Monsalvo, V. M., Lopez, J., Somer, M. M., Mohedano, A. F., and Rodriguez, J. J. (2015). Short-term fouling control by cyclic aeration in membrane bioreactors for cosmetic wastewater treatment. *Desalination and Water Treatment,* 56, 3599-3606.

Mueller, J., Boyle, W. C., and Popel, H. J. (2002). Aeration: principles and practice, Vol 11: CRC press).

Nagaoka, H., and Nemoto, H. (2005). Influence of extracellular polymeric substances on nitrogen removal in an intermittently-aerated membrane bioreactor. *Water Science and Technology*, 51, 151-158.

Nagaoka, H., Ueda, S., and Miya, A. (1996). Influence of bacterial extracellular polymers on the membrane separation activated sludge process. *Water Science and Technology*, 34, 165-172.

Navarro, J., and Durand, G. (1977). Modification of yeast metabolism by immobilization onto porous glass. *European journal of applied microbiology and biotechnology*, 4, 243-254.

Ngo, H. H., Nguyen, M. C., Sangvikar, N. G., Hoang, T. T. L., and Guo, W. S. (2006). Simple approaches towards the design of an attached-growth sponge bioreactor (AGSB) for wastewater treatment and reuse. *Water Science and Technology,* 54, 191-197.

Nguyen, L. N., Hai, F. I., Kang, J., Price, W. E., and Nghiem, L. D. (2012). Removal of trace organic contaminants by a membrane bioreactor–granular activated carbon (MBR–GAC) system. *Bioresource Technology,* 113, 169-173.

Novick, R. P., and Muir, T. W. (1999). Virulence gene regulation by peptides in staphylococci and other Gram-positive bacteria. *Current Opinion in Microbiology*, 2, 40-45.

Oh, H.-S., Kim, S.-R., Cheong, W.-S., Lee, C.-H., and Lee, J.-K. (2013). Biofouling inhibition in MBR by Rhodococcus sp. BH4 isolated from real MBR plant. *Applied microbiology and biotechnology*, 97, 10223-10231.

Oh, H.-S., Yeon, K.-M., Yang, C.-S., Kim, S.-R., Lee, C.-H., Park, S. Y., Han, J. Y., and Lee, J.-K. (2012). Control of Membrane Biofouling in MBR for Wastewater Treatment by Quorum Quenching Bacteria Encapsulated in Microporous Membrane. *Environmental Science & Technology*, 46, 4877-4884.

Olsen, J. A., Severinsen, R., Rasmussen, T. B., Hentzer, M., Givskov, M., and Nielsen, J. (2002). Synthesis of new 3- and 4-substituted analogues of acyl homoserine lactone quorum sensing autoinducers. *Bioorganic & Medicinal Chemistry Letters*, 12, 325-328.

Park, J., and Chang, H. (2000). Microencapsulation of microbial cells. *Biotechnology advances*, 18, 303-319.

Parsek, M. R., and Greenberg, E. P. (2000). Acyl-homoserine lactone quorum sensing in gram-negative bacteria: a signaling mechanism involved in associations with higher organisms. *Proceedings of the National Academy of Sciences*, 97, 8789-8793.

Parsek, M. R., and Greenberg, E. P. (2005). Sociomicrobiology: the connections between quorum sensing and biofilms. *Trends in Microbiology*, 13, 27-33.

Parsek, M. R., Val, D. L., Hanzelka, B. L., Cronan, J. E., and Greenberg, E. (1999). Acyl homoserine-lactone quorum-sensing signal generation. *Proceedings of the National Academy of Sciences*, 96, 4360-4365.

Parveen, N., and Cornell, K. A. (2011). Methylthioadenosine/S-adenosylhomocysteine nucleosidase, a critical enzyme for bacterial metabolism. *Molecular Microbiology*, 79, 7-20.

Petersen, F. C., Tao, L., and Scheie, A. A. (2005). DNA Binding-Uptake System: a Link between Cell-to-Cell Communication and Biofilm Formation. *Journal of Bacteriology*, 187, 4392-4400.

Pham, Q. P., Sharma, U., and Mikos, A. G. (2006). Electrospinning of polymeric nanofibers for tissue engineering applications: a review. *Tissue engineering*, 12, 1197-1211.

Pombo, F., Magrini, A., and Szklo, A. (2011). Technology Roadmap for Wastewater Reuse in Petroleum Refineries in Brazil: *INTECH* Open Access Publisher).

Ramakrishna, S., and Prakasham, R. (1999). Microbial fermentations with immobilized cells. *Current Science*, 77.

Rana, D., and Matsuura, T. (2010). Surface modifications for antifouling membranes.

Chemical Reviews, 110, 2448-2471.

Randall, C. W., and Sen, D. (1996). Full-scale evaluation of an integrated fixed-film activated sludge (IFAS) process for enhanced nitrogen removal. *Water Science and Technology*, 33, 155-162.

Raychaudhuri, A., Jerga, A., and Tipton, P. A. (2005). Chemical mechanism and substrate specificity of RhlI, an acylhomoserine lactone synthase from Pseudomonas aeruginosa. *Biochemistry*, 44, 2974-2981.

Rosenberger, S., Helmus, F., Krause, S., Bareth, A., and Meyer-Blumenroth, U. (2011). Principles of an enhanced MBR-process with mechanical cleaning. *Water Science & Technology*, 64.

Rosenberger, S., Laabs, C., Lesjean, B., Gnirss, R., Amy, G., Jekel, M., and Schrotter, J.-C. (2006). Impact of colloidal and soluble organic material on membrane performance in membrane bioreactors for municipal wastewater treatment. *Water Research*, 40, 710-720.

Santos, A., and Judd, S. (2010). The Commercial Status of Membrane Bioreactors for Municipal Wastewater. *Separation Science and Technology*, 45, 850-857.

Sauer, K., Camper, A. K., Ehrlich, G. D., Costerton, J. W., and Davies, D. G. (2002). Pseudomonas aeruginosa displays multiple phenotypes during development as a biofilm. *Journal of Bacteriology*, 184, 1140-1154.

Schmid, C. F., Switzer, L. H., and Klingenberg, D. J. (2000). Simulations of fiber flocculation: Effects of fiber properties and interfiber friction. *Journal of Rheology*, 44, 781-809.

Shim, S. N., Kim, S.-R., Jo, S. J., Yeon, K.-M., and Lee, C.-H. (2015). Evaluation of mechanical membrane cleaning with moving beads in MBR using Box–Behnken response surface methodology. *Desalination and Water Treatment*, 56, 2797-2806.

Siembida, B., Cornel, P., Krause, S., and Zimmermann, B. (2010). Effect of mechanical cleaning with granular material on the permeability of submerged membranes in the MBR process. *Water Research*, 44, 4037-4046.

Skjetne, P., Ross, R. F., and Klingenberg, D. J. (1997). Simulation of single fiber dynamics. *The Journal of Chemical Physics*, 107, 2108-2121.

Smith, K. M., Bu, Y., and Suga, H. (2003). Induction and inhibition of Pseudomonas aeruginosa quorum sensing by synthetic autoinducer analogs. *Chemistry & Biology*, 10, 81-89.

Solano, C., Echeverz, M., and Lasa, I. (2014). Biofilm dispersion and quorum sensing. *Current Opinion in Microbiology*, 18, 96-104.

Song, S. H., Choi, S. S., Park, K., and Yoo, Y. J. (2005). Novel hybrid immobilization of microorganisms and its applications to biological denitrification. Enzyme and Microbial Technology 37, 567-573.

Steindler, L., and Venturi, V. (2007). Detection of quorum-sensing N-acyl homoserine lactone signal molecules by bacterial biosensors. *FEMS Microbiology Letters*, 266, 1-9.

Stolarzewicz, I., Białecka-Florjańczyk, E., Majewska, E., and Krzyczkowska, J. (2011). Immobilization of yeast on polymeric supports. *Chemical and Biochemical Engineering Quarterly*, 25, 135-144.

Sze Chai Kwok, H. L. a. P. O. C. (2010). Water Technology Market 2010: Key opportunities and emerging trends. *Global Water Intelligence*.

Talabardon, M., Schwitzguébel, J. P., Peringer, P., and Yang, S. T. (2000). Acetic Acid Production from Lactose by an Anaerobic Thermophilic Coculture Immobilized in a Fibrous-Bed Bioreactor. *Biotechnology progress*, 16, 1008-1017.

Tan, C. H., Koh, K. S., Xie, C., Tay, M., Zhou, Y., Williams, R., Ng, W. J., Rice, S. A., and Kjelleberg, S. (2014). The role of quorum sensing signalling in EPS production and the assembly of a sludge community into aerobic granules. *The ISME journal*, 8, 1186-1197.

Teplitski, M., Eberhard, A., Gronquist, M. R., Gao, M., Robinson, J. B., and Bauer, W. D. (2003). Chemical identification of N-acyl homoserine lactone quorum-sensing signals produced by Sinorhizobium meliloti strains in defined medium. *Archives of Microbiology*, 180, 494-497.

Thiel, V., Vilchez, R., Sztajer, H., Wagner-Döbler, I., and Schulz, S. (2009). Identification, Quantification, and Determination of the Absolute Configuration of the Bacterial Quorum-Sensing Signal Autoinducer-2 by Gas Chromatography–Mass Spectrometry. *ChemBioChem*, 10, 479-485.

Tomlin, K. L., Malott, R. J., Ramage, G., Storey, D. G., Sokol, P. A., and Ceri, H. (2005). Quorum-sensing mutations affect attachment and stability of Burkholderia cenocepacia biofilms. Applied and Environmental Microbiology, 71, 5208-5218.

Toyofuku, M., Nomura, N., Fujii, T., Takaya, N., Maseda, H., Sawada, I., Nakajima, T., and Uchiyama, H. (2007). Quorum sensing regulates denitrification in Pseudomonas aeruginosa PAO1. *Journal of bacteriology*, 189, 4969-4972.

Tsuyuhara, T., Hanamoto, Y., Miyoshi, T., Kimura, K., and Watanabe, Y. (2010). Influence of membrane properties on physically reversible and irreversible fouling in membrane bioreactors. *Water Science and Technology*, 61, 2235-2240.

Uroz, S., Chhabra, S. R., Camara, M., Williams, P., Oger, P., and Dessaux, Y. (2005). N-Acylhomoserine lactone quorum-sensing molecules are modified and degraded by Rhodococcus erythropolis W2 by both amidolytic and novel oxidoreductase activities. *Microbiology*, 151, 3313-3322.

van 't Oever, R. (2005). MBR focus: is submerged best? *Filtration & Separation*, 42, 24-27.

Verma, M., Brar, S., Blais, J., Tyagi, R., and Surampalli, R. (2006). Aerobic biofiltration processes—Advances in wastewater treatment. *Practice Periodical of Hazardous, Toxic, and Radioactive Waste Management*, 10, 264-276.

Verrecht, B., Maere, T., Nopens, I., Brepols, C., and Judd, S. (2010). The cost of a large-scale hollow fibre MBR. *Water Research*, 44, 5274-5283.

Wang, G., Yu, W., and Zhou, C. (2006). Optimization of the rod chain model to simulate the motions of a long flexible fiber in simple shear flows. *European Journal of Mechanics - B/Fluids*, 25, 337-347.

Wang, J., Quan, C., Wang, X., Zhao, P., and Fan, S. (2011). Extraction, purification and identification of bacterial signal molecules based on N-acyl homoserine lactones. *Microbial Biotechnology*, 4, 479-490.

Wang, L.-H., Weng, L.-X., Dong, Y.-H., and Zhang, L.-H. (2004). Specificity and enzyme kinetics of the quorum-quenching N-acyl homoserine lactone lactonase (AHL-lactonase). *Journal of Biological Chemistry*, 279, 13645-13651.

Wang, Z., Wu, Z., and Tang, S. (2009). Extracellular polymeric substances (EPS) properties and their effects on membrane fouling in a submerged membrane bioreactor. *Water research*, 43, 2504-2512.

Waters, C. M., and Bassler, B. L. (2005). QUORUM SENSING: Cell-to-Cell Communication in Bacteria. *Annual Review of Cell and Developmental Biology*, 21, 319-346.

Weerasekara, N. A., Choo, K.-H., and Lee, C.-H. (2014). Hybridization of physical cleaning and quorum quenching to minimize membrane biofouling and energy consumption in a membrane bioreactor. *Water research*, 67, 1-10.

Weiner, R., and Matthews, R. (2003). Environmental engineering: Butterworth-Heinemann).

Welty, J. R., Wicks, C. E., Rorrer, G., and Wilson, R. E. (2009). Fundamentals of momentum, heat, and mass transfer: John Wiley & Sons).

Wisniewski, C., and Grasmick, A. (1998). Floc size distribution in a membrane bioreactor and consequences for membrane fouling. *Colloids and Surfaces*

A: Physicochemical and Engineering Aspects, 138, 403-411.

Wu, H., Song, Z., Hentzer, M., Andersen, J. B., Heydorn, A., Mathee, K., Moser, C., Eberl, L., Molin, S., Hoiby, N., and Givskov, M. (2000). Detection of N-acylhomoserine lactones in lung tissues of mice infected with Pseudomonas aeruginosa. *Microbiology*, 146 (Pt 10), 2481-2493.

Wu, J., and He, C. (2012). Effect of cyclic aeration on fouling in submerged membrane bioreactor for wastewater treatment. *Water Research*, 46, 3507-3515.

Wu, J., Le-Clech, P., Stuetz, R. M., Fane, A. G., and Chen, V. (2008). Effects of relaxation and backwashing conditions on fouling in membrane bioreactor. *Journal of Membrane Science*, 324, 26-32.

Xiong, Y., and Liu, Y. (2010). Biological control of microbial attachment: a promising alternative for mitigating membrane biofouling. *Applied Microbiology and Biotechnology*, 86, 825-837.

Xu, H., and Liu, Y. (2011). Control and Cleaning of Membrane Biofouling by Energy Uncoupling and Cellular Communication. *Environmental Science & Technology*, 45, 595-601.

Yamamoto, K., Hiasa, M., Mahmood, T., and Matsuo, T. (1989). Direct Solid-Liquid Separation Using Hollow Fiber Membrane in an Activated Sludge Aeration Tank. *Water Science and Technology*, 21, 43-54.

Yamato, N., Kimura, K., Miyoshi, T., and Watanabe, Y. (2006). Difference in membrane fouling in membrane bioreactors (MBRs) caused by membrane polymer materials. *Journal of Membrane Science*, 280, 911-919.

Yang, X., Wang, R., Fane, A. G., Tang, C. Y., and Wenten, I. (2013). Membrane module design and dynamic shear-induced techniques to enhance liquid separation by hollow fiber modules: a review. *Desalination and Water Treatment*, 51, 3604-3627.

Yeom, I.-T., Nah, Y.-M., and Ahn, K.-H. (1999). Treatment of household wastewater using an intermittently aerated membrane bioreactor. *Desalination*, 124, 193-203.

Yeon, K.-M., Cheong, W.-S., Oh, H.-S., Lee, W.-N., Hwang, B.-K., Lee, C.-H., Beyenal, H., and Lewandowski, Z. (2009a). Quorum Sensing: A New Biofouling Control Paradigm in a Membrane Bioreactor for Advanced Wastewater Treatment. *Environmental Science & Technology*, 43, 380-385.

Yeon, K. M., Lee, C. H., and Kim, J. (2009b). Magnetic enzyme carrier for effective biofouling control in the membrane bioreactor based on enzymatic quorum quenching. *Environmental Science & Technology*, 43, 7403-7409.

Yoon, S.-H. (2015). Membrane bioreactor processes: Principles and applications.

Yu, H., Xu, G., Qu, F., Li, G., and Liang, H. (2016). Effect of solid retention time on membrane fouling in membrane bioreactor: from the perspective of quorum sensing and quorum quenching. *Applied Microbiology and Biotechnology*.

Yuniarto, A., Noor, Z. Z., Ujang, Z., Olsson, G., Aris, A., and Hadibarata, T. (2013). Bio-fouling reducers for improving the performance of an aerobic submerged membrane bioreactor treating palm oil mill effluent. *Desalination*, 316, 146-153.

Yusuf, Z., Abdul Wahab, N., and Sahlan, S. (2015). Fouling control strategy for submerged membrane bioreactor filtration processes using aeration airflow, backwash, and relaxation: a review. *Desalination and Water Treatment*, 1-13.

ZHANG, H., Jie, X., Yang, Y., Zixing, W., and Fenglin, Y. (2009). Mechanism of calcium mitigating membrane fouling in submerged membrane bioreactors. *Journal of Environmental Sciences*, 21, 1066-1073.

Zhou, H., and Smith, D. W. (2002). Advanced technologies in water and wastewater treatment. *Journal of Environmental Engineering and Science*, 1, 247-264.

Zong, X., Kim, K., Fang, D., Ran, S., Hsiao, B. S., and Chu, B. (2002). Structure and process relationship of electrospun bioabsorbable nanofiber membranes. *Polymer*, 43, 4403-4412.

Zsirai, T., Buzatu, P., Aerts, P., and Judd, S. (2012). Efficacy of relaxation, backflushing, chemical cleaning and clogging removal for an immersed hollow fibre membrane bioreactor. *Water Research*, 46, 4499-4507.